



HAL
open science

Diversity-oriented synthesis and bioactivity evaluation of N-substituted ferrocifen compounds as novel antiproliferative agents against TNBC cancer cells

Yong Wang, Pascal Pigeon, Wei Li, Jiangkun Yan, Patrick M Dansette,
Mohamed Othman, Michael Mcglinchey, Gérard Jaouen

► To cite this version:

Yong Wang, Pascal Pigeon, Wei Li, Jiangkun Yan, Patrick M Dansette, et al.. Diversity-oriented synthesis and bioactivity evaluation of N-substituted ferrocifen compounds as novel antiproliferative agents against TNBC cancer cells. *European Journal of Medicinal Chemistry*, 2022, 234, pp.114202. 10.1016/j.ejmech.2022.114202 . hal-03599161

HAL Id: hal-03599161

<https://hal.science/hal-03599161>

Submitted on 13 Jun 2022

HAL is a multi-disciplinary open access archive for the deposit and dissemination of scientific research documents, whether they are published or not. The documents may come from teaching and research institutions in France or abroad, or from public or private research centers.

L'archive ouverte pluridisciplinaire **HAL**, est destinée au dépôt et à la diffusion de documents scientifiques de niveau recherche, publiés ou non, émanant des établissements d'enseignement et de recherche français ou étrangers, des laboratoires publics ou privés.

Diversity-oriented Synthesis and Bioactivity Evaluation of N-substituted Ferrocifen Compounds as Novel Antiproliferative Agents against TNBC Cancer Cells

Yong Wang,*^{[a],[b]} Pascal Pigeon,^{[c],[d]} Wei Li,^{[a],[b]} Jiangkun Yan,^{[a],[b]} Patrick M. Dansette,^[e] Mohamed Othman,^[f] Michael J. McGlinchey,^[g] and Gérard Jaouen*^{[c],[d]}

- [a] Prof. Yong Wang, Wei Li, Jiangkun Yan, Key Laboratory of Marine Drugs, Chinese Ministry of Education, School of Medicine and Pharmacy, Ocean University of China, Qingdao, 26003, Shandong, China
E-mail: wangyong8866@ouc.edu.cn
- [b] Prof. Yong Wang, Wei Li, Jiangkun Yan, Laboratory for Marine Drugs and Bioproducts, Pilot National Laboratory for Marine Science and Technology, Qingdao, 266200, China
- [c] Dr. Pascal Pigeon; Prof. G. Jaouen, PSL, Chimie ParisTech, 11 rue Pierre et Marie Curie, F-75005 Paris, France
E-mail: gerard.jaouen@chimie-paristech.fr
- [d] Dr. Pascal Pigeon; Prof. G. Jaouen, Sorbonne Universités, UPMC Univ Paris 6, UMR 8232, CNRS, IPCM, 4 Place Jussieu, F-75005 Paris, France
- [e] Dr. P. M. Dansette, Laboratoire de Chimie et Biochimie Pharmacologiques et Toxicologiques, UMR 8601 CNRS, Université de Paris, 45 rue des Saints Pères, 75270 Paris Cedex 06, France
- [f] Mohamed Othman, Normandie Univ., URCOM, UNIHAVRE, FR3032, EA 3221, 25 rue P. Lebon, BP 540, 76058 Le Havre (France).
- [g] Prof. Michael J. McGlinchey, UCD School of Chemistry, University College Dublin, Belfield, Dublin 4, Ireland

Abstract

Ferrociphenols are characterized by the presence of a biologically active redox motif [ferrocenyl-ene-*p*-phenol], and are known to exhibit anticancer properties. Recent studies have identified a new series of ferrociphenols that bear an imido-type heterocycle at the terminus of a short alkyl chain, and which showed very strong antiproliferativity against multiple types of cancer cells. This work describes the syntheses and an SAR study of ferrociphenols bearing a diversity-based range of nitrogen-containing substituents on the alkyl chain. Preliminary oxidative metabolism experiments and ROS-related bioactivity measurements were also carried out to probe the origin of the cytotoxicity of the imido-ferrociphenols. Furthermore, an interesting dimerization phenomenon was observed in the X-ray crystal structure of the 2,3-naphthalenedicarboximidopropyl-ferrocidiphenol, **21**, which may be a factor in decreasing its rate of oxidation to form the corresponding quinone methide, **21-QM**, thereby affecting its antitumor activity. These results suggest that both the formation rate and the stability of QMs could affect the antiproliferative activity of their ferrociphenol precursors.

Key words: anticancer agents; bioorganometallic chemistry; ferrocene; quinones; imides

1. Introduction

Bioorganometallic chemistry is a multidisciplinary field focused on the bioactivity of molecules with at least one metal-carbon bond.[1-5] This unifying neologism arose in the mid-1980s and encompasses some aspects of radiopharmaceuticals, natural and artificial enzymes, toxicology, metallomics, biosensors, bioanalysis, and medicinal chemistry.[6-9] Amongst several fields of note, medicinal organometallic chemistry is in fact now one of the major areas that has garnered most interest, thanks to its potential to provide new approaches in oncology.[10-14] A number of series of transition metal organometallic complexes have been explored in an attempt to treat malignant tumors, including those of Ru, Os, Au, Ir, Ti, as well as of Fe, which is the most abundant transition metal in the human body.[15-20] In the latter case, the iron is generally present as a ferrocenyl moiety, whereby it can be stabilized as Fe(II) in a non-oxidizing medium.

Ferrocene derivatives have attracted significant interest in the antibacterial, antiviral, antifungal, and especially anticancer and antiparasitic areas.[21-24] Ferrocifens, which were patented in 1994 as a consequence of their exceptional bioactivity,[25, 26] are organometallic derivatives of Fe(II) in which a phenyl group in tamoxifen, the current first-line treatment for hormone-dependent breast cancers, has been replaced by a ferrocenyl substituent. They exhibit the unusual characteristic of possessing a [ferrocenyl-ene-*p*-phenol] motif which, at low concentrations in cancerous cells, gives rise to ROS (Reactive Oxygen Species), in particular H₂O₂. The metal, easily reversibly oxidized, provides access to a range of quinone methides (QMs), whose identity depends on the substituents present on the carbon skeleton.[27-29] This first type of electrophilic metabolite can itself react with overexpressed nucleophilic proteins in the cancer cell, or it can evolve to form indenones or other cyclic species capable of inhibiting other proteic targets (*vide infra*).[30, 31] The particular feature of interest for the ferrocifens was that they not only exhibited antiproliferative behavior against hormone-dependent tumours (such as MCF-7) comparable to, or in some cases even better than hydroxytamoxifen, they were also active on triple-negative breast cancers (TNBC), i.e. hormone-independent cell-lines such as MDA-MB-231, for which tamoxifen is ineffective. This dramatic result prompted us to focus on the ferrocifens, not only by modifying the phenol group, but also by adding functional groups to the original ethyl side-chain.[32-34]

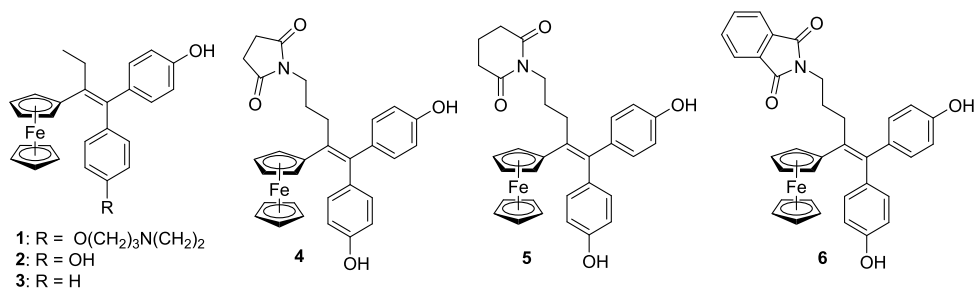
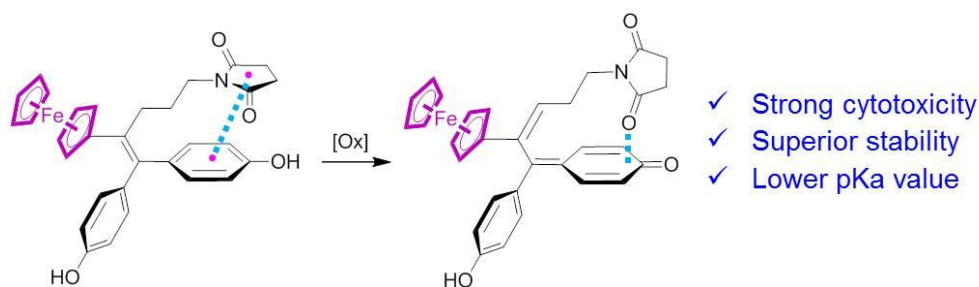


Figure 1. A selection of ferrociphenols **1-6**; (**1** is specifically designated as hydroxyferrocifen).

Recently, modification of the initial alkyl chain by attaching an imido-type heterocycle has been explored. Gratifyingly, this approach has yielded molecules with particularly low IC₅₀ values, notably for complexes **4**, **5** and **6**, on multiple cancer cells including TNBC MDA-MB-231 cells, epithelial ovarian cancer cells A2780 and A2780-Cis (cisplatin resistant).[35] It was demonstrated that the potent cytotoxicity of imido-ferrociphenols correlates strongly with the specific lone pair- π (lp- π) interaction between a carbonyl group of the imide and the quinone ring of the corresponding QMs, as depicted in Scheme 1, thus enhancing the stability of the QMs and lowering the pKa values of the corresponding phenolates.[36]

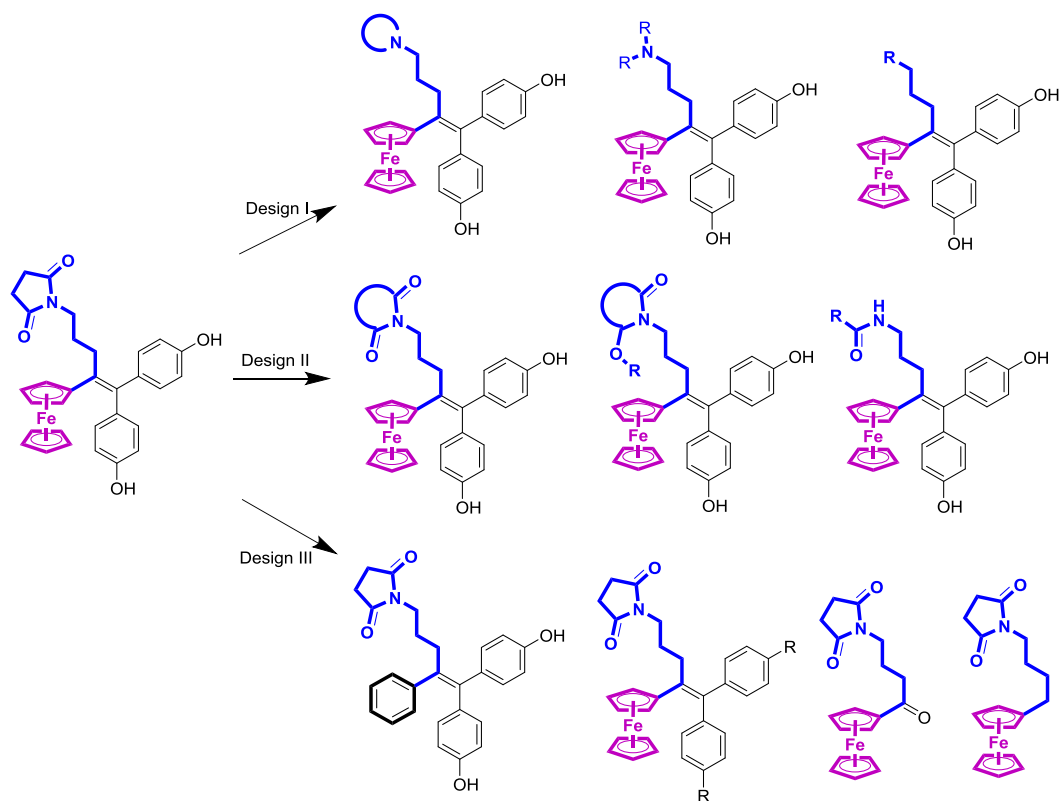


Scheme 1. Oxidation of a ferrociphenol to form a quinone methide.

The unprecedented behaviour of these initial systems, i.e. the imido-ferrociphenols, led us towards their systematic modification by incorporating diversity-based nitrogen-containing substituents. Consequently, the syntheses of a wide variety of ferrocenyl complexes, together with an SAR analysis, are described herein, and the preliminary oxidative metabolic behaviour of some typical compounds has also been undertaken.

To generate a diverse range of substituents, three design strategies were envisaged (Scheme 2). In the first case, the imido substituent in the terminal position was replaced by an amino group, such as dialkylamino, cycloalkylamino or pyridinium. The second approach maintained the presence of an

imido group, but expanded the scope by the fusion of naphthalene or pyridine rings to the succinimido core, or by the incorporation of a morpholine-type structure. Moreover, ring-opened derivatives were prepared. Finally, in the third strategy, the ferrocenyl moiety was replaced by phenyl, or the phenolic groups were removed to leave the succinimido unit at the terminus of a simple alkyl or acyl chain.



Scheme 2. Design strategy of selected ferrociphenols bearing diverse nitrogen-containing substituents.

2. Results and discussion

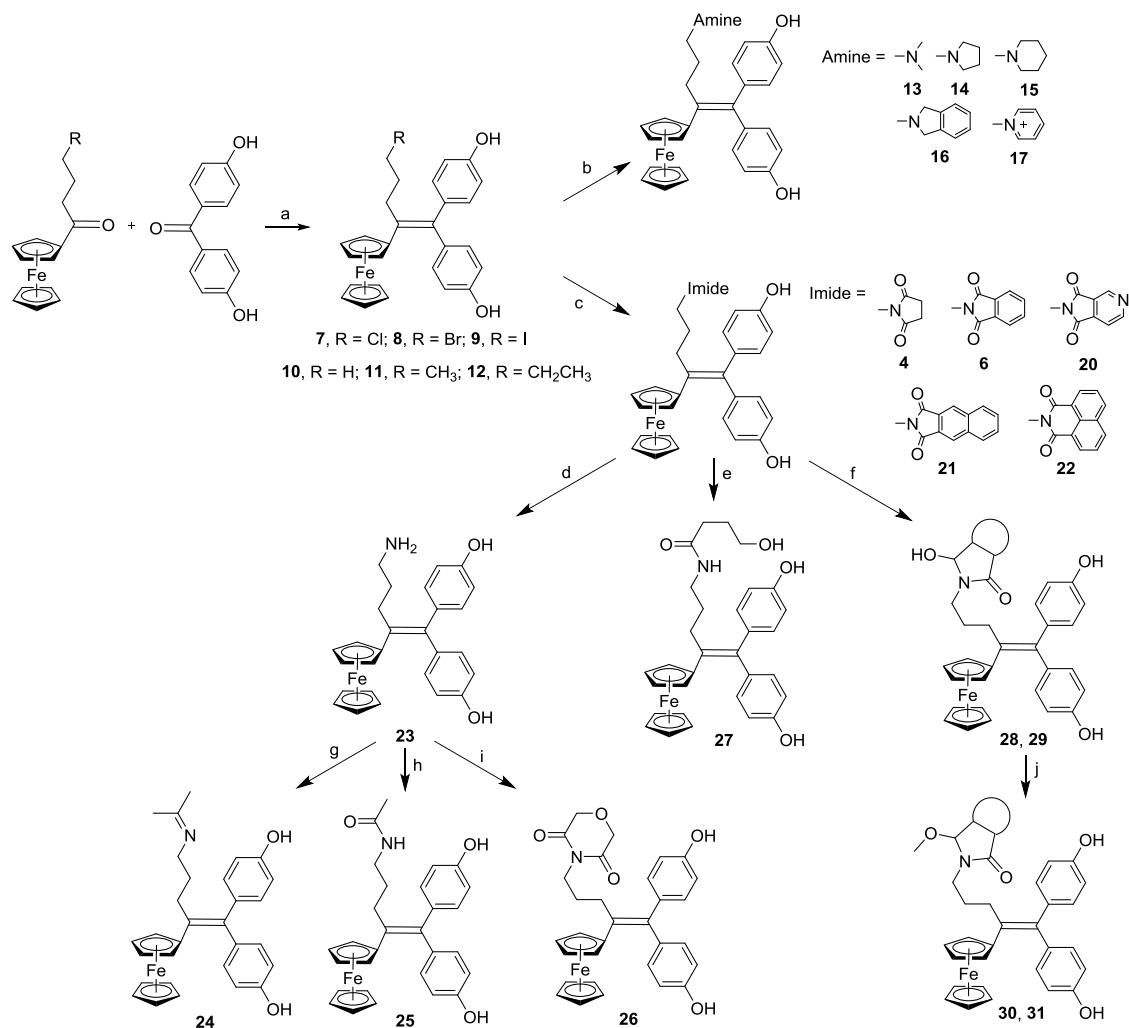
2.1 Synthesis and characterization of products

As shown in Scheme 3, the scaffold of the ferrociphenols was readily constructed by McMurry coupling of the appropriate ferrocenyl ketone and a suitable benzophenone; the iodo-ferrociphenol **9** was prepared in quantitative yield by displacement of the bromine atom of bromo-ferrociphenol **8** by action of KI; subsequent incorporation of the nitrogen-containing alkyl chain furnished the corresponding ferrociphenols via a nucleophilic displacement of the halide under basic conditions.[35, 36] Amongst the imido-ferrociphenols, hydrolysis of the phthalimido group of **6** in the presence of hydrazine hydrate gave **23** that now bears a primary amino group at the end of the alkyl chain. This compound reacted readily with acetone to yield imine **24** in 72% yield. Treatment of the amine **23** with

acetic anhydride delivered amide **25** in 95% yield, without acetylating the phenolic substituents. The primary amine **23** was also used to prepare other imides, such as the morpholine-dione derivative **26**, in 40% yield, by reaction with diglycolic anhydride (see Scheme 4, Scheme 5).

The selective reduction of only one carbonyl of the imido group of the succinimido- and phthalimido-ferrocenylphenols, **4** and **6** respectively, can be achieved with sodium borohydride in a short time (< 1 h), to give the α -hydroxylactams **28** and **29** in moderate yields. Under similar conditions, but with an increased amount of sodium borohydride for a longer time (2 days), the equilibrium favours formation of the ring-opened aldehyde-amide isomers of **28** (**29**). In this case, one can do a second reduction of the aldehyde to generate the alcohol-amide **27** in 93% yield, as we have done previously with other imides.[37] Formation of α -methoxylactam-ferrocenylphenols **30** and **31** from **28** and **29** in very high yield was catalyzed by *p*-toluenesulfonic acid.

The succinimido-alkyl and -acyl ferrocenes **38** and **39** (shown in Design III in Scheme 2, also in Table 3) were readily prepared from the appropriate ferrocenyl ketone intermediate via nucleophilic substitution and ketone reduction. The purely organic compound **34** was synthesized by McMurry coupling and nucleophilic displacement of halide by analogy to the preparation of **6**. In addition to all the standard spectroscopic data, several of these new ferrocenylphenols have also been unambiguously characterized by X-ray crystallography.



Scheme 3. Synthetic routes to target compounds. Reagents and conditions: a) Zn, TiCl₄, THF, reflux; b) amines, MeOH, reflux; c) imides, K₂CO₃, DMF, 60 or 80 °C; d) NH₂NH₂, EtOH, rt; e) NaBH₄, MeOH, 2 days; f) NaBH₄, MeOH, 45 mins; g) acetone, rt; h) acetic anhydride, pyridine, rt; i) diglycolic anhydride, TEA, toluene, reflux; j) MeOH, 4-toluenesulfonic acid, DCM, rt.

The molecular structures of the morpholino-imido-type ferrocidiphenol, **26**, and of the 4-succinimidobutylferrocene, **38**, are shown in Figure 2. In **26**, the ring oxygen is folded 52° out of the plane containing the nitrogen and four carbons of the imido group; more interestingly, the imido ring is oriented such that the interplanar angle between it and the neighbouring phenol is 62°, and the distance from the nearer carbonyl oxygen to the phenol ring plane is 3.724 Å. This may imply the existence of a lone pair- π (lp- π) interaction, somewhat weaker than those previously observed in imidopropyl-ferrocifenyl quinone methides.[36] In **38**, the ferrocenyl and succinimido moieties are maximally separated on the butyl chain.

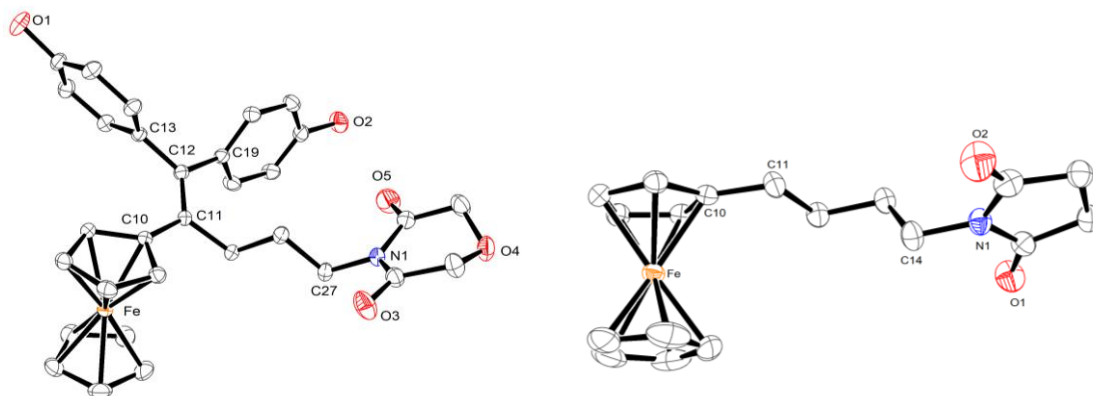


Figure 2. Molecular structures of complexes **26** (left) and **38** (right).

It is noteworthy that the X-ray crystallographic data for **21** revealed the existence of a dimeric structure, shown in Figure 3, whereby the two molecules are linked via hydrogen bonding between the phenols (Figure 4), which may be stabilized by the six-membered envelope conformation. The dimer forms a three-layer sandwich structure in which the naphthalene rings are almost parallel, as are the phenols (interplanar angles of 3.16° and 8.77° , respectively). Intriguingly, the distance of two phenolic oxygens (O3 and O8) to the aryl ring planes ranges from 3.18 to 3.93 Å, once again suggesting involvement of the increasingly invoked lp- π interaction, a phenomenon involving a stabilizing association between a lone pair of electrons and the face of a π system.[38-40]

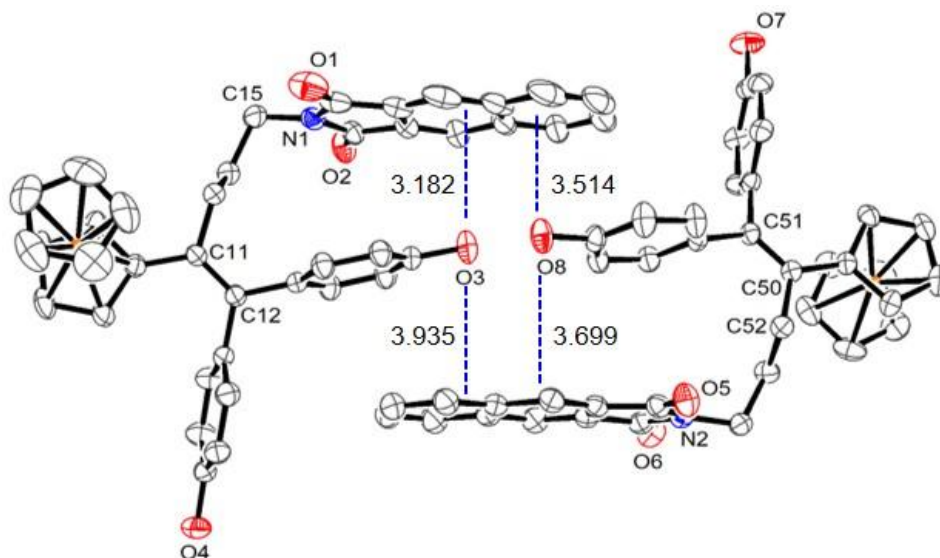


Figure 3. Molecular structure of the naphthalenedicarboximido-ferrocidiphenol, **21**, with probability ellipsoids shown at 50%; all distances in Å.

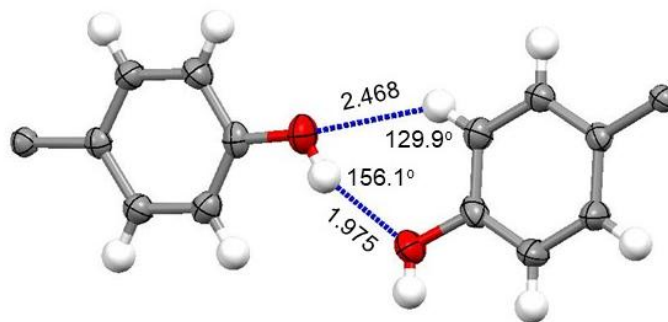


Figure 4. View of the dimer-forming interactions between the two phenols in **21**.

2.2 Anticancer and lipophilicity evaluation

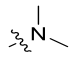
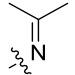
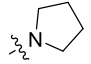
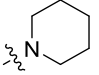
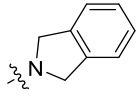
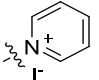
The anticancer tests on MDA-MB-231 cells have been performed via our usual in-house protocol. The cytotoxicity data of some known molecules from our library of ferrociphenols have also been included for comparison.[25] Recognizing the importance of imido-type heterocycles for increasing the antiproliferative activity of ferrocidiphenols, it was decided to replace the two carbonyl units of the imides by methylene groups, so as to form the corresponding cycloalkylamines. Moreover, we have also prepared ferrocifen derivatives with alkyl- or halogen- substituents in the chain. Bioactivity data for the different series of molecules are collected in Tables 1-3.

As shown in Table 1, the introduction of substituents lacking a nitrogen considerably lowers the cytotoxic activity of ferrocidiphenols. Only the simple propyl derivative, **10**, shows moderate antitumor activity comparable to that of its ethyl counterpart, **2**, the prototypical ferrocidiphenol; evidently, simple extension of the alkyl chain significantly weakens the cytotoxicity. The chloro-, bromo- and iodo-propyl ferrocidiphenols, **7-9**, show very similar potency with IC₅₀ values ranging from 2 to 4.5 μM. The comparable physical properties of these halides also led to similar lipophilicity values. Interestingly, positioning of a primary amine group at the terminus of the alkyl chain, as in **23**, prepared from the hydrolysis of the phthalimide complex, **6**, triggers a two-fold loss of activity compared to **6**. However, the cytotoxicity of the primary amine, **23**, is still much better than that of the corresponding n-butyl derivative, **11**, or the halogenated species **7-9**. Indeed, the presence of an aliphatic tertiary amino (or cycloalkylamino) functionality at the chain terminus, as in compounds **13-16**, brings about a strong antiproliferative effect against TNBC cells. The high polarity of tertiary amines improves the hydrophilicity of ferrocifens, as reflected in their lipophilicity values. We note, however, that in **17**,

which bears a terminal pyridinium moiety, antitumor activity is almost completely lost ($> 50 \mu\text{M}$), even though it exhibits similar lipophilicity to that of the related tertiary amines. Presumably, one can attribute this observed deactivation to the presence of the positive charge.

Table 1. Activity of several selected products ($\text{IC}_{50} \mu\text{M}$) on TNBC MDA-MB-231.

Product	R	Log Po/w	MDA-MB-231 ^a
4		4.0	0.035 ± 0.005^b
5		4.2	0.07 ± 0.01^b
6		4.8	0.145 ± 0.0005^b
10	H	--	0.83 ± 0.02
11		--	2.73 ± 0.25
12		--	5.19 ± 0.04
7	Cl	5.2	1.94 ± 0.43
8	Br	5.5	3.83 ± 0.05
9	I	5.8	4.52 ± 0.1
23		--	0.32 ± 0.04

13		1.4	0.59 ± 0.07
24		--	0.63 ± 0.06
14		1.6	0.53 ± 0.02
15		1.6	0.61 ± 0.03
16		3.5	0.75 ± 0.09
17		1.2	> 50

(a) Measured after 5 days of culture (mean of two independent experiments \pm SD); (b) Values taken from ref. 35.

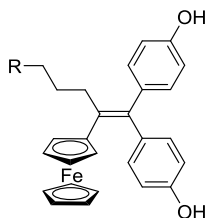
Having demonstrated that imido-type heterocycles exert a prominent role in the cytotoxicity of ferrociphenols, we decided to expand their range by implementing structural modifications of the imido moiety. It was found that increasing the ring size from succinimido, as in **4**, to glutarimido in **5**, resulted in a slight loss of activity.[35] Moreover, introduction of the morpholine-3,5-dione group, as in **26**, diminished its anticancer activity relative to **5** by a factor of three. Apparently, the fine tuning of the conformation of six-membered imide ring brought about by the presence of the extra oxygen affects the cytotoxicity of ferrociphenols.

Remarkably, the minor structural modification of incorporating a nitrogen atom into the phthalimido ring of **6**, as in **20**, lowers its antiproliferative effect by a factor of seventeen! This seems to indicate that the presence of nitrogen in the conjugated aromatic system affects the lp- π interaction in the QM scaffold, which has been identified as the potentially cytotoxic species. In this context, one can ask whether a more extended conjugated system might also have a negative influence on the lp- π interaction, thus weakening the antitumor behaviour of their precursors. To this end, the complexes **21** and **22**, which bear a linear 2,3-naphthalenedicarboximide and a tricyclic 1,8-naphthalimide at the end of the aliphatic chain, respectively, were prepared. 1,8-Naphthalimide compounds have received considerable recent attention;[41] they are known as DNA intercalators as a consequence of their

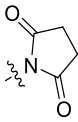
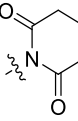
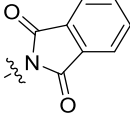
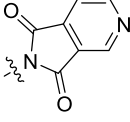
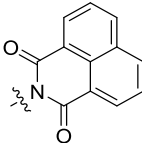
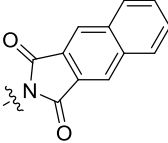
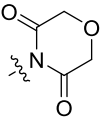
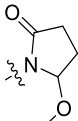
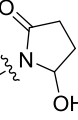
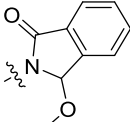
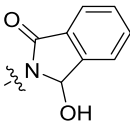
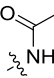
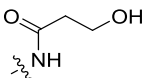
tricyclic planar structure, and several of them, in particular amonafide, elinafide, mitonafide and bisnafide, are in phase II clinical trials.[42, 43] Some naphthalimide derivatives linked to ferrocene have also been reported as having DNA binding activity.[44] However, in our current case, the introduction of naphthyl units did not improve the antiproliferativity of their ferrociphenols in comparison to other imido-ferrociphenols.

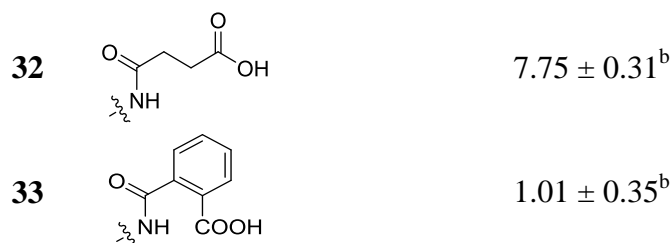
Cyclic amides are known to form α -hydroxylactams and ring opening analogues by reduction and hydrolysis respectively, which prompted us to synthesize the ferrociphenols **27** through **33** (Table 2). In the case of succinimide analogues, the transformation of one of the carbonyls to methoxy reduces its cytotoxicity (IC_{50} value increases from 0.035 μ M in **4** to 0.14 μ M in **30**). Meanwhile, **28**, in which a hydroxyl group is attached to the 2-pyrrolidone ring, shows even weaker antitumor activity. Furthermore, the methoxy, **31**, and hydroxy, **29**, counterparts of the phthalimido-ferrocidiphenol complex **6**, both displayed slightly weaker antiproliferative behaviour. Although the ring-opened products **32** and **33**, prepared from **4** and **6**, respectively, can only inhibit cellular growth at the micromolar level, perhaps due to the high polarity of the carboxylic acid substituent, the complexes **25** and **27** have IC_{50} μ M values in the sub-micromolar range. Despite their bioactivity being much worse than that of the succinimido-ferrocidiphenol, **4**, these compounds are still better than the historically first ferrocidiphenol, **2**, with its simple ethyl side-chain.

Table 2. Activity of a series of amide products (IC_{50} μ M) on TNBC MDA-MB-231.



Product	R	Log Po/w	MDA-MB-231 ^a
---------	---	----------	-------------------------

4		4.0	0.035 ± 0.005^b
5		4.2	0.07 ± 0.01^b
6		4.8	0.145 ± 0.0005^b
20		--	2.45 ± 0.15
22		5.3	0.40 ± 0.08
21		5.5	0.41 ± 0.05
26			0.22 ± 0.05
30			0.14 ± 0.02
28			0.82 ± 0.22
31			0.28 ± 0.02
29		4.4	0.27 ± 0.01
25			0.19 ± 0.07
27			0.31 ± 0.05

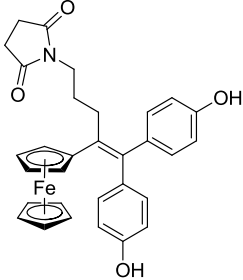
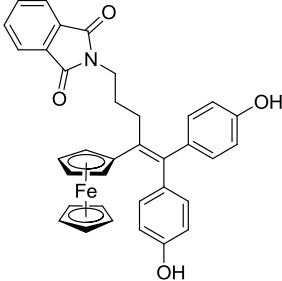
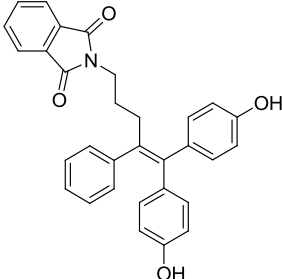
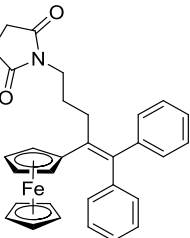
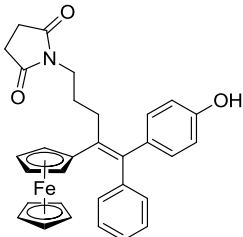
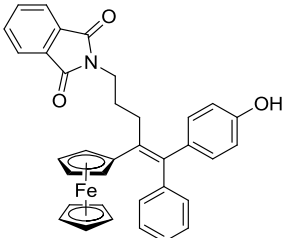


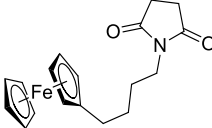
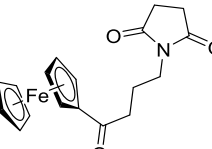
(a) Measured after 5 days of culture (mean of two independent experiments \pm SD); (b) Values taken from ref. 35.

In our previous reports, we have identified the [ferrocenyl-ene-*p*-phenol] motif as an indispensable pharmacophore as a result of its redox properties.[25, 26] In the case of ferrocidiphenols bearing imido heterocycles, replacement of ferrocenyl by phenyl reduces the activity very sharply, as in the purely organic compound **34** (Table 3). This result highlights the crucial role of the organometallic sandwich moiety in the bioactivity of ferrocifens.

It is noteworthy that the removal of one phenolic hydroxyl does not affect the anticancer effect, as in the succinimido-ferrociphenol, **36**, which possesses the lowest IC₅₀ value. At first sight, this observation appears to be incompatible with the initial discovery that all previously studied ferrociphenols exhibited a weaker anticancer effect than that of their corresponding di-phenol analogues, as in the ethylferrociphenols **2** and **3**. This latter fact can be rationalized in terms of the established requirement of the *trans*-ferrociphenol motif that is always available in the diphenols, whereas the monophenols exist as *cis/trans* mixtures.[45] The exceptional cytotoxicities of the mono- and di-phenolic succinimido complexes, **36** and **4**, respectively, emphasize the fact that their QMs have the strongest lp- π interaction among all imido-type analogues. Interestingly, even when there is no phenolic hydroxyl, as in the diphenyl system **35**, it still has moderate antiproliferative activity, lying in the sub-micromolar range. One might venture to suggest that this molecule can be transformed into a ferrociphenol inside cells, just as is well-established for tamoxifen whose potent antitumor activity is dependent on its *in vivo* conversion into hydroxytamoxifen.[46] Further simplification of the skeleton of ferrocidiphenols by removal of the aryl substituents, as for **38** and **39**, each of which possess only a ferrocenyl and succinimide group, very dramatically diminishes their cytotoxicities. All these observations again confirm the unique character of the [ferrocenyl-ene-*p*-phenol] motif as a paradigm of bioorganometallic versatility.

Table 3. Activity of products bearing a heterocycle (IC_{50} μ M) on TNBC MDA-MB-231.

Product	Structure	Log Po/w	MDA-MB-23 ^a
4		4.0	0.035 ± 0.005^b
6		4.8	0.145 ± 0.005^b
34		4.3	22.48 ± 1.26
35		--	0.79 ± 0.29
36		--	0.035 ± 0.015^c
37		--	0.41 ± 0.01^c

38		--	27.08 ± 1.42
39		--	> 50

(a) Measured after 5 days of culture (mean of two independent experiments \pm SD); (b) Values taken from ref. 35; (c) Values taken from ref. 36.

Inspired by the above results, the antiproliferative effects of certain molecules were also evaluated on other cancers including ER⁺ cancer (MCF-7), colorectal cancer (HCT116), melanoma (A-375), leukemia (K562), as well as ferroptosis-sensitive fibrosarcoma (HT1080) [47] (Table 4). Compounds **4** and **36** exhibited much stronger cytotoxicity than that of **14** on all the cancer cells tested, a result consistent with that observed on MDA-MB-231 cells. Together with the particularly high activity of diphenol complex **4** on leukemia cells, the monophenol complex **36** also showed high potency towards both colorectal cancer and melanoma cells. These results encouraged us to undertake further research to evaluate the drug-like properties of **36** as an optimal compound. Indeed, the higher lipophilicity of **36** (Log Po/w equals 4.4/4.8 for its two isomers, see Table 3) than that of **4** makes it more suitable for encapsulation into lipid nanocapsules (LNP), and in vivo studies with our collaborators will be presented in due course.

Table 4. IC₅₀ (μM) of selected molecules on other cell lines: ER⁺ cancer (MCF-7), colorectal cancer (HCT116), melanoma (A-375), leukemia (K562) and fibrosarcoma (HT1080).

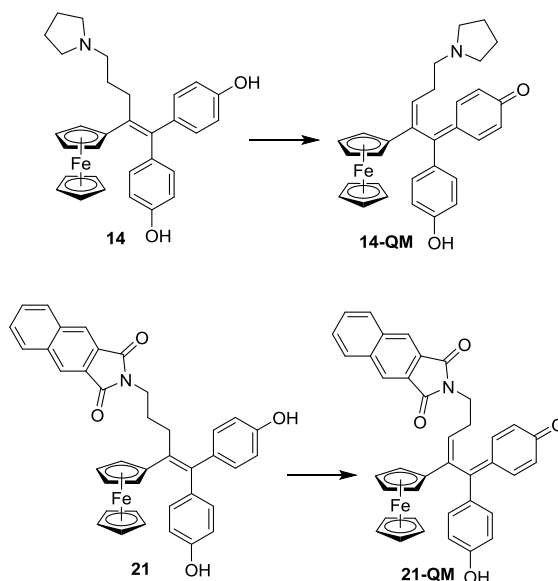
Compd.	MCF-7	HCT116	A-375	K562	HT1080
4	0.51 ± 0.15	0.14 ± 0.01^a	NT ^b	0.05 ± 0.01^a	7.45 ± 2.08
14	11.60 ± 1.07	16.66 ± 0.66	2.68 ± 0.25	> 20	NT ^b
36	0.31 ± 0.05	0.09 ± 0.04	0.02 ± 0.01	0.30 ± 0.08	9.23 ± 1.61

(a) Values taken from ref. 35; (b) NT: Not Tested.

2.3 Chemical oxidation of typical imido-ferrociphenol Compounds

One of the likely mechanisms that we have previously identified to explain the cytotoxic effect of ferrocenyl phenols on various cancer cells is based on their *in situ* transformation to electrophilic quinone methides (QM), which are potentially cytotoxic species.[25, 26] This process is mediated by the ferrocenyl group and allows QM formation to occur under comparatively mild (i.e. biologically relevant) oxidation conditions. We propose that the strong antiproliferative activity of **4** as a precursor compound is also related to QM formation inside cells. We have performed the chemical oxidation of **4** (by Ag₂O) to produce the vinyl quinone methide **4-QM** which showed superior stability profile and strong cytotoxicity.[36] This phenomenon drove us to explore the oxidation of more N-substituted ferrocifens. The elimination of the two carbonyl groups of the imide, in the case of **14**, evidently decreases the stability of the corresponding QMs. The degradation of **14-QM** was observed by NMR monitoring, but our attempts to isolate the subsequent products failed due to the poor solubility of **14** and its derivatives. As for the naphthyl derivatives **21** and **22**, which bear a larger conjugated system at the end of the chain, the corresponding QMs were obtained via chemical oxidation (see Scheme 4). The resulting QMs showed comparable stability profile to that of **4** and **6**, and might benefit from an lp- π interaction between the imido and quinone scaffolds.

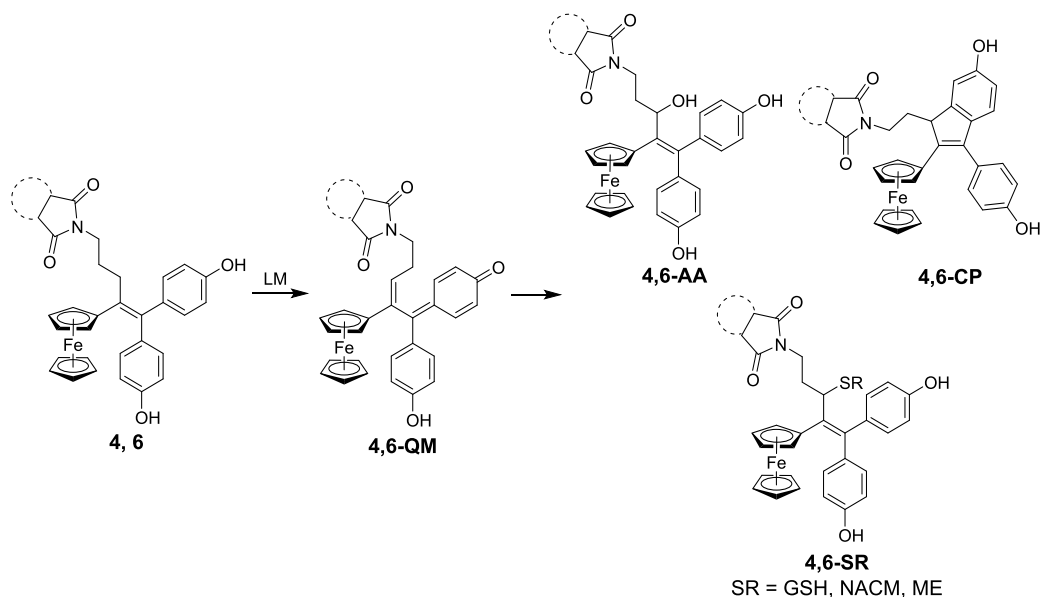
Interestingly, we observed that the oxidation of **21** takes a significantly longer time than for other ferrocifens; when its rate of QM formation using Ag₂O was monitored by NMR spectroscopy, it was found to be much slower than that of the succinimido and phthalimido complexes, **4** and **6**, ($t_{1/2} \approx 3500$ s for the former vs. $t_{1/2} \approx 120$ s for the latter two). This may account for the differences in toxicity obtained for **4**, **6** and **21** since QMs are considered to be a major factor in the high cytotoxicity of ferrocifens. The slowed rate of formation of **21-QM** may perhaps be rationalized by its X-ray crystallographically observed dimeric structure. The steric effect resulting from the presence of two bulky conjugated imido scaffolds, plus the intermolecular hydrogen bonding between the two phenols, could reduce the ability of the phenols to undergo proton abstraction, and then formation of phenoxy radical species, thereby decreasing the rate of QM formation.[48]



Scheme 4. The oxidation of **14** and **21** by Ag_2O .

2.4 Metabolism transformations

As noted in preliminary work, under similar oxidative conditions, the succinimido- and phthalimido quinone methides, **4-QM** and **6-QM**, were prepared; they exhibited a high stability profile and displayed strong antiproliferative effects.[36] To establish the metabolic behaviour of ferrocenylphenols bearing imido-type heterocycles, their transformation when treated with liver microsomes containing the main enzymes responsible for xenobiotic metabolism was studied. Incubation of the ferrocenylphenols **4** and **6** (100 μM) with an aerobic suspension of rat liver microsomes (1 μM cytochrome P450) in phosphate buffer (pH 7.4) containing 1 mM nicotinamide adenine dinucleotide phosphate (NADPH) for 30 min at 37 °C led to the formation of **4-QM** or **6-QM** that were detected by HPLC-MS. Their mass spectra (ESI) exhibited typical QM molecular ions at m/z $[\text{M}+\text{H}]^+$ 534 and 582, respectively, presumably attributable to protonation of the quinone oxygen atom. Furthermore, their UV/Vis spectra displayed characteristic vinyl QM behavior ($\lambda_{\text{max}} \sim 430$ nm). Formation of these QMs upon microsomal oxidation was also confirmed by comparison of their HPLC retention times and spectroscopic characteristics with those of authentic samples prepared by chemical oxidation.



Scheme 5. The metabolites obtained from **4/6** after incubation with rat liver microsomes and NADPH (+/- thiols).

Moreover, because of the high reactivity of QMs under physiological incubation of **4** and **6** with liver microsomes, a number of metabolites were detected by LC-MS. They included cyclized indene and allylic alcohols in approximately equivalent amounts, paralleling the metabolic behaviour of the ethyl-ferrociphenol **2**. In addition, the incubation of **4** and **6** with rat liver microsomes in the presence of NADPH and various thiols, such as glutathione (GSH), N-acetyl-*L*-cysteine methyl ester (NACM) or mercaptoethanol (ME) led to QM-thiol adducts, as well as the metabolites mentioned above (see Scheme 5). The approximate proportions of thiol conjugates formed relative to all metabolites varied from 30-60%. They were characterized by comparison of their HPLC, MS and UV properties with those previously reported for **2**, [29, 49] as shown in Table S4. We note that, under the same conditions, these metabolites were not generated in the absence of NADPH.

It is evident, not only that vinyl QMs are formed from the ferrocenyl diphenols **4** and **6** when treated with rat liver microsomes, but also that they can react with electrophiles under physiological conditions. The formation of **4/6-QM** inside cells, together with their superior stability established previously, may account for the excellent antiproliferative activity of their precursor diphenols, **4/6**.

2.5 ROS related bioactivity evaluation

It is known that the formation of ROS (Reactive Oxygen Species), via a Fenton-type reaction, play an important role in the cytotoxicity of ferrocifens. [25] Consequently, ROS generation was measured

after 10 mins incubation of MDA-MB-231 cells in the presence of several typical complexes (at 1 μ M). As shown in Figure 5, monophenol analogues produced much more ROS relative to their corresponding diphenols, in full accord with an earlier report.[30] This observation might be explained by a phenomenon that we have termed the *kronotropic* effect, whereby the ROS generated in cancer cells by ferrocifens could in turn interact with them in a feedback process, and so be consumed.[25] It is the base level of ROS in cancer cells that initiates the oxidation of Fe(II) to Fe(III), thereby triggering the sequence of reactions leading to the stepwise synthesis of quinone methides. However, in those species possessing two phenolic substituents in their molecular scaffold, their rate of oxidation is faster than that of monophenols and so may consume more ROS, as we have previously reported.[45, 48]

It is particularly noteworthy that only small amounts of ROS were generated in the case of the succinimido-ferrocidiphenol, **4**, and its corresponding monophenol, **37**, both of which display a very strong antiproliferative effect on breast cancer cells. We propose that this result could be related to the formation rate and the stability of their quinone methides, which are generated very quickly, and exhibit relatively long half-lives. Thus, in cancer cells the generation of ROS brings about the oxidation sequence whereby ferrocifens are oxidized to form quinone methides. Moreover, the ability of the QMs to undergo nucleophilic addition of cellular electrophiles plays a crucial role in their bioactivity.

Ferroptosis is an iron-dependent form of programmed cell death whose most significant features are the accumulation of ROS and lipid peroxidation products (LPO) [47]. Several pathways can induce ferroptosis, most of which act directly via using covalent inhibitors to bind glutathione peroxidase 4 (GPX4), a unique selenoprotein that can reduce lipid hydroperoxides and maintain the cellular redox balance [50]. Considering the importance of ROS in the cytotoxicity of ferrocifens and the potential nucleophilicity of the QMs, it is rational to envision the potential relationship of ferrocifens and ferroptosis. Thus, the ferroptosis-inducing activities of ferrocifens were determined on ferroptosis-sensitive HT1080 cells with or without ferrostatin-1 (fer-1), which is a specific ferroptosis inhibitor [47]. Primary screening was carried out for eight typical ferrocifen complexes at two concentrations (1 and 10 μ M, see Table S5). Unfortunately, although ferrocifens can inhibit the proliferation of HT1080 cells at micromolar level, these cytotoxicities cannot be reversed significantly by the ferroptosis inhibitor fer-1, as shown by the anticancer activities of **4** and **36**. These results indicated that the antiproliferative effect of ferrocifens may not be relevant with respect to ferroptosis,

probably the ROS induced by ferrocifen does not occur in a lipid environment. We proposed previously that ferrocifen can induce the inactivation or cell death by apoptosis or by the senescence pathway, depending on the dosages of organometallics [25].

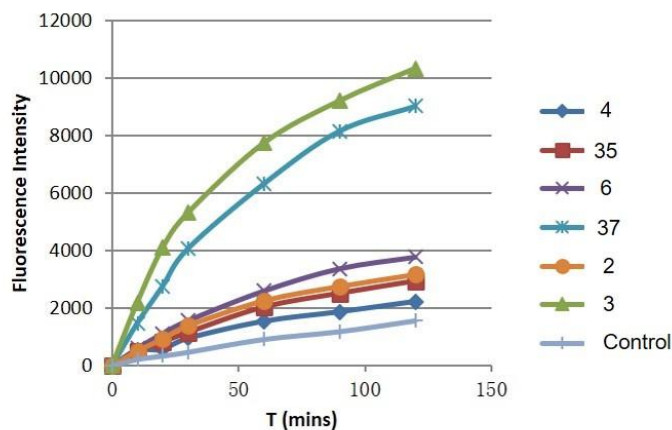
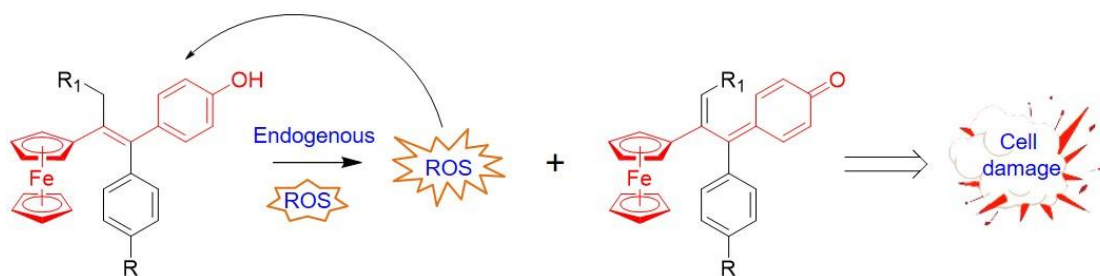


Figure 5. ROS measurements of typical compounds in MDA-MB-231 breast cancer cells.



Scheme 6. Illustration of the mechanism of action of ferrociphenols in cancer cells.

3. Conclusion

The ferrociphenol family is characterized by the presence of a [ferrocenyl-ene-*p*-phenol] redox motif that can be activated by ROS to generate an electrophilic quinone methide in cancer cells. Thus, ROS levels mediated by a Fenton reaction involving the redox versatility of ferrocene and the *in situ* formation of QMs are mainly responsible for the bioactivity of ferrociphenol. Since the latter process is a dominant factor, the formation rates of QMs and their stability profiles appear to play a crucial role (Scheme 6). With the aim of regulating the reactivity of ferrociphenols and the stability of their corresponding QMs, we have carried out a wide range of chemical modifications of the ferrociphenol scaffold, and have obtained a series of imido-ferrociphenols that exhibit particularly low IC₅₀ values on TNBC MDA-MB-231 cells. Extensive structural modification of the alkyl chain by attaching diversity-based nitrogen-containing substituents has been explored, together with a systematic SAR

study. This has shown that a suitable imido group, preferentially a small one, is required to maintain strong cytotoxicity. Chemical and enzymatic oxidation confirmed that vinyl-QMs are formed from imido-ferrociphenols under physiological conditions.

Furthermore, the X-ray crystal structure of naphthalenedicarboximido-ferrocidiphenol, **21**, revealed an interesting dimerization phenomenon; its slow oxidation to give **21-QM**, and only moderate antitumor activity, emphasizes the importance of QMs in the cytotoxicity of ferrociphenols. Overall, these results indicate that both the formation rate and the stability profile of the QMs strongly affect the antiproliferative activity of the corresponding ferrociphenol precursors. In-depth mechanistic research, and preclinical *in vivo* studies of representative compounds are currently being carried out in a collaborating laboratory;^[51] in particular, the immunological anticancer behaviour of succinimido-ferrocidiphenol, **4** and **36**.

4. Experiments

4.1 General Synthetic Methods. All reagents and solvents were obtained from commercial suppliers. THF was obtained by distillation from sodium/benzophenone. Thin layer chromatography (TLC) was performed on silica gel 60 GF₂₅₄. Column chromatography was performed on silica gel Merck 60 (40-63 μm). All NMR experiments (¹H, ¹³C, 2D) were carried out at room temperature on Bruker 300 and 400 NMR spectrometers. Mass spectrometry was performed with a Nermag R 10–10C spectrometer. HRMS measurements were performed on a Thermo Fischer LTQ-Orbitrap XL apparatus equipped with an electrospray source by IPCM (UMR 8232). Elemental analyses were performed by the microanalysis service of ICSN (Gif sur Yvette, France).

4.2 General procedure for McMurry coupling. Titanium chloride was added dropwise to a suspension of zinc powder in dry THF at 10-20 °C. The mixture was heated at reflux for 2 hours. A second solution was prepared by dissolving the two ketones in dry THF. This latter solution was added dropwise to the first solution and then the reflux was continued for the indicated time. After cooling to room temperature, the mixture was stirred with water and dichloromethane. The mixture was acidified with dilute hydrochloric acid until the dark color disappeared and was then decanted. The aqueous layer was extracted with dichloromethane and the combination of organic layers was dried on magnesium sulfate. After concentration under reduced pressure, the crude product was flash chromatographed on silica gel

column with the indicated eluent to afford the alkenes.

2-Ferrocenyl-1,1-bis-(4-hydroxyphenyl)-hex-1-ene, 11. Following the general McMurry coupling procedure, **11** was prepared using 1-ferrocenyl-pentan-1-one (0.582 g, 2.15 mmol), 4,4'-dihydroxybenzophenone (0.923 g, 4.3 mmol), zinc (0.845 g, 12.9 mmol), titanium(IV) chloride (2.044 g, 1.18 mL, 10.8 mmol), heating overnight, eluent dichloromethane/acetone 90/10, yield: 42%. ¹H NMR (CDCl₃): δ 0.78 (t, *J* = 7.3 Hz, 2H, CH₃), 1.12-1.35 (m, 4H, CH₂), 2.54 (t, *J* = 7.9 Hz, 2H, CH₂), 3.92 (t, *J* = 1.9 Hz, 2H, CH C₅H₄), 4.08 (t, *J* = 1.9 Hz, 2H, CH C₅H₄), 4.12 (s, 5H, Cp), 4.81 (s, 1H, OH), 4.86 (s, 1H, OH), 6.67 (d, *J* = 8.6 Hz, 2H, C₆H₄), 6.78 (d, *J* = 8.6 Hz, 2H, C₆H₄), 6.90 (d, *J* = 8.6 Hz, 2H, C₆H₄), 7.05 (d, *J* = 8.6 Hz, 2H, C₆H₄). ¹³C NMR (CDCl₃): δ 14.2 (CH₃), 23.2 (CH₂), 33.3 (CH₂), 35.0 (CH₂), 68.4 (2CH C₅H₄), 69.6 (5CH Cp), 69.7 (2CH C₅H₄), 88.2 (C C₅H₄), 115.3 (2CH C₆H₄), 115.4 (2CH C₆H₄), 131.1 (2CH C₆H₄), 131.7 (2CH C₆H₄), 135.7 (C), 137.7 (C), 137.8 (C), 138.1 (C), 154.1 (C), 154.2 (C). MS (CI, NH₃) *m/z* : 453 [M+H]⁺. HRMS (ESI, C₂₈H₂₈FeO₂: [M]⁺) calcd: 452.1439, found: 452.1448.

2-Ferrocenyl-1,1-bis-(4-hydroxyphenyl)-hept-1-ene, 12. Analogously, **12** was prepared using 1-ferrocenyl-hexan-1-one (1.17 g, 4.12 mmol), 4,4'-dihydroxybenzophenone (0.882 g, 4.1 mmol), zinc (1.615 g, 24.7 mmol), titanium(IV) chloride (3.124 g, 1.81 mL, 16.5 mmol), heating overnight, eluent dichloromethane/acetone 90/10, yield: 32%. ¹H NMR (acetone-d₆): δ 0.85 (t, *J* = 8.0 Hz, 2H, CH₃), 1.19-1.30 (m, 4H, CH₂), 1.47-1.59 (m, 2H, CH₂), 2.66 (t, *J* = 8.0 Hz, 2H, CH₂), 3.95 (t, *J* = 1.9 Hz, 2H, CH C₅H₄), 4.09 (t, *J* = 1.9 Hz, 2H, CH C₅H₄), 4.15 (s, 5H, Cp), 6.74 (d, *J* = 8.7 Hz, 2H, C₆H₄), 6.85 (d, *J* = 8.7 Hz, 2H, C₆H₄), 6.90 (d, *J* = 8.7 Hz, 2H, C₆H₄), 7.09 (d, *J* = 8.7 Hz, 2H, C₆H₄), 8.26 (s, 1H, OH), 8.29 (s, 1H, OH). ¹³C NMR (acetone-d₆): δ 15.1 (CH₃), 23.8 (CH₂), 31.9 (CH₂), 33.5 (CH₂), 36.2 (CH₂), 69.3 (2CH C₅H₄), 70.6 (5CH Cp), 70.7 (2CH C₅H₄), 89.3 (C C₅H₄), 116.5 (2x2CH C₆H₄), 132.1 (2CH C₆H₄), 132.5 (2CH C₆H₄), 136.2 (C), 138.0 (C), 138.3 (C), 139.8 (C), 157.3 (C), 157.4 (C). MS (CI, NH₃) *m/z* : 467 [M+H]⁺. HRMS (ESI, C₂₉H₃₀FeO₂: [M]⁺) calcd: 466.1595, found: 466.1603.

5-Bromo-2-ferrocenyl-1,1-bis-(4-hydroxyphenyl)-pent-1-en, 8. Similarly, using 4-bromo-1-ferrocenyl-butan-1-one (7.5 g, 22.39 mmol), 4,4'-dihydroxybenzophenone (5.995 g, 28

mmol), zinc (8.781 g, 134.3 mmol), titanium(IV) chloride (16.988 g, 9.84 mL, 89.5 mmol), heating overnight, eluent dichloromethane/acetone 90/10, yield: 71%. ¹H NMR (acetone-d₆): δ 1.96-2.10 (m, 2H, CH₂), 2.83 (t, *J* = 7.9 Hz, 2H, CH₂), 3.38-3.49 (m, 2H, CH₂Br), 3.99 (t, *J* = 1.9 Hz, 2H, CH C₅H₄), 4.11 (t, *J* = 1.9 Hz, 2H, CH C₅H₄), 4.17 (s, 5H, Cp), 6.72 (d, *J* = 8.7 Hz, 2H, C₆H₄), 6.84 (d, *J* = 8.7 Hz, 2H, C₆H₄), 6.88 (d, *J* = 8.7 Hz, 2H, C₆H₄), 7.07 (d, *J* = 8.7 Hz, 2H, C₆H₄), 8.73 (s, 1H, OH), 8.77 (s, 1H, OH). ¹³C NMR (acetone-d₆): δ 35.1 (CH₂), 35.3 (CH₂), 35.8 (CH₂), 69.5 (2CH C₅H₄), 70.6 (5CH Cp), 70.7 (2CH C₅H₄), 89.2 (C C₅H₄), 116.5 (2CH C₆H₄), 116.8 (2CH C₆H₄), 132.0 (2CH C₆H₄), 132.5 (2CH C₆H₄), 134.6 (C), 137.6 (C), 138.0 (C), 140.8 (C), 157.6 (2C). MS (EI, 70 eV) *m/z* : 516 [M]⁺, 437, 371, 343, 286. HRMS (ESI, C₂₇H₂₅BrFeO₂: [M]⁺) calcd: 516.0387, found: 516.0405.

2-Ferrocenyl-1,1-bis-(4-hydroxyphenyl)-5-iodo-pent-1-ene, 9. Bromo compound **8** (3.04 g, 5.88 mmol) was heated overnight in a mixture of acetone and potassium iodide (22.44 g, 135.2 mmol). After cooling, the mixture was evaporated then was poured into water and extracted with diethyl ether twice. After drying on magnesium sulfate, the solvent was removed to give pure **9** as an orange solid in a quantitative yield. ¹H NMR (acetone-d₆): δ 1.95-2.06 (m, 2H, CH₂), 2.81 (t, *J* = 8.0 Hz, 2H, CH₂), 3.21 (m, 3H, CH₂I), 4.01 (t, *J* = 1.9 Hz, 2H, CH C₅H₄), 4.11 (t, *J* = 1.9 Hz, 2H, CH C₅H₄), 4.18 (s, 5H, Cp), 6.75 (d, *J* = 8.7 Hz, 2H, C₆H₄), 6.87 (d, *J* = 8.7 Hz, 2H, C₆H₄), 6.90 (d, *J* = 8.7 Hz, 2H, C₆H₄), 7.09 (d, *J* = 8.7 Hz, 2H, C₆H₄), 8.30 (s, 1H, OH), 8.35 (s, 1H, OH). ¹³C NMR (acetone-d₆): δ 30.9 (CH₂), 36.0 (CH₂), 37.4 (CH₂), 69.4 (2CH C₅H₄), 70.5 (5CH Cp), 70.6 (2CH C₅H₄), 89.2 (C C₅H₄), 116.5 (2CH C₆H₄), 116.8 (2CH C₆H₄), 131.9 (2CH C₆H₄), 132.5 (2CH C₆H₄), 134.3 (C), 137.5 (C), 137.9 (C), 140.8 (C), 157.5 (C). MS (EI, 70 eV) *m/z* : 564 [M]⁺, 436 [M-HI]⁺. HRMS (ESI, C₂₇H₂₅FeIO₂: [M]⁺) calcd: 564.0249, found: 564.0236.

5-Amino-2-ferrocenyl-1,1-bis-(4-hydroxyphenyl)-pent-1-ene, 23. Phthalimide **6** (0.4 g, 0.686 mmol), hydrazine monohydrate (0.275 g, 0.27 mL, 5.5 mmol) and ethanol (60 mL) were stirred at r. t. for 24 hours. The mixture was poured into water, extracted twice with ethyl acetate then was dried over magnesium sulfate. The residue was recrystallized from methanol to afford pure **23** as an orange solid in a 73% yield. ¹H NMR (DMSO-d₆): δ 1.40-1.59 (m, 2H, -CH₂-CH₂-CH₂-N), 2.32-2.47 (m, 4H, -CH₂-C= + CH₂N), 3.81 (s, 2H, C₅H₄), 4.06 (s, 2H, C₅H₄), 4.10 (s, 5H, Cp), 4.63-5.75 (s very broad, 4H, OH +

NH₂), 6.63 (d, *J* = 8.2 Hz, 2H, C₆H₄), 6.71 (d, *J* = 8.2 Hz, 2H, C₆H₄), 6.78 (d, *J* = 8.1 Hz, 2H, C₆H₄), 6.95 (d, *J* = 8.1 Hz, 2H, C₆H₄). ¹³C NMR (DMSO-d₆): δ 31.6 (CH₂), 34.4 (CH₂), 41.6 (CH₂), 67.6 (2CH C₅H₄), 68.8 (2CH C₅H₄), 68.9 (5CH Cp), 86.8 (C C₅H₄), 114.9 (2CH C₆H₄), 115.0 (2CH C₆H₄), 129.9 (2CH C₆H₄), 130.3 (2CH C₆H₄), 133.7 (C), 135.3 (C), 135.7 (C), 137.8 (C), 155.6 (C), 155.7 (C). HRMS (ESI, C₂₇H₂₈FeNO₂: [M+H]⁺) calcd: 454.1464, found: 454.1461.

***N*-[4-ferrocenyl-5,5-bis-(4-hydroxyphenyl)-pent-4-enyl]-2-propanimine, 24.** The same method as for **23** was followed, but in place of pouring the mixture into water, it was poured into acetone. After evaporation under reduced pressure, the mixture was chromatographed on a silica gel column with acetone as the eluent to furnish pure **24** as an orange solid in a 72% yield. ¹H NMR (DMSO-d₆): δ 1.55-1.67 (m, 2H, -CH₂-CH₂-CH₂-N), 1.69 (s, 3H, Me), 1.87 (s, 3H, Me), 2.52-2.60 (m, 2H, -CH₂-C=), 3.00 (t, *J* = 7.0 Hz, 2H, CH₂N), 3.86 (t, *J* = 1.9 Hz, 2H, C₅H₄), 4.06 (t, *J* = 1.9 Hz, 2H, C₅H₄), 4.09 (s, 5H, Cp), 6.62 (d, *J* = 8.1 Hz, 2H, C₆H₄), 6.70 (d, *J* = 7.9 Hz, 2H, C₆H₄), 6.77 (d, *J* = 7.9 Hz, 2H, C₆H₄), 6.95 (d, *J* = 8.1 Hz, 2H, C₆H₄), 9.17 (s broad, 2H, OH). ¹³C NMR (DMSO-d₆): δ 17.9 (CH₃), 28.7 (CH₃), 31.5 (CH₂), 32.0 (CH₂), 50.6 (CH₂), 67.7 (2CH C₅H₄), 68.7 (2CH C₅H₄), 68.9 (5CH Cp), 87.0 (C C₅H₄), 114.9 (2CH C₆H₄), 115.0 (2CH C₆H₄), 129.9 (2CH C₆H₄), 130.3 (2CH C₆H₄), 133.7 (C), 135.3 (C), 135.7 (C), 137.9 (C), 155.5 (C), 155.6 (C), 165.4 (C=N). HRMS (ESI, C₃₀H₃₂FeNO₂: [M+H]⁺) calcd: 494.1777, found: 494.1772.

***N*-{4-ferrocenyl-5,5-bis-(4-hydroxyphenyl)-pent-4-enyl}pyridinium iodide, 17.** Compound **9** (1.049 g, 1.86 mmol) was dissolved in dry tetrahydrofuran and pyridine (0.588 g, 0.6 mL, 7.4 mmol) was added. The solution was heated for 5 hours, cooled to room temperature then the solid was filtered off and rinsed with acetone. After drying, **17** was obtained as an orange solid with a 61% yield. Mp : 224 °C. ¹H NMR (DMSO D₆): δ 1.94-2.16 (m, 2H, CH₂), 2.34-2.48 (m, 2H, CH₂), 3.83 (s, 2H, C₅H₄), 4.10 (s, 7H, Cp + C₅H₄), 4.55 (t, *J* = 6.0 Hz, 2H, CH₂N), 6.58 (d, *J* = 8.4 Hz, 2H, C₆H₄), 6.61 (d, *J* = 8.4 Hz, 2H, C₆H₄), 6.75 (d, *J* = 8.4 Hz, 2H, C₆H₄), 6.83 (d, *J* = 8.4 Hz, 2H, C₆H₄), 8.05 (dd, *J* = 8.5, 7.6 Hz, 2H, pyridinium), 8.56 (t, *J* = 7.6 Hz, 1H, pyridinium), 8.91 (s, 1H, OH), 8.93 (s, 1H, OH), 9.29 (t, *J* = 8.5 Hz, 2H, pyridinium). ¹³C NMR (DMSO D₆): δ 30.2 (CH₂), 31.6 (CH₂), 60.8 (CH₂), 67.9 (2CH, C₅H₄), 68.6 (2CH, C₅H₄), 69.0 (5CH, Cp), 86.2 (C, C₅H₄), 115.0 (2CH, C₆H₄), 115.2 (2CH, C₆H₄), 127.9 (2CH,

pyridinium), 129.5 (2CH, C₆H₄), 130.2 (2CH, C₆H₄), 132.0 (C), 134.6 (C), 135.1 (C), 138.7 (C), 144.5 (2CH, pyridinium), 145.2 (CH, pyridinium), 155.6 (C), 155.8 (C). IR (KBr, ν cm⁻¹): 3425 (OH), 3261, 3200 (CH, CH₂). HRMS (ESI, C₃₂H₃₀FeNO₂) calcd: 516.162593, found: 516.16164.

General procedure for synthesis of amines 13-16. Compound **7** or **9** was transferred into a pressure tube with the corresponding amine and methanol. The mixture was heated at 60 °C for 24 h and then cooled to room temperature. The solution was concentrated under reduced pressure, dissolved in dichloromethane, washed with a solution of saturated sodium hydrogen carbonate then with water, dried on magnesium sulfate and concentrated under reduced pressure. The crude mixture was chromatographed on silica gel column using acetone/trimethylamine 90/10 as the eluent. Compounds were crystallized from acetone to obtain pure orange solids.

2-Ferrocenyl-1,1-bis-(4-hydroxyphenyl)-5-dimethylamino-pent-1-ene, 13. Accordingly, compound **7** (0.452 g, 0.96 mmol), commercial 2 M solution of dimethylamine in methanol (4.8 mL, 9.6 mmol), 36% yield. mp: 218 °C. ¹H NMR (DMSO-d₆): δ 1.46-1.61 (m, 2H, CH₂), 2.02 (s, 6H, NMe₂), 2.12 (t, J = 8.0 Hz, 2H, CH₂), 3.46-3.54 (m, 2H, CH₂N), 3.85 (t, J = 1.9 Hz, 2H, C₅H₄), 4.11 (t, J = 1.9 Hz, 2H, C₅H₄), 4.14 (s, 5H, Cp), 6.65 (d, J = 8.7 Hz, 2H, C₆H₄), 6.74 (d, J = 8.7 Hz, 2H, C₆H₄), 6.81 (d, J = 8.7 Hz, 2H, C₆H₄), 7.00 (d, J = 8.7 Hz, 2H, C₆H₄), 9.33 (s broad, 2H, OH). ¹³C NMR (DMSO-d₆): δ 29.1 (CH₂), 32.9 (CH₂), 45.9 (NMe₂), 60.1 (CH₂N), 68.7 (2CH, C₅H₄), 69.6 (2CH, C₅H₄), 69.9 (5CH, Cp), 87.9 (C, C₅H₄), 116.0 (2X2CH, C₆H₄), 130.9 (2CH, C₆H₄), 131.3 (2CH, C₆H₄), 134.7 (C), 136.3 (C), 136.6 (C), 138.8 (C), 156.5 (C), 156.6 (C). IR (KBr, ν cm⁻¹): 3398 (OH). MS (CI, NH₃) m/z : 482 [M+H]⁺. HRMS (ESI, C₂₉H₃₁FeNO₂: [M]⁺) calcd: 481.1704, found: 481.1689. Anal. Calcd for C₂₉H₃₁FeNO₂(H₂O)_{1.25}: C, 69.12; H, 6.70; N, 2.77. Found: C, 68.99; H, 6.57; N, 2.65.

N-{4-ferrocenyl-5,5-bis-(4-hydroxyphenyl)-pent-4-enyl}pyrrolidine, 14. Analogously, compound **7** (1.46 g, 3.09 mmol), pyrrolidine (2.196 g, 2.58 mL, 30.9 mmol), 77% yield. Mp: 216 °C. ¹H NMR (DMSO-d₆): δ 1.45-1.65 (m, 6H, CH₂), 2.16-2.33 (m, 6H, CH₂), 2.46-2.59 (m, 2H, CH₂N), 3.81 (t, J = 1.9 Hz, 2H, CH C₅H₄), 4.07 (t, J = 1.9 Hz, 2H, CH C₅H₄), 4.10 (s, 5H, Cp), 6.61 (d, J = 8.5 Hz, 2H, C₆H₄), 6.71 (d, J = 8.5 Hz, 2H, C₆H₄), 6.76 (d, J = 8.5 Hz, 2H, C₆H₄), 6.95 (d, J = 8.5 Hz, 2H, C₆H₄),

9.27 (s broad, 2H, OH). ^{13}C NMR (DMSO- d_6): δ 23.0 (2CH₂), 29.4 (CH₂), 32.1 (CH₂), 53.4 (CH₂NCH₂), 55.6 (CH₂N), 67.7 (2CH C₅H₄), 68.7 (2CH C₅H₄), 68.9 (5CH Cp), 87.0 (C C₅H₄), 114.9 (2CH C₆H₄), 115.0 (2CH C₆H₄), 130.0 (2CH C₆H₄), 130.4 (2CH C₆H₄), 133.7 (C), 135.3 (C), 135.7 (C), 137.8 (C), 155.6 (2C). IR (KBr, ν cm⁻¹): 3420 (OH). HRMS (ESI, C₃₁H₃₄FeNO₂: [M+H]⁺) calcd: 508.19335, found: 508.19270. Anal. Calcd for C₃₁H₃₃FeNO₂(H₂O)_{0.75}: C, 71.47; H, 6.67; N, 2.69. Found: C, 71.44; H, 6.35; N, 2.47.

***N*-{4-ferrocenyl-5,5-bis-(4-hydroxyphenyl)-pent-4-enyl}piperidine, 15.** Compound **7** (1.23 g, 2.6 mmol), piperidine (2.215 g, 2.57 mL, 26 mmol), 87% yield. Mp: 197 °C. ^1H NMR (DMSO- d_6): δ 1.27-1.65 (m, 10 H, CH₂), 2.15-2.33 (m, 6H, CH₂N), 3.83 (s broad, 2H, CH C₅H₄), 4.06 (s broad, 2H, CH C₅H₄), 4.10 (s, 5H, Cp), 6.62 (d, J = 8.3 Hz, 2H, C₆H₄), 6.71 (d, J = 8.3 Hz, 2H, C₆H₄), 6.77 (d, J = 8.3 Hz, 2H, C₆H₄), 6.96 (d, J = 8.3 Hz, 2H, C₆H₄), 9.34 (s very broad, 2H, OH). ^{13}C NMR (DMSO- d_6): δ 23.7 (CH₂), 25.0 (2CH₂), 26.9 (CH₂), 31.9 (CH₂), 53.5 (CH₂NCH₂), 57.9 (CH₂N), 67.7 (2CH C₅H₄), 68.7 (2CH C₅H₄), 68.9 (5CH Cp), 86.9 (C C₅H₄), 115.0 (2X2CH C₆H₄), 129.9 (2CH C₆H₄), 130.3 (2CH C₆H₄), 133.5 (C), 135.2 (C), 135.6 (C), 138.0 (C), 155.7 (2C). IR (KBr, ν cm⁻¹): 3388 (OH). HRMS (ESI, C₃₂H₃₆FeNO₂: [M+H]⁺) calcd: 522.20900, found: 522.20832. Anal. Calcd for C₃₂H₃₅FeNO₂(H₂O): C, 71.24; H, 6.91; N, 2.59. Found: C, 71.57; H, 6.90; N, 2.83.

***N*-{4-ferrocenyl-5,5-bis-(4-hydroxyphenyl)-pent-4-enyl}isoindoline, 16.** Compound **9** (0.655 g, 1.16 mmol), isoindoline (0.24 g, 2 mmol), 39% yield. Mp: 203 °C. ^1H NMR (DMSO- d_6): δ 1.56-1.76 (m, 2H, CH₂), 2.54-2.74(m, 4H, CH₂), 3.64 (s, 4H, CH₂), 3.86 (t, J = 1.7 Hz, 2H, C₅H₄), 4.08 (t, J = 1.7 Hz, 2H, C₅H₄), 4.11 (s, 5H, Cp), 6.63 (d, J = 8.7 Hz, 2H, C₆H₄), 6.75 (d, J = 8.5 Hz, 2H, C₆H₄), 6.79 (d, J = 8.7 Hz, 2H, C₆H₄), 7.01 (d, J = 8.5 Hz, 2H, C₆H₄), 7.19 (s, 4H, isoindoline). ^{13}C NMR (DMSO- d_6): δ 28.9 (CH₂), 31.8 (CH₂), 54.9 (CH₂), 57.9 (2CH₂, isoindoline), 67.7 (2CH, C₅H₄), 68.7 (2CH, C₅H₄), 68.9 (5CH, Cp), 86.9 (C, C₅H₄), 114.97 (2CH, C₆H₄), 115.03 (2CH, C₆H₄), 122.0 (2CH, isoindoline), 126.6 (2CH, isoindoline), 130.0 (2CH, C₆H₄), 130.3 (2CH, C₆H₄), 133.6 (C), 135.3 (C), 135.6 (C), 137.9 (C), 139.4 (2C, isoindoline), 155.6 (2C). IR (KBr, ν cm⁻¹): 3420 (OH). HRMS (ESI, C₃₅H₃₄FeNO₂: [M+H]⁺) calcd: 556.19335, found: 556.19305. Anal. Calcd for C₃₅H₃₃FeNO₂(H₂O)₂: C, 71.06; H, 6.30; N, 2.37. Found: C, 71.24; H, 6.04; N, 2.15.

5-*N*-acetamido-2-ferrocenyl-1,1-bis-(4-hydroxyphenyl)-pent-1-ene, 25. Compound **23** (0.13 g, 0.287 mmol) was dissolved into dry tetrahydrofuran and pyridine (0.136 g, 0.14 mL, 1.7 mmol) was added. Acetic anhydride (0.176 g, 0.16 mL, 1.7 mmol) was added and the solution was stirred overnight. After concentration under reduced pressure, the residue was chromatographed on a silica gel column with acetone as the eluent. The solid was recrystallized from acetone to furnish pure **25** as an orange solid in a 95% yield. ¹H NMR (DMSO-*d*₆): δ 1.45-1.61 (m, 2H, -CH₂-CH₂-CH₂-N), 1.75 (s, 3H, Me), 2.41-2.54 (m, 2H, -CH₂-C=), 2.88 (q, *J* = 6.6 Hz, 2H, CH₂N), 3.80 (t, *J* = 1.9 Hz, 2H, C₅H₄), 4.06 (t, *J* = 1.9 Hz, 2H, C₅H₄), 4.10 (s, 5H, Cp), 6.62 (d, *J* = 8.5 Hz, 2H, C₆H₄), 6.71 (d, *J* = 8.5 Hz, 2H, C₆H₄), 6.77 (d, *J* = 8.5 Hz, 2H, C₆H₄), 6.94 (d, *J* = 8.5 Hz, 2H, C₆H₄), 7.72 (t, *J* = 5.7 Hz, 1H, NH), 9.28 (s, 1H, OH), 9.32 (s, 1H, OH). ¹³C NMR (DMSO-*d*₆): δ 22.6 (Me), 30.5 (CH₂), 31.8 (CH₂), 38.6 (CH₂), 67.7 (2CH, C₅H₄), 68.7 (2CH, C₅H₄), 69.0 (5CH, Cp), 86.5 (C, C₅H₄), 115.0 (2x2CH, C₆H₄), 129.9 (2CH, C₆H₄), 130.3 (2CH, C₆H₄), 133.3 (C), 135.3 (C), 135.6 (C), 138.0 (C), 155.6 (C), 155.7 (C), 168.9 (CO).

General procedure for the synthesis of imides 20, 21, 22 and 34. A mixture of potassium carbonate and imide in dimethylformamide (DMF) was heated at 60-80 °C for 15 min. Halogenated compound was added and the stirring was continued at 60 or 80 °C overnight. The mixture was cooled to room temperature, was poured into a diluted hydrochloric acid solution, was extracted with diethyl ether, then the organic layer was dried on magnesium sulfate and concentrated under reduced pressure. The residue was purified by flash-chromatography to afford the imide.

N-{4-ferrocenyl-5,5-bis-(4-hydroxyphenyl)-pent-4-enyl}-3,4-pyridinedicarboximide, 20. This compound was synthesized using the general procedure for the synthesis of imides using compound **7** (2.59 g, 5.48 mmol), potassium carbonate (1.514 g, 11 mmol), 3,4-pyridinedicarboximide (1.217 g, 8.2 mmol), temperature 80 °C, overnight, 24% yield. ¹H NMR (acetone-*d*₆): δ 1.82-1.97 (m, 2H, CH₂), 2.60-2.72 (m, 2H, CH₂=), 3.61 (t, *J* = 6.6 Hz, 2H, CH₂N), 3.92 (t, *J* = 1.9 Hz, 2H, C₅H₄), 4.05 (t, *J* = 1.9 Hz, 2H, C₅H₄), 4.09 (s, 5H, Cp), 6.58 (d, *J* = 8.5 Hz, 2H, C₆H₄), 6.68 (d, *J* = 8.5 Hz, 2H, C₆H₄), 6.84 (d, *J* = 8.5 Hz, 2H, C₆H₄), 6.93 (d, *J* = 8.5 Hz, 2H, C₆H₄), 7.79 (d, *J* = 4.7 Hz, 1H, pyridine), 8.22 (s broad, 1H, OH), 8.41 (s broad, 1H, OH), 9.05 (s, 1H, pyridine), 9.08 (d, *J* = 4.7 Hz, 1H, pyridine). ¹³C

NMR (acetone- d_6): δ 30.5 (CH₂), 33.0 (CH₂), 38.8 (CH₂), 68.6 (2CH C₅H₄), 69.8 (5CH Cp), 69.9 (2CH C₅H₄), 88.1 (C C₅H₄), 116.7 (2x2CH C₆H₄), 117.4 (CH pyridine), 127.0 (C pyridine), 130.9 (2CH C₆H₄), 131.6 (2CH C₆H₄), 134.2 (C), 136.5 (C), 137.0 (C), 139.7 (C), 140.3 (C), 144.6 (CH pyridine), 156.5 (C + CH pyridine), 156.8 (C), 167.6 (CO), 168.0 (CO).

5-(1,8-naphthalimido)-2-ferrocenyl-1,1-bis-(4-hydroxyphenyl)-pent-1-en, 22. This compound was synthesized using the general procedure for the synthesis of imides using compound **9** (2.821 g, 5 mmol), potassium carbonate (1.382 g, 10 mmol), 1,8-naphthalimide (1.479 g, 7.5 mmol), temperature 60 °C, 3 days, 67% yield. Mp: 228 °C. ¹H NMR (DMSO- d_6): δ 1.73-1.92 (m, 2H, CH₂), 2.59 (t, J = 7.6 Hz, 2H, CH₂), 3.78 (t, J = 1.7 Hz, 2H, C₅H₄), 3.96 (t, J = 7.4 Hz, 2H, CH₂N), 4.01 (s broad, 7 H, Cp + C₅H₄), 6.60 (d, J = 8.3 Hz, 2H, C₆H₄), 6.61 (d, J = 8.3 Hz, 2H, C₆H₄), 6.77 (d, J = 8.3 Hz, 2H, C₆H₄), 6.92 (d, J = 8.3 Hz, 2H, C₆H₄), 7.86 (t, J = 7.7 Hz, 2H, imide), 8.45 (d, J = 7.7 Hz, 2H, imide), 8.49 (d, J = 7.7 Hz, 2H, imide), 9.19 (s, 1H, OH), 9.27 (s, 1H, OH). ¹³C NMR (DMSO- d_6): δ 28.6 (CH₂), 31.8 (CH₂), 39.4 (CH₂), 67.7 (2CH C₅H₄), 68.6 (2CH C₅H₄), 68.9 (5CH Cp), 86.8 (C C₅H₄), 114.9 (2CH C₆H₄), 115.0 (2CH C₆H₄), 122.0 (2 C_{imide}), 127.2 (2CH_{imide}), 127.3 (C_{imide}), 129.9 (2CH_{imide}), 130.4 (2CH C₆H₄), 130.7 (2CH C₆H₄), 131.3 (C), 132.7 (C), 134.4 (2CH_{imide}), 135.1 (C), 135.5 (C), 138.4 (C), 155.6 (C), 155.7 (C), 163.4 (2 CO). IR (KBr, ν cm⁻¹): 3407 (OH), 1702 (CO). HRMS (ESI, C₃₉H₃₁FeNNaO₄: [M+Na]⁺) calcd: 656.149468, found: 656.14883. Anal. Calcd for C₃₉H₃₁FeNO₄(H₂O): C, 71.89; H, 5.10; N, 2.15. Found: C, 71.80; H, 5.20; N, 1.88.

5-(2,3-naphthalenedicarboximido)-2-ferrocenyl-1,1-bis-(4-hydroxyphenyl)-pent-1-en, 21. This compound was synthesized using the general procedure for the synthesis of imides using compound **7** (1.909 g, 3.38 mmol), potassium carbonate (0.701 g, 5.1 mmol), 2,3-naphthalenedicarboximide (0.667 g, 3.4 mmol), temperature 60 °C, 3 days, 79% yield. Mp: >270 °C. ¹H NMR (DMSO- d_6): δ 1.71-1.89 (m, 2H, CH₂), 2.51-2.59 (m, 2H, CH₂), 3.53 (t, J = 6.7 Hz, 2H, CH₂N), 3.77 (t, J = 1.7 Hz, 2H, C₅H₄), 4.02 (s broad, 7 H, Cp + C₅H₄), 6.58 (d, J = 8.5 Hz, 2H, C₆H₄), 6.59 (d, J = 8.5 Hz, 2H, C₆H₄), 6.75 (d, J = 8.5 Hz, 2H, C₆H₄), 6.90 (d, J = 8.5 Hz, 2H, C₆H₄), 7.72-7.82 (m, 2H, imide), 8.20-8.31 (m, 2H, imide), 8.49 (s, 2H, imide), 9.14 (s, 1H, OH), 9.29 (s, 1H, OH). ¹³C NMR (DMSO- d_6): δ 29.1 (CH₂), 31.7 (CH₂), 37.7 (CH₂), 67.8 (2CH C₅H₄), 68.6 (2CH C₅H₄), 69.0 (5CH Cp), 86.8 (C C₅H₄), 115.0 (2X2CH C₆H₄),

124.4 (2CH_{imide}), 127.4 (2C_{imide}), 129.2 (2CH_{imide}), 129.8 (2CH_{arom}), 130.4 (2X2CH_{arom}), 132.7 (2C_{imide}), 134.8 (C), 135.1 (C), 135.5 (C), 138.5 (C), 155.6 (C), 155.7 (C), 167.6 (2CO). IR (KBr, ν cm⁻¹): 3426 (OH), 1755 (CO). HRMS (ESI, C₃₉H₃₁FeNNaO₄: [M+Na]⁺) calcd: 656.149468, found: 656.14882. Anal. Calcd for C₃₉H₃₁FeNO₄(H₂O)_{0.5}: C, 72.89; H, 5.02; N, 2.18. Found: C, 72.68; H, 5.01; N, 2.03.

***N*-{5,5-bis-(4-hydroxyphenyl)-4-phenyl-pent-4-enyl}phthalimide, 34.** This compound was synthesized using the general procedure for the synthesis of imides using compound 5-Chloro-1,1-bis-(4-hydroxyphenyl)-2-phenyl-pent-1-ene (2.01 g, 5.51 mmol, can be prepared following the general procedure of the McMurry coupling), potassium carbonate (1.523 g, 11 mmol), phthalimide (1.621 g, 11 mmol), temperature 80 °C, overnight, 84% yield. ¹H NMR (acetone-d₆): δ 1.64-1.80 (m, 2H, CH₂), 2.50 (t, J = 8.3 Hz, 2H, CH₂-C=C), 3.56 (t, J = 6.9 Hz, 2H, CH₂N), 6.47 (d, J = 8.6 Hz, 2H, C₆H₄), 6.67 (d, J = 8.6 Hz, 2H, C₆H₄), 6.69 (d, J = 8.6 Hz, 2H, C₆H₄), 6.99 (d, J = 8.6 Hz, 2H, C₆H₄), 7.02-7.18 (m, 5H, C₆H₅), 7.82 (s, 4H, phthalimide), 8.08 (s, 1H, OH), 8.17 (s, 1H, OH). ¹³C NMR (acetone-d₆): δ 28.8 (CH₂), 34.1 (CH₂), 38.4 (CH₂), 115.0 (2CH C₆H₄), 115.7 (2CH C₆H₄), 123.6 (2CH phthalimide), 126.8 (CH C₆H₅), 128.7 (2CH_{arom}), 130.4 (2CH_{arom}), 131.1 (2CH_{arom}), 132.6 (2CH_{arom}), 133.0 (2C_{phthalimide}), 134.9 (2CH_{arom}), 135.4 (C), 135.6 (C), 138.7 (C), 140.4 (C), 143.7 (C), 156.3 (C), 157.0 (C), 168.7 (2CO). IR (KBr, ν cm⁻¹): 3421 (OH), 1768, 1705 (CO). HRMS (ESI, C₃₁H₂₅NNaO₄: [M+Na]⁺) calcd: 498.167579, found: 498.16718. Anal. Calcd for C₃₁H₂₅NO₄: C, 78.29; H, 5.29; N, 2.94. Found: C, 77.95; H, 5.07; N, 2.84.

***N*-(4-ferrocenyl-5,5-bis-phenyl-pent-4-enyl)succinimide, 35.** The mixture of compounds obtained from the McMurry reaction being unseparable, this mixture was used in the next step without separation. The McMurry reaction was done using the general procedure for the McMurry coupling using 4-chloro-1-ferrocenyl-butan-1-one (2.3 g, 7.92 mmol), titanium chloride (4.505 g, 2.61 mL, 23.7 mmol), zinc powder (2.587 g, 39.6 mmol), benzophenone (4.327 g, 23.7 mmol). Imide **35** was then prepared using the general procedure for the synthesis of imides using potassium carbonate (1.44 g, 10.4 mmol) and succinimide (1.033 g, 10.4 mmol), with a yield 5%. ¹H NMR (CDCl₃): δ 1.72-1.91 (m, 2H, CH₂), 2.48-2.62 (m, 6H, 2CH₂ succinimide + CH₂-C=C), 3.44 (t, J = 6.6 Hz, 2H, CH₂N), 3.87 (t, J = 1.9 Hz, 2H, C₅H₄), 4.09 (t, J = 1.9 Hz, 2H, C₅H₄), 4.13 (s, 5H, Cp), 7.03-7.46 (m, 10H, 2Ph). ¹³C NMR (CDCl₃):

δ 28.1 (2CH₂ succinimide), 29.3 (CH₂), 32.2 (CH₂), 38.8 (CH₂), 68.5 (2CH C₅H₄), 69.3 (2CH C₅H₄), 69.4 (5CH Cp), 86.3 (C C₅H₄), 126.3 (CH Ph), 126.5 (CH Ph), 128.5 (2CH Ph), 128.4 (2CH Ph), 129.4 (2CH Ph), 129.8 (2CH Ph), 134.9 (C), 138.9 (C), 144.4 (C), 144.5 (C), 177.1 (2CO). IR (KBr, ν cm⁻¹): 1690 (CO). HRMS (ESI, C₃₁H₂₉FeNO₂: [M]⁺) calcd: 503.1542, found: 503.1541.

***N*-(4-ferrocenylbutyl)succinimide, 38.** Compound **39** was dissolved into a solution of 20 mL of dry dichloromethane and 12 mL of trifluoroacetic acid. Triethylsilane (1.803 g, 2.48 mL, 15.5 mmol) was added and the solution was stirred for 7 days. The solution was slowly poured into a solution of sodium hydrogen carbonate under stirring and solid sodium hydrogen carbonate was added until the gassing stops. The mixture was extracted three times with dichloromethane and the combination of organic layers was washed with water, dried on magnesium sulfate, and concentrated under reduced pressure. The residue was chromatographed on silica gel with a 1/1 dichloromethane/petroleum ether solution as the eluent and was recrystallized from diethyl ether to afford compound **38** as a yellow solid in a yield 7%. ¹H NMR (CDCl₃): δ 1.40-1.65 (m, 4H, CH₂-CH₂), 2.34 (t, J = 7.5 Hz, 2H, CH₂=), 2.69 (s, 4H, succinimide), 3.51 (t, J = 7.2 Hz, 2H; CH₂N), 4.00-4.10 (m, 9H, ferrocene). ¹³C NMR (CDCl₃): δ 27.6 (CH₂), 28.3 (2CH₂; succinimide), 28.5 (CH₂), 29.2 (CH₂), 38.8 (CH₂), 67.5 (2CH; C₅H₄), 68.5 (2CH; C₅H₄), 68.9 (5CH; Cp), 177.4 (CO-N-CO). IR (KBr, ν cm⁻¹): 1690 (CO). MS (ESI) m/z : 339 [M]⁺. HRMS (ESI, C₁₈H₂₁FeNO₂: [M]⁺) calcd: 339.0922, found: 339.0919.

***N*-(4-ferrocenyl-4-oxobutyl)succinimide, 39.** 4-Chloro-1-ferrocenyl-1-butanone (5.811 g, 20 mmol), potassium carbonate (4.15 g, 30 mmol), succinimide (3.964 g, 40 mmol) and DMF (60 mL) were placed into a flask and the mixture was heated at 80 °C under stirring for two days. After cooling, the mixture was poured into water and extracted three times with diethyl ether and the combination of organic layers was washed with water, dried on magnesium sulfate, and concentrated under reduced pressure. The residue was chromatographed on silica gel with a 3/1 dichloromethane/petroleum ether solution as the eluent to afford compound **39** as an orange-red solid in a yield 41%. ¹H NMR (CDCl₃): δ 1.90-2.05 (m, 2H, CH₂), 2.69 (s, 4H, succinimide), 2.74 (t, J = 7.3 Hz, 2H, CH₂), 3.60 (t, J = 7.1 Hz, 2H, CH₂), 4.17 (s, 5H, Cp), 4.48 (t, J = 2.0 Hz, 2H, C₅H₄), 4.74 (t, J = 2.0 Hz, 2H, C₅H₄). ¹³C NMR (CDCl₃): δ 22.5 (CH₂), 28.3 (2CH₂; succinimide), 37.0 (CH₂), 38.6 (CH₂), 69.4 (2CH; C₅H₄), 69.9 (5CH; Cp), 72.3 (2CH;

C₅H₄), 78.8 (C; C₅H₄), 177.4 (CO-N-CO), 203.2 (CO; ketone). MS (ESI) m/z: 354 [M+H]⁺. HRMS (ESI, C₁₈H₂₀FeNO₃: [M+H]⁺) calcd: 354.0793, found: 354.0797.

***N*-{4-ferrocenyl-5,5-bis-(4-hydroxyphenyl)-pent-4-enyl}diglycolimide, 26.** A solution of compound **23** (0.2 g, 0.441 mmol), diglycolic anhydride (0.077 g, 0.662 mmol) and triethylamine (0.089 g, 0.12 mL, 0.882 mmol) in toluene was refluxed overnight then cooled to room temperature. After concentration under reduced pressure, the product was purified by flash chromatography (ethyl acetate/cyclohexane 3/1) to give the desired compound **26** as an orange solid with a yield of 54%. ¹H NMR (acetone-d₆): δ 1.64-1.81 (m, 2H, -CH₂-CH₂-CH₂-N), 2.56-2.68 (m, 2H, -CH₂-C=), 3.66 (t, *J* = 7.1 Hz, 2H, CH₂N), 3.92 (t, *J* = 2.0 Hz, 2H, C₅H₄), 4.06 (t, *J* = 2.0 Hz, 2H, C₅H₄), 4.12 (s, 5H, Cp), 4.34 (s, 4H, -CH₂-O-CH₂-), 6.69 (d, *J* = 8.5 Hz, 2H, C₆H₄), 6.81 (d, *J* = 8.5 Hz, 2H, C₆H₄), 6.87 (d, *J* = 8.5 Hz, 2H, C₆H₄), 7.03 (d, *J* = 8.5 Hz, 2H, C₆H₄), 8.22 (s, 1H, OH), 8.30 (s, 1H, OH). ¹³C NMR (acetone-d₆): δ 29.7 (CH₂), 33.0 (CH₂), 38.9 (CH₂), 68.1 (-CH₂-O-CH₂-), 68.7 (2CH C₅H₄), 69.9 (5CH Cp), 70.0 (2CH C₅H₄), 88.3 (C C₅H₄), 115.8 (2CH C₆H₄), 115.9 (2CH C₆H₄), 131.2 (2CH C₆H₄), 131.7 (2CH C₆H₄), 134.3 (C), 136.9 (C), 137.2 (C), 139.6 (C), 156.6 (C), 156.7 (C), 170.2 (2CO).

***5-N*-(4-hydroxybutanoyl)amino-2-ferrocenyl-1,1-bis-(4-hydroxyphenyl)-pent-1-ene, 27.** A mixture of **4** (0.6 g, 1.12 mmol), tetrahydrofuran (50 mL) and methanol (350 mL) was stirred at room temperature then sodium borohydride (0.678 g, 18 mmol) was added for 5 hours. After an additional stirring time of 2 days the mixture was poured into water and extracted 3 times with ethyl acetate. After concentration under reduced pressure, the residue was dissolved into hot ethanol and crystallized to give the desired compound as an orange solid in a 93% yield. ¹H NMR (DMSO-d₆): δ 1.44-1.61 (m, 2H, -CH₂-CH₂-CH₂-N), 1.58-1.72 (m, 2H, -CH₂-CH₂-CH₂-O), 2.01-2.15 (m, 2H, CH₂-CO), 2.42-2.53 (m, 2H, -CH₂-C=), 2.84-2.97 (m, 2H, CH₂N), 3.34-3.43 (m, 2H, CH₂-O), 3.81 (s broad, 2H, C₅H₄), 4.07 (s broad, 2H, C₅H₄), 4.10 (s, 5H, Cp), 4.48 (t, *J* = 5.1 Hz, 1H, OH), 6.63 (d, *J* = 8.1 Hz, 2H, C₆H₄), 6.72 (d, *J* = 8.1 Hz, 2H, C₆H₄), 6.78 (d, *J* = 8.1 Hz, 2H, C₆H₄), 6.95 (d, *J* = 8.1 Hz, 2H, C₆H₄), 7.70 (t, *J* = 5.7 Hz, 1H, NH), 9.28 (s, 1H, OH), 9.32 (s, 1H, OH). ¹³C NMR (DMSO-d₆): δ 28.5 (CH₂), 30.3 (CH₂), 31.5 (CH₂), 32.1 (CH₂), 38.4 (CH₂), 60.2 (CH₂), 67.5 (2CH, C₅H₄), 68.5 (2CH, C₅H₄), 68.8 (5CH, Cp), 86.7 (C, C₅H₄), 115.1 (2x2CH, C₆H₄), 129.9 (2CH, C₆H₄), 130.3 (2CH, C₆H₄), 133.3 (C), 135.3 (C), 135.7

(C), 138.0 (C), 155.6 (C), 155.7 (C), 172.0 (CO). HRMS (ESI, C₃₁H₃₄FeNO₄: [M+H]⁺) calcd: 540.1832, found: 540.1828.

1-[4-ferrocenyl-5,5-bis-(4-hydroxyphenyl)-pent-4-enyl]-5-hydroxy-2-pyrrolidone, 28. A mixture of compound **4** (1.88 g, 3.51 mmol), tetrahydrofuran (10 mL) and methanol (200 mL) was stirred at room temperature then sodium borohydride (1.063 g, 28.1 mmol) was slowly added for 30 minutes. After an additional time of 15 minutes the reaction was quenched with a saturated aqueous solution of sodium hydrogen carbonate and extracted twice with dichloromethane. The organic layer was dried on magnesium sulfate and concentrated under reduced pressure. The product was purified by flash chromatography (ethyl acetate/cyclohexane 3/1) to give the desired compound **28** as an orange solid with a yield of 58%. ¹H NMR (acetone-d₆): δ 1.61-1.88 (m, 3H, -CH₂-CH₂-CH₂- + -CH₂-CH₂-CH-O), 2.11-2.30 (m, 2H, -CO-CH₂-CH₂-CH-O), 2.33-2.47 (m, 1H, -CH₂-CO), 2.47-2.73 (m, 2H, CH₂-C=C), 2.98-3.13 (m, 1H, CH₂N), 3.37-3.54 (m, 1H, CH₂N), 3.81-3.85 (m, 1H, C₅H₄), 3.98-4.16 (m, 8H, Cp+C₅H₄), 4.90 (d broad, *J* = 4.0 Hz, CH-O), 6.70 (d, *J* = 8.5 Hz, 2H, C₆H₄), 6.83 (d, *J* = 8.5 Hz, 2H, C₆H₄), 6.87 (d, *J* = 8.5 Hz, 2H, C₆H₄), 7.05 (d, *J* = 8.5 Hz, 2H, C₆H₄), 8.55 (s broad, 2H, OH). ¹³C NMR (acetone-d₆): δ 28.6 (CH₂), 29.1 (CH₂), 29.3 (CH₂), 33.0 (CH₂), 39.5 (CH₂N), 68.6 (CH, C₅H₄), 68.7 (CH, C₅H₄), 69.9 (5CH, Cp), 70.0 (CH, C₅H₄), 70.1 (CH, C₅H₄), 82.7 (CH-O), 88.3 (C, C₅H₄), 115.8 (2CH, C₆H₄), 115.9 (2CH, C₆H₄), 131.3 (2CH, C₆H₄), 131.8 (2CH, C₆H₄), 134.9 (C), 137.1 (C), 137.3 (C), 139.2 (C), 156.7 (C), 156.8 (C), 174.2 (CO). HRMS (ESI, C₃₁H₃₂FeNO₄: [M+H]⁺) calcd: 538.1675, found: 538.1674.

2,3-Dihydro-3-hydroxy-2-[4-ferrocenyl-5,5-bis-(4-hydroxyphenyl)-pent-4-enyl]-1H-isoindol-1-one, 29. The same procedure as for the synthesis of **29** was used starting from compound **6** (1.167 g, 2 mmol) to afford **29** as an orange solid with a yield of 92%. Mp: 187 °C. ¹H NMR (acetone-d₆): δ 1.85-1.98 (m, 2H, CH₂), 2.62-2.83 (m, 2H, CH₂-C=C), 3.29-3.38 (m, 1H, CH₂N), 3.67-3.81 (m, 1H, CH₂N), 3.82-3.86 (m, 1H, C₅H₄), 4.03-4.06 (m, 1H, C₅H₄), 4.06-4.15 (m, 7H, Cp + C₅H₄), 5.35 (d, *J* = 4.7 Hz, 1H, OH), 5.53 (d, *J* = 4.7 Hz, 1H, CH), 6.72 (d, *J* = 8.6 Hz, 2H, C₆H₄), 6.75 (d, *J* = 8.6 Hz, 2H, C₆H₄), 6.89 (d, *J* = 8.6 Hz, 2H, C₆H₄), 7.06 (d, *J* = 8.6 Hz, 2H, C₆H₄), 7.53-7.71 (m, 4H, isoindole), 8.28 (s, 1H, OH), 8.29 (s, 1H, OH). ¹³C NMR (acetone-d₆): δ 29.3 (CH₂), 32.9 (CH₂), 39.1 (CH₂), 68.3 (CH C₅H₄), 68.4 (CH

C₅H₄), 69.6 (5CH Cp + 1CH C₅H₄), 69.8 (CH C₅H₄), 81.2 (CH-OH), 88.2 (C C₅H₄), 115.5 (2CH C₆H₄), 115.6 (2CH C₆H₄), 122.9 (CH isoindole), 124.0 (CH isoindole), 129.8 (CH isoindole), 131.0 (2CH C₆H₄), 131.5 (2CH C₆H₄), 132.2 (CH isoindole), 134.4 (C), 136.6 (C), 137.0 (C), 139.0 (2C), 145.6 (C), 156.7 (C), 156.8 (C), 167.2 (CO). IR (KBr, ν cm⁻¹): 3406 (OH), 1665 (CO). MS (EI, 70 eV) m/z : 585 [M]⁺, 520 [M-Cp]⁺, 502 [M-Cp-H₂O]⁺, 474, 369, 341, 146. HRMS (ESI, C₃₅H₃₁FeNO₄: [M]⁺) calcd: 585.1602, found: 585.1623. Anal. Calcd for C₃₅H₃₁FeNO₄(H₂O): C, 69.66; H, 5.50; N, 2.32. Found: C, 69.61; H, 5.32; N, 2.50.

1-[4-ferrocenyl-5,5-bis-(4-hydroxyphenyl)-pent-4-enyl]-5-methoxy-2-pyrrolidone, 30. A solution of compound **28** (0.21 g, 0.391 mmol), methanol (5 mL), dichloromethane (40 mL) and 4-toluenesulfonic acid (0.007 g, 0.04 mmol) was stirred for 30 minutes at room temperature. After completion of the reaction (TLC), the solution was poured into water, extracted twice with dichloromethane, dried on magnesium sulfate then concentrated under reduced pressure to afford **30** as an orange solid with a yield of 97%. ¹H NMR (DMSO-d₆): δ 1.42-1.73 (m, 2H, -CH₂-CH₂-CH₂), 1.73-1.98 (m, 2H, -CH₂-CH₂-CH-O), 1.98-2.18 (m, 1H, -CH₂-CO), 2.20-2.42 (m, 2H, -CH₂-CO + CH-C=), 2.42-2.57 (m, 1H, CH₂-C=C), 2.75-2.93 (m, 1H, CH₂N), 3.11 (s, 3H, OMe), 3.23-3.40 (m, 1H, CH₂N), 3.71 (s broad, 1H, C₅H₄), 3.92 (s broad, 1H, C₅H₄), 4.04 (s broad, 1H, C₅H₄), 4.09 (s broad, 6H, Cp+C₅H₄), 4.50 (dd, J = 4.5 and 1.7 Hz, CH-O), 6.62 (d, J = 8.5 Hz, 2H, C₆H₄), 6.73 (d, J = 8.5 Hz, 2H, C₆H₄), 6.77 (d, J = 8.5 Hz, 2H, C₆H₄), 6.95 (d, J = 8.5 Hz, 2H, C₆H₄), 9.30 (s broad, 1H, OH), 9.35 (s broad, 1H, OH). ¹³C NMR (DMSO-d₆): δ 23.3 (CH₂), 28.1 (CH₂), 28.5 (CH₂), 31.7 (CH₂), 39.4 (CH₂N), 52.4 (OMe), 67.78 (CH, C₅H₄), 67.84 (CH, C₅H₄), 68.6 (CH, C₅H₄), 68.8 (CH, C₅H₄), 69.0 (5CH, Cp), 86.7 (C, C₅H₄), 88.9 (CH-O), 115.1 (2x2CH, C₆H₄), 130.0 (2CH, C₆H₄), 130.4 (2CH, C₆H₄), 133.2 (C), 135.2 (C), 135.5 (C), 138.0 (C), 155.7 (2C), 174.0 (CO). HRMS (ESI, C₃₂H₃₄FeNO₄: [M+H]⁺) calcd: 552.1832, found: 552.183.

2,3-Dihydro-3-methoxy-2-[4-ferrocenyl-5,5-bis-(4-hydroxyphenyl)-pent-4-enyl]-1H-isoindol-1-one, 31. This compound was obtained with the same procedure as for compound **30** with compound **28** (0.119 g, 0.203 mmol), methanol (3 mL), dichloromethane (25 mL) and 4-toluenesulfonic acid (0.004 g, 0.02 mmol) to afford **31** as an orange solid with a yield of 89%. ¹H NMR (acetone-d₆): δ 1.76-1.93 (m,

2H, CH₂), 2.55-2.76 (m, 2H, CH₂C=C), 2.87 (s, 3H, CH₃), 3.03-3.18 (m, 1H, CH₂N), 3.68-3.82 (m, 1H, CH₂N), 3.89-3.84 (m, 1H, C₅H₄), 3.97-4.03 (m, 1H, C₅H₄), 4.04-4.14 (m, 7H, C₅H₄+Cp), 5.42 (s, 1H, CH), 6.63-6.76 (m, 4H, C₆H₄), 6.85 (d, *J* = 8.6 Hz, 2H, C₆H₄), 7.02 (d, *J* = 8.6 Hz, 2H, C₆H₄), 7.52-7.76 (m, 4H, isoindole), 8.19 (s broad, 1H, OH), 8.22 (s broad, 1H, OH). ¹³C NMR (acetone-d₆): δ 29.4 (CH₂), 32.9 (CH₂), 39.4 (CH₂), 49.8 (OCH₃), 68.4 (CH, C₅H₄), 68.5 (CH, C₅H₄), 69.6 (6CH, C₅H₄+Cp), 69.8 (CH, C₅H₄), 86.3 (CH-O), 88.6 (C, C₅H₄), 115.5 (2CH, C₆H₄), 115.7 (2CH, C₆H₄), 123.0 (CH, isoindole), 124.3 (CH, isoindole), 130.3 (CH, isoindole), 131.0 (2CH, C₆H₄), 131.5 (2CH, C₆H₄), 132.4 (CH, isoindole), 133.9 (C), 134.6 (C), 136.9 (C), 137.3 (C), 139.5 (C), 142.0 (C), 156.7 (C), 156.8 (C), 167.7 (CO). HRMS (ESI, C₃₆H₃₄FeNO₄: [M+H]⁺) calcd: 600.1832, found: 600.1831.

4.3 X-Ray crystal structure determination of **21**, **26** and **38**

A suitable crystal of compound **21**, **26** and **38** was mounted and transferred into a cold nitrogen gas stream. Intensity data was collected with a Bruker Kappa-APEX2 system using micro-source Cu-Kα radiation. Data collection was carried out with the Bruker APEX2 suite of programs. Unit-cell parameters determination, integration and data reduction were performed with SAINT. SADABS was used for scaling and multi-scan absorption corrections. The structure was solved with SHELXT-2014[52] and refined by full-matrix least-squares methods with SHELXL-2014[52] using the WinGX suite.[53] All non-hydrogen atoms were refined anisotropically. Hydrogen atoms were placed at calculated positions and refined with a riding model. The structure was deposited at the Cambridge Crystallographic Data Centre with number CCDC 2114457 for **21**, 2114461 for **26**, 1542076 for **38** and can be obtained free of charge via www.ccdc.cam.ac.uk.

4.4 Chemical Oxidation

Freshly prepared Ag₂O was added to solutions of the compounds in acetone-d₆ at 20 °C, and the mixtures were stirred to allow contact between Ag₂O, which is insoluble in acetone, and the molecule to be oxidized. The formation of QMs was then monitored by NMR spectroscopy. At specific times, aliquots (0.5 mL) of the solutions were taken and filtered to remove Ag₂O. The samples were kept in liquid nitrogen until they were analyzed by NMR spectroscopy. The QMs are mainly characterized by a multiplet and a triplet signals of their —CH₂CH=C— group. The variation of methylene signals was

used for calculation of rate constants (k) and half-lives ($t_{1/2}$).

4.5 Incubation of 4 and 6 with liver microsomes in the absence or presence of thiols.

Rat liver microsomes were isolated from rat pre-treated for 7 days by 1g/L phenobarbital in drinking water (2 nmole P450/mg protein). All the experiments with animals were performed in accordance with the French Agricultural and Fishing Ministry regulations, following an agreement from the French Ministry of Education and Research (Nb APAFIS#794-2016102716338280 v2). Male Sprague Dawley rats (220-250 g) were used for the study. Human liver microsomes were obtained from Corning as UltraPool HLM-150 containing 350 pmol P450/mg protein. Typical incubations were performed in potassium phosphate buffer (0.1 M, pH 7.4) containing microsomes (0.5-1 mg protein/mL for rat microsomes and 1 mg/mL for HLM), 1 mM NADP, 15 mM glucose-6-phosphate, 2 unit/mL of glucose-6-phosphate dehydrogenase, and substrate (5-500 μ M) at 37 °C. Reactions were stopped either by adding one-half volume of CH₃CN:CH₃COOH (9:1) and centrifugation of precipitated proteins (12000 g, 10 min) or by solid-phase extraction using Oasis columns (Waters, St. Quentin en Yvelines, France) (1 mL loading, 1 mL water wash, and 1 mL CH₃OH elution), evaporation of the solvent with N₂, and redissolution in HPLC mobile phase.

4.6 HPLC-MS analyses.

HPLC-MS studies were performed on a Surveyor HPLC instrument coupled to a LCQ Advantage ion trap mass spectrometer (Thermo, Les Ulis, France), using a Biobasic C18 column (100 mm x 2 mm, 3 μ m) and a 20 min linear gradient of A) ammonium acetate (10 mM, pH 4.6) to B) CH₃CN:CH₃OH:H₂O (7:2:1) mixture at 200 μ L/min. For some compounds an alternative gradient system was used: A) H₂O:HCOOH 0.5% and B) CH₃CN:HCOOH 0.1%. Mass spectra were obtained by electrospray ionization (ESI) in positive ionization mode detection under the following conditions: source parameters: sheath gas, 20; auxiliary gas, 5; spray voltage, 4.5 kV; capillary temperature, 200 °C; capillary voltage, 15 V; and m/z range for MS recorded generally between 200 and 900. Semiquantitative analysis of the yield of different metabolites from the two quinone methide pathways was achieved by comparing the areas under the respective peaks of different compounds visible in the UV traces of the LC-MS analysis. High resolution HPLC-MS was performed with a Shimadzu Prominence HPLC system coupled to an Exactive-Orbitrap mass spectrometer (Thermo, Les Ulis, France), using a Satisfaction C18 column 100

mm x 2 mm, 3 μ m) (CIL, Sainte Foix la Grande, France) and the above alternative gradient and the same source parameters.

4.7 Lipophilicity.

Measurements of the octanol/water partition coefficient ($\log P_{o/w}$) were made by the HPLC technique according to a method described previously.[54] Measurement of the chromatographic capacity factors (k) for each molecule was done at various concentrations in the range of 95–75% methanol containing 0.25% (v/v) 1-octanol and an aqueous phase consisting of 0.15% (v/v) n-decylamine in the buffering agent MOPS (3-morpholinopropane-1-sulfonic acid, prepared in 1-octanol saturated water) adjusted to pH 7.4. These capacity factors (k') are extrapolated to 100% of the aqueous component given the value of $k'w$. The $\log P_{o/w}$ is obtained by the formula $\log P_{o/w} = 0.13418 + 0.98452 \log k'$.

4.8 ROS Measurements.

Intracellular ROS levels in live MDA-MB-231 cells were measured by using the fluorogenic probe H₂DCFDA (dihydro-2',7'-dichlorofluorescein diacetate; C2938, Molecular Probes Inc., Eugene, OR). Cells (9500 per well) were seeded in 96-well plates and left to grow overnight. At 24 h, medium was replaced with a solution of H₂DCFDA in HBSS (1 μ M) and cells were incubated at 37°C for 30 min. This solution was then removed, the 96-wells rinsed twice with buffer then the medium added and the cells left to recover at 37°C for 30 min, before addition of the compounds investigated (1 μ M) or a control solution. DCF fluorescence emission at 525 nm was then measured at 0, 10, 20, 30, 60, 90 and 120 min using excitation at 495 nm with a microplate reader (Fluorostar Optima, BMG Labtech).

4.9 Cell Culture and Proliferation Assay.

Human HCT-116 colorectal carcinoma and K562 leukemia were grown in RPMI 1640 supplemented with 10% fetal calf serum (FCS) and 1% glutamine. MCF-7, A-375 and HT1080 carcinoma cells were grown in Gibco medium DMEM supplemented with 10% fetal calf serum (FCS) and 1% glutamine. Cells were maintained at 37 °C in a humidified atmosphere containing 5% CO₂. Cell growth inhibition was determined by an CCK-8 assay according to the manufacturer's instructions (Promega, Madison, WI, USA). Briefly, the cells were seeded in 96-well plates (2.5×10^3 cells/well) containing 100 μ L of

growth medium. After 24 h of culture, the cells were treated with the tested compounds at 8 different final concentrations. After 48 h of incubation, 10 μ L of CCK-8 stock solution was added for 2 h before recording absorbance at 450 nm with a spectrophotometric plate reader. The dose-response curves were plotted with Graph Prism software and the IC₅₀ values were calculated using the Graph Prism software from polynomial curves (four or five-parameter logistic equations).

MDA-MB-231: stock solutions (10 mM) of the compounds to be tested were prepared in DMSO and were kept at -20 °C in the dark. Serial dilutions in Dulbecco's modified eagle medium (DMEM) without phenol red/Glutamax I were prepared just prior to use. DMEM without phenol red, Glutamax I and fetal bovine serum were purchased from Gibco; MDA-MB-231 cells were obtained from ATCC (Manassas, VA, USA). Cells were maintained in a monolayer culture in DMEM with phenol red/Glutamax I supplemented with 9% fetal bovine serum at 37 °C in a 5% CO₂/air-humidified incubator. For proliferation assays, MDA-MB-231 cells were plated in 1 mL of DMEM without phenol red, supplemented with 9% decompartmented and hormone-depleted fetal bovine serum, 1% kanamycin, 1% Glutamax I and incubated. The following day (D0), 1 mL of the same medium containing the compounds to be tested was added to the plates. After 3 days (D3) the incubation medium was removed and 2 mL of the fresh medium containing the compounds was added. At different days (D4, D5), the protein content of each well was quantified by methylene blue staining as follows: cell monolayers were fixed for 1 h at room temperature with methylene blue (1mg mL⁻¹ in 50:50 water/MeOH mixture), then washed with water. After addition of HCl (0.1 M, 2 mL), the plate was incubated for 1 h at 37 °C and then the absorbance of each well (4 wells for each concentration) was measured at 655 nm with a Biorad spectrophotometer. The results are expressed as the percentage of proteins versus the control. Two independent experiments, run in quadruplicate, were performed.

Declaration of competing interest

The authors declare that they have no known competing financial interests or personal relationships that could have appeared to influence the work reported in this paper.

Acknowledgements.

Yong received funding from the Starting Fund of Shandong Province for Pilot National Laboratory for

Marine Science and Technology (Qingdao) (LMDBCXRC202002) and Taishan Scholar Youth Expert Program in Shandong Province (tsqn202103035). We thank the PGG foundation, PSL University, Feroscan and ANR (NaTeMOc Project) for financial support, and we thank Geoffrey Gontard (IPCM, CNRS UMR 8232) for the X-ray structure determinations.

Supplementary Information.

Supplementary crystallographic data Tables S1-3, and MS data Table S4. This material is available free of charge via the Internet at [xxx](#).

References

- [1] S. Top, G. Jaouen, A. Vessieres, J.P. Abjean, D. Davoust, C.A. Rodger, B.G. Sayer, M.J. McGlinchey, Chromium tricarbonyl complexes of estradiol derivatives: differentiation of .alpha.- and .beta.-diastereoisomers using 1- and 2-dimensional NMR spectroscopy at 500 MHz, *Organometallics*, 4 (1985) 2143-2150.
- [2] G. Jaouen, A. Vessieres, I.S. Butler, *Bioorganometallic Chemistry - a Future-Direction for Transition-Metal Organometallic Chemistry*, *Acc. Chem. Res.*, 26 (1993) 361-369.
- [3] C.G. Hartinger, P.J. Dyson, *Bioorganometallic chemistry-from teaching paradigms to medicinal applications*, *Chem. Soc. Rev.*, 38 (2009) 391-401.
- [4] G. Jaouen, N. Metzler-Nolte, *Medicinal Organometallic Chemistry*, Vol. 32, Springerlink ed., 2010.
- [5] *Bioorganometallic Chemistry*, De Gruyter, 2020.
- [6] G. Jaouen, *Bioorganometallics: biomolecules, labeling, medicine*, John Wiley & Sons, 2006.
- [7] K.D. Mjos, C. Orvig, *Metallodrugs in Medicinal Inorganic Chemistry*, *Chemical Reviews*, 114 (2014) 4540-4563.
- [8] K. Kowalski, *Ferrocenyl-nucleobase complexes: Synthesis, chemistry and applications*, *Coord. Chem. Rev.*, 317 (2016) 132-156.
- [9] M.A. Cinellu, I. Ott, A. Casini, in: G. Jaouen, M. Salmain (Eds.) *Bioorganometallic Chemistry*, Wiley-VCH, 2015, pp. 117-140.
- [10] P. Zhang, P.J. Sadler, *Advances in the design of organometallic anticancer complexes*, *J. Organomet. Chem.*, 839 (2017) 5-14.
- [11] R. Wang, H. Chen, W. Yan, M. Zheng, T. Zhang, Y. Zhang, *Ferrocene-containing hybrids as potential anticancer agents: Current developments, mechanisms of action and structure-activity relationships*, *European Journal of Medicinal Chemistry*, 190 (2020) 112109.
- [12] Z. Yang, G. Jiang, Z. Xu, S. Zhao, W. Liu, *Advances in alkynyl gold complexes for use as potential anticancer agents*, *Coordination Chemistry Reviews*, 423 (2020) 213492.
- [13] J.P.C. Coverdale, I. Romero-Canelón, C. Sanchez-Cano, G.J. Clarkson, A. Habtemariam, M. Wills, P.J. Sadler, *Asymmetric transfer hydrogenation by synthetic catalysts in cancer cells*, *Nature Chemistry*, 10 (2018) 347.
- [14] A. Terenzi, C. Pirker, B.K. Keppler, W. Berger, *Anticancer metal drugs and immunogenic cell death*, *J. Inorg. Biochem.*, 165 (2016) 71-79.
- [15] W.A. Wani, U. Baig, S. Shreaz, R.A. Shiekh, P.F. Iqbal, E. Jameel, A. Ahmad, S.H. Mohd-Setapar, M. Mushtaque, L.T. Huna, *Recent advances in iron complexes as potential anticancer agents*, *New Journal of Chemistry*, 40 (2016) 1063-1090.

- [16] M. Patra, G. Gasser, *Nature Rev. Chem.*, (2017) 0066.
- [17] R.G. Kenny, C.J. Marmion, *Toward Multi-Targeted Platinum and Ruthenium Drugs—A New Paradigm in Cancer Drug Treatment Regimens?*, *Chemical Reviews*, 119 (2019) 1058-1137.
- [18] J.-J. Zhang, M.A. Abu el Maaty, H. Hoffmeister, C. Schmidt, J.K. Muenzner, R. Schobert, S. Wölfel, I. Ott, *A Multitarget Gold(I) Complex Induces Cytotoxicity Related to Aneuploidy in HCT-116 Colorectal Carcinoma Cells*, *Angewandte Chemie International Edition*, 59 (2020) 16795-16800.
- [19] S. Schoch, M. Hadjij, S.A.P. Pereira, M.L.M.F.S. Saraiva, S. Braccini, F. Chiellini, T. Biver, S. Zacchini, G. Pampaloni, P.J. Dyson, F. Marchetti, *A Strategy to Conjugate Bioactive Fragments to Cytotoxic Diiron Bis(cyclopentadienyl) Complexes*, *Organometallics*, 40 (2021) 2516-2528.
- [20] Y. Long, B. Cao, X. Xiong, A.S.C. Chan, R.W.-Y. Sun, T. Zou, *Bioorthogonal Activation of Dual Catalytic and Anti-Cancer Activities of Organogold(I) Complexes in Living Systems*, *Angewandte Chemie International Edition*, 60 (2021) 4133-4141.
- [21] J. Skiba, Q. Yuan, A. Hildebrandt, *Ferrocenyl GNA Nucleosides: A Bridge between Organic and Organometallic Xeno - nucleic Acids*, *ChemPlusChem*, 83 (2018) 77-86.
- [22] S. Sansook, S. Hassell-Hart, C. Ocasio, J. Spencer, *Ferrocenes in medicinal chemistry; a personal perspective*, *Journal of Organometallic Chemistry*, 905 (2020) 121017.
- [23] A. Singh, I. Lumb, V. Mehra, V. Kumar, *Ferrocene-appended pharmacophores: an exciting approach for modulating the biological potential of organic scaffolds*, *Dalton Transactions*, 48 (2019) 2840-2860.
- [24] B. Sharma, V. Kumar, *Has Ferrocene Really Delivered Its Role in Accentuating the Bioactivity of Organic Scaffolds?*, *Journal of Medicinal Chemistry*, 64 (2021) 16865-16921.
- [25] G. Jaouen, A. Vessières, S. Top, *Ferrocifen type anti cancer drugs*, *Chem. Soc. Rev.*, 44 (2015) 8802-8817.
- [26] A. Vessières, Y. Wang, M.J. McGlinchey, G. Jaouen, *Multifaceted chemical behaviour of metallocene (M = Fe, Os) quinone methides. Their contribution to biology*, *Coordination Chemistry Reviews*, 430 (2021) 213658.
- [27] Y. Wang, P. Pigeon, S. Top, M.J. McGlinchey, G. Jaouen, *Organometallic Antitumor Compounds: Ferrocifens as Precursors to Quinone Methides*, *Angew. Chem.-Int. Edit.*, 54 (2015) 10230-10233.
- [28] W. Yong, R. Marie-Aude, T. Siden, D.P. M., P. Pascal, V. Anne, M. Daniel, J. Gérard, *Ferrocenyl Quinone Methide–Thiol Adducts as New Antiproliferative Agents: Synthesis, Metabolic Formation from Ferrociphenols, and Oxidative Transformation*, *Angewandte Chemie International Edition*, 55 (2016) 10431-10434.
- [29] Y. Wang, P.M. Dansette, P. Pigeon, S. Top, *A new generation of ferrociphenols leads to a great diversity of reactive metabolites, and exhibits remarkable antiproliferative properties*, *Chem. Sci.*, 9 (2018) 70-78.
- [30] A. Citta, A. Folda, A. Bindoli, P. Pigeon, S. Top, A. Vessières, M. Salmain, G. Jaouen, M.P. Rigobello, *Evidence for targeting thioredoxin reductases with ferrocenyl quinone methides. A possible molecular basis for the antiproliferative effect of hydroxyferrocifens on cancer cells.*, *J. Med. Chem.*, 57 (2014) 8849-8859.
- [31] V. Scalcon, A. Citta, A. Folda, A. Bindoli, M. Salmain, I. Ciofini, S. Blanchard, J. de Jesús Cázares-Marinero, Y. Wang, P. Pigeon, G. Jaouen, A. Vessières, M.P. Rigobello, *Enzymatic oxidation of ansa-ferrocifen leads to strong and selective thioredoxin reductase inhibition in vitro*, *Journal of Inorganic Biochemistry*, 165 (2016) 146-151.
- [32] Y. Wang, P. Pigeon, M.J. McGlinchey, S. Top, G. Jaouen, *Synthesis and antiproliferative evaluation of novel hydroxypropyl-ferrociphenol derivatives, resulting from the modification of hydroxyl groups*, *Journal of Organometallic Chemistry*, 829 (2017) 108-115.
- [33] L. Cunningham, Y. Wang, C. Nottingham, J. Pagsulingan, G. Jaouen, M.J. McGlinchey, P.J. Guiry, *Enantioselective Synthesis of Planar Chiral Ferrocifens that Show Chiral Discrimination in Antiproliferative Activity on Breast Cancer Cells*, *ChemBioChem*, 21 (2020) 2974-2981.
- [34] Y. Wang, F. Heinemann, S. Top, A. Dazzi, C. Policar, L. Henry, F. Lambert, G. Jaouen, M. Salmain, A. Vessières, *Ferrocifens labelled with an infrared rhenium tricarbonyl tag: synthesis, antiproliferative activity, quantification and nano IR mapping in*

cancer cells, Dalton Transactions, 47 (2018) 9824-9833.

[35] P. Pigeon, Y. Yong, S. Top, F. Najlaoui, A New Series of Succinimido-ferrociphenols and Related Heterocyclic Species Induce Strong Antiproliferative Effects, Especially against Ovarian Cancer Cells Resistant to Cisplatin, J. Med. Chem., 60 (2017) 8358-8368.

[36] Y. Wang, P. Pigeon, S. Top, J. Sanz García, C. Troufflard, I. Ciofini, M.J. McGlinchey, G. Jaouen, Atypical Lone Pair- π Interaction with Quinone Methides in a Series of Imido-Ferrociphenol Anticancer Drug Candidates, Angewandte Chemie International Edition, 58 (2019) 8421-8425.

[37] B. Decroix, P. Pigeon, J. Sikoraiova, S. Marchalin, Intramolecular Addition of a Hydroxyl to an N-Acyliminium System. Application to the Synthesis of Isoindolo[2,1-a][3,1]benzoxazine and Isoindolo[1,2-c][2,4]benzoxazepine Derivatives, Heterocycles, 56 (2002).

[38] M. Egli, S. Sarkhel, Lone Pair-Aromatic Interactions: To Stabilize or Not to Stabilize, Accounts of Chemical Research, 40 (2007) 197-205.

[39] S.K. Singh, A. Das, The $n \rightarrow \pi^*$ interaction: a rapidly emerging non-covalent interaction, Physical Chemistry Chemical Physics, 17 (2015) 9596-9612.

[40] J. Kozelka, Lone pair- π interactions in biological systems: occurrence, function, and physical origin, European Biophysics Journal, 46 (2017) 729-737.

[41] A. Kamal, N.R. Bolla, P.S. Srikanth, A.K. Srivastava, Naphthalimide derivatives with therapeutic characteristics: a patent review, Expert Opinion on Therapeutic Patents, 23 (2013) 299-317.

[42] S. Banerjee, E.B. Veale, C.M. Phelan, S.A. Murphy, G.M. Tocci, L.J. Gillespie, D.O. Frimannsson, J.M. Kelly, T. Gunnlaugsson, Recent advances in the development of 1,8-naphthalimide based DNA targeting binders, anticancer and fluorescent cellular imaging agents, Chemical Society Reviews, 42 (2013) 1601-1618.

[43] G. Gellerman, Recent Developments in the Synthesis and Applications of Anticancer Amonafide Derivatives. A Mini Review, Letters in Drug Design & Discovery, 13 (2016) 47-63.

[44] D.-G. Jia, J.-A. Zheng, Y.-R. Fan, J.-Q. Yu, X.-L. Wu, B.-J. Wang, X.-B. Yang, Y. Huang, Ferrocene appended naphthalimide derivatives: Synthesis, DNA binding, and in vitro cytotoxic activity, Journal of Organometallic Chemistry, 888 (2019) 16-23.

[45] F. Tonolo, M. Salmain, V. Scalcon, S. Top, P. Pigeon, A. Folda, B. Caron, M.J. McGlinchey, R.-A. Toillon, A. Bindoli, G. Jaouen, A. Vessières, M.P. Rigobello, Small Structural Differences between Two Ferrocenyl Diphenols Determine Large Discrepancies of Reactivity and Biological Effects, ChemMedChem, 14 (2019) 1717-1726.

[46] K.V. Ramakrishna, P.W. Fan, C.S. Boyer, D. Dalvie, J.L. Bolton, Oxo Substituents Markedly Alter the Phase II Metabolism of α -Hydroxybutenylbenzenes: Models Probing the Bioactivation Mechanisms of Tamoxifen, Chemical Research in Toxicology, 10 (1997) 887-894.

[47] Scott J. Dixon, Kathryn M. Lemberg, Michael R. Lamprecht, R. Skouta, Eleina M. Zaitsev, Caroline E. Gleason, Darpan N. Patel, Andras J. Bauer, Alexandra M. Cantley, Wan S. Yang, B. Morrison, III, Brent R. Stockwell, Ferroptosis: An Iron-Dependent Form of Nonapoptotic Cell Death, Cell, 149 (2012) 1060-1072.

[48] H.Z.S. Lee, O. Buriez, F. Chau, E. Labbé, R. Ganguly, C. Amatore, G. Jaouen, A. Vessières, W.K. Leong, S. Top, Synthesis, Characterization, and Biological Properties of Osmium-Based Tamoxifen Derivatives – Comparison with Their Homologues in the Iron and Ruthenium Series, European Journal of Inorganic Chemistry, 2015 (2015) 4217-4226.

[49] M.-A. Richard, D. Hamels, P. Pigeon, S. Top, P.M. Dansette, H.Z.S. Lee, A. Vessières, D. Mansuy, G. Jaouen, Oxidative Metabolism of Ferrocene Analogues of Tamoxifen: Characterization and Antiproliferative Activities of the Metabolites, Chemmedchem, 10 (2015) 981-990.

[50] Wan S. Yang, R. SriRamaratnam, Matthew E. Welsch, K. Shimada, R. Skouta, Vasanthi S. Viswanathan, Jaime H. Cheah, Paul A. Clemons, Alykhan F. Shamji, Clary B. Clish, Lewis M. Brown, Albert W. Girotti, Virginia W. Cornish, Stuart L. Schreiber, Brent R. Stockwell, Regulation of Ferroptotic Cancer Cell Death by GPX4, Cell, 156 (2014) 317-331.

- [51] S. Topin-Ruiz, A. Mellinger, E. Lepeltier, C. Bourreau, J. Fouillet, J. Riou, G. Jaouen, L. Martin, C. Passirani, N. Clere, p722 ferrocifen loaded lipid nanocapsules improve survival of murine xenografted-melanoma via a potentiation of apoptosis and an activation of CD8+ T lymphocytes, *International Journal of Pharmaceutics*, 593 (2021) 120111.
- [52] G. Sheldrick, A Short History of ShelX, *Acta crystallographica. Section A, Foundations of crystallography*, 64 (2008) 112-122.
- [53] L. Farrugia, WinGX Suite for Single Crystal Small Molecule Crystallography, *Journal of Applied Crystallography*, 32 (1999) 837-838.
- [54] D.J. Minick, J.H. Frenz, M.A. Patrick, D.A. Brent, A comprehensive method for determining hydrophobicity constants by reversed-phase high-performance liquid chromatography, *Journal of Medicinal Chemistry*, 31 (1988) 1923-1933.

Supplementary Information

Diversity-oriented Synthesis and Bioactivity Evaluation of N-substituted Ferrocifen Compounds as Novel Antiproliferative Agents against TNBC Cancer Cells

Yong Wang,^{* [a]} Pascal Pigeon,^[b] Wei Li,^[a] Jiangkun Yan,^[a] Patrick M. Dansette,^[c] Mohamed Othman^[e]
Michael J. McGlinchey,^[d] and Gérard Jaouen^{*[b]}

Table S1. Crystallographic Data for **21**.

Formula	C ₃₉ H ₃₁ FeNO ₄ X2	Selected bond lengths (Å)	
Molecular Weight	633.53 X2	C(1)-C(2)	1.400
Crystal description	Orange prism	C(31)-O(3)	1.363
Crystal size (mm)	0.65x 0.25x 0.15	C(15)-N(1)	1.465
Temperature (K)	200(1)	Fe(1)-C(1)	2.028
Crystal system	Monoclinic		
Space group	P 2 ₁ /c		
<i>a</i> (Å)	10.9124		
<i>b</i> (Å)	25.6124	Selected Bond Angles (°)	
<i>c</i> (Å)	21.7237	C(28)-C(12)-C(34)	113.6(1)
α (°)	90	C(12)-C(11)-C(13)	119.9(1)
β (°)	94.295	C(14)-C(15)-N(1)	112.2(2)
γ (°)	90	C(31)-O(3)-H(3A)	109.5
Volume (Å ³)	6054.57	C(30)-C(31)-O(3)	123.2(2)
Z	8	C(1)-Fe(1)-C(2)	40.3(1)
R	0.0532		
GOF	1.020		

Table S2. Crystallographic Data for **26**.

Formula	C ₃₁ H ₂₉ FeNO ₅	Selected bond lengths (Å)	
Molecular Weight	551.42	C(1)-C(2)	1.416
Crystal description	Orange fragment	C(28)-O(3)	1.224
Crystal size (mm)	0.6 x 0.5 x 0.5	C(27)-N(1)	1.472
Temperature (K)	200(1)	C(30)-O(4)	1.408
Crystal system	Monoclinic		
Space group	P 2 ₁ /n		
<i>a</i> (Å)	11.6859(2)		
<i>b</i> (Å)	17.1430(3)	Selected Bond Angles (°)	
<i>c</i> (Å)	13.6951(2)	C(10)-C(11)-C(12)	124.2(1)
<i>α</i> (°)	90	C(12)-C(11)-C(25)	121.2(1)
<i>β</i> (°)	110.8040	C(27)-N(1)-C(31)	117.8(1)
<i>γ</i> (°)	90	C(29)-O(4)-C(30)	110.8
Volume (Å ³)	2564.68	C(1)-Fe(1)-C(10)	127.12(5)
Z	4	C(1)-Fe(1)-C(2)	40.21(5)
R	0.0363		
GOF	1.023		

Table S3. Crystallographic Data for **38**.

Formula	C ₁₈ H ₂₁ FeNO ₂	Selected bond lengths (Å)	
Molecular Weight	339.22	C(1)-C(2)	1.382
Crystal description	Yellow plate	C(14)-N(1)	1.461
Crystal size (mm)	0.01 x 0.15 x 0.25	C(15)-N(1)	1.382
Temperature (K)	200(1)	C(15)-O(1)	1.208
Crystal system	Monoclinic		
Space group	P 2 ₁ /c		
<i>a</i> (Å)	12.1082(6)		
<i>b</i> (Å)	10.4928(5)	Selected Bond Angles (°)	
<i>c</i> (Å)	12.2853(5)	C(10)-C(11)-C(12)	115.8(2)
<i>α</i> (°)	90	C(11)-C(10)-Fe(1)	128.9(1)
<i>β</i> (°)	99.270(3)	C(14)-N(1)-C(15)	122.6(2)
<i>γ</i> (°)	90	O(1)-C(15)-N(1)	124.0(2)
Volume (Å ³)	1540.45	O(1)-C(15)-C(16)	127.7(2)
Z	4		
R	0.0714		
GOF	1.011		

Table S4. MS, and MS², and UV/Vis properties of main metabolites resulting from **4** and **6**.

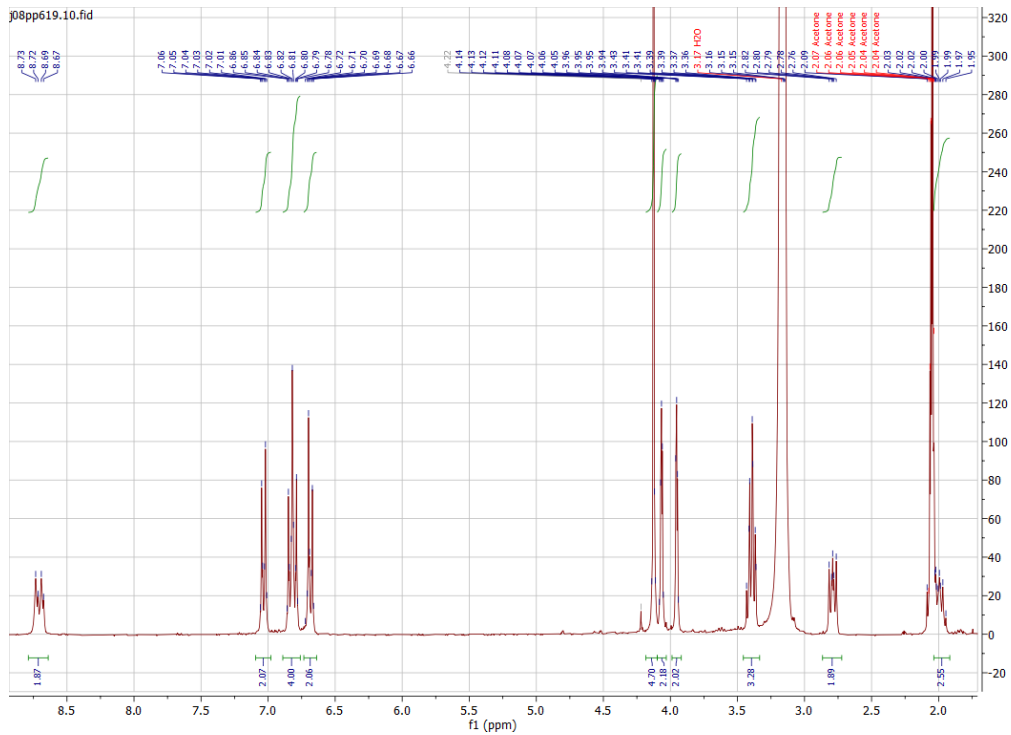
Compound	Mr (Calc.)	<i>m/z</i>		λ_{\max} [nm] UV/Vis
		MS	MS ²	
4-AA	551	551 [M] ⁺	533, 486, 353	210
4-CP	533	533 [M] ⁺	468, 407, 355	321
4-SG	841	841 [M] ⁺	535, 468, 267	209
4-NACM	710	710 [M] ⁺	502, 468, 293	208
4-ME	611	611 [M] ⁺	546, 517, 281	210
6-AA	599	599 [M] ⁺	534, 516, 401	220
6-CP	581	581 [M] ⁺	516, 407, 355	322
6-SG	889	889 [M] ⁺	582, 516, 489	211
6-NACM	758	758 [M] ⁺	597, 532, 407	213
6-ME	659	659 [M] ⁺	594, 516, 437	214

Table S5. Ferroptosis inducing activity of selected compounds were measured on ferroptosis sensitive fibrosarcoma cells HT1080.

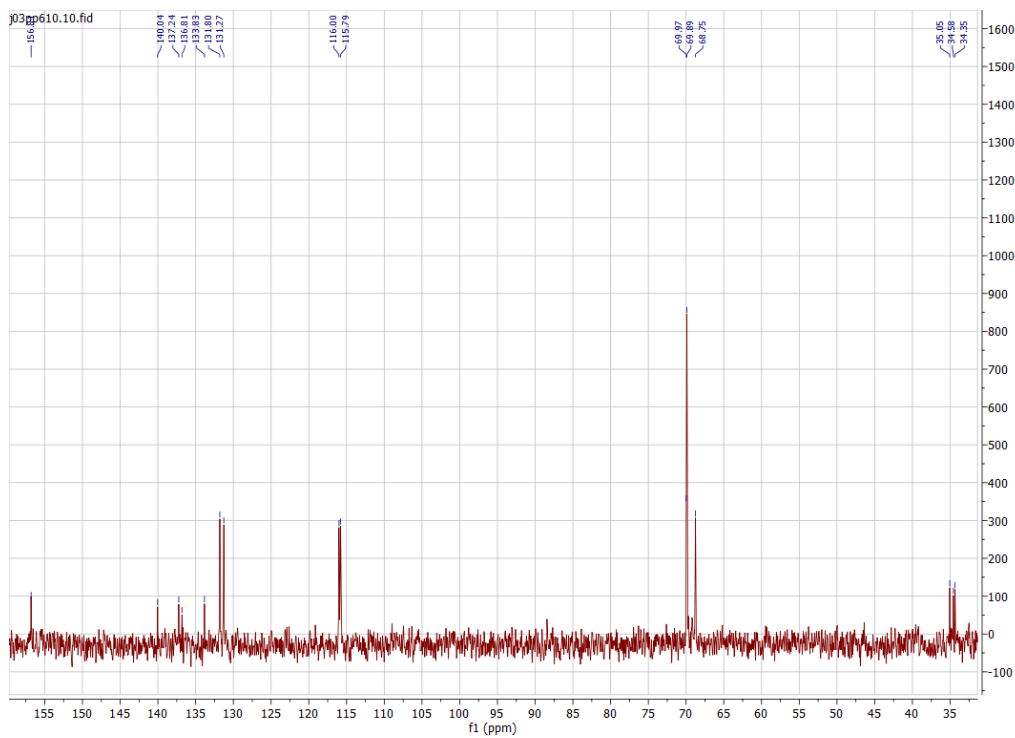
Compd.	Conc. (μ M)	Inhibition (%) ^a	
		-fer-1	+fer-1
1	10	66.72	67.10
	1	16.21	15.87
2	10	35.89	38.38
	1	29.45	14.59
3	10	50.92	54.59
	1	25.62	22.08
4	10	49.12	58.53
	1	34.46	38.61
5	10	36.73	38.78
	1	21.26	18.95
6	10	46.92	51.89
	1	27.21	33.98
36	10	50.34	50.64
	1	48.62	43.38
37	10	50.92	54.59
	1	25.62	22.08

(a) Inhibition of the growth of HT1080 cells were measured with or without 1.5 μ M fer-1.

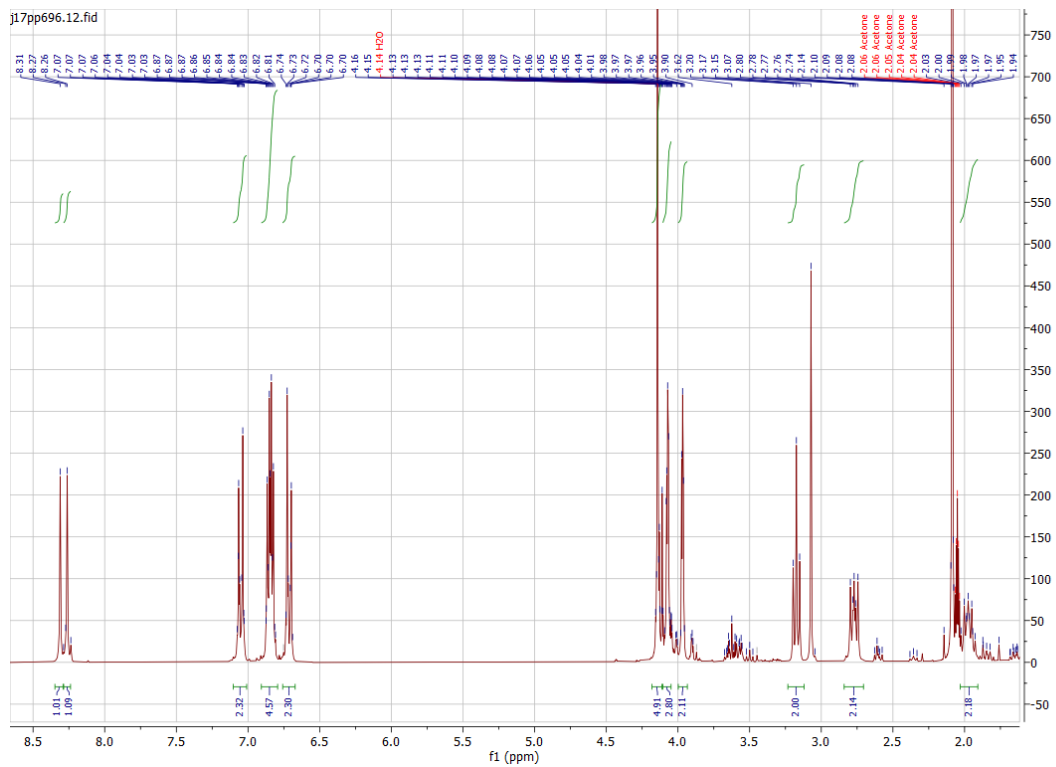
Supplementary NMR spectra



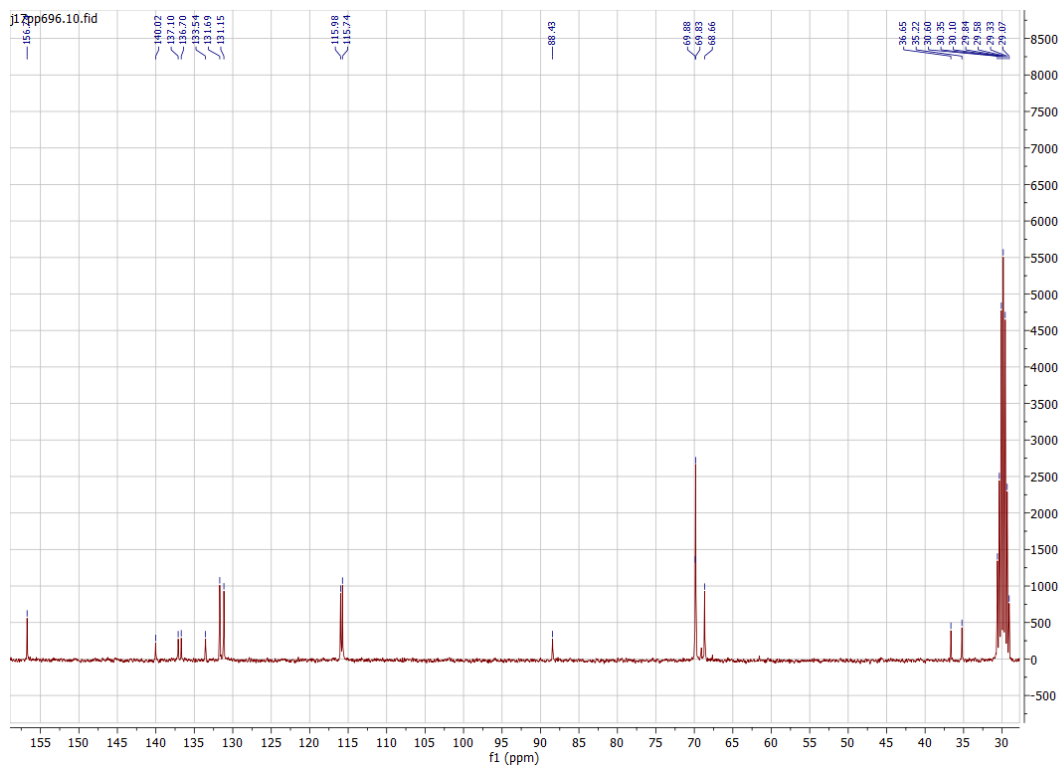
¹H spectrum of 8.



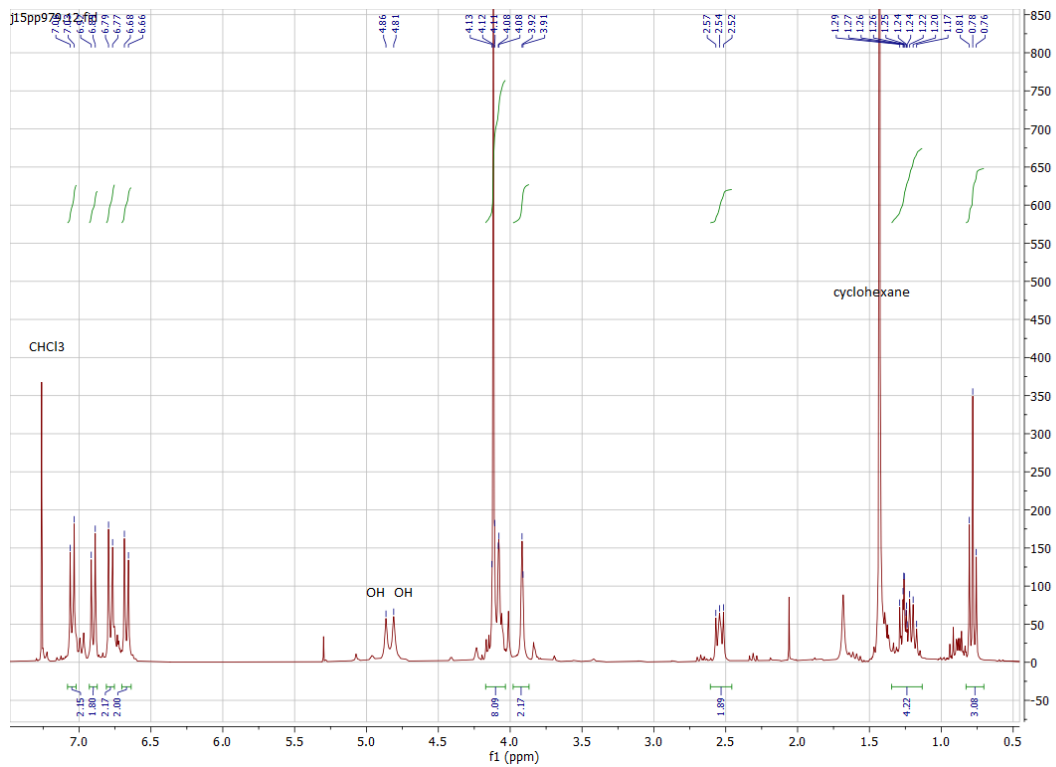
¹³C spectrum of 8.



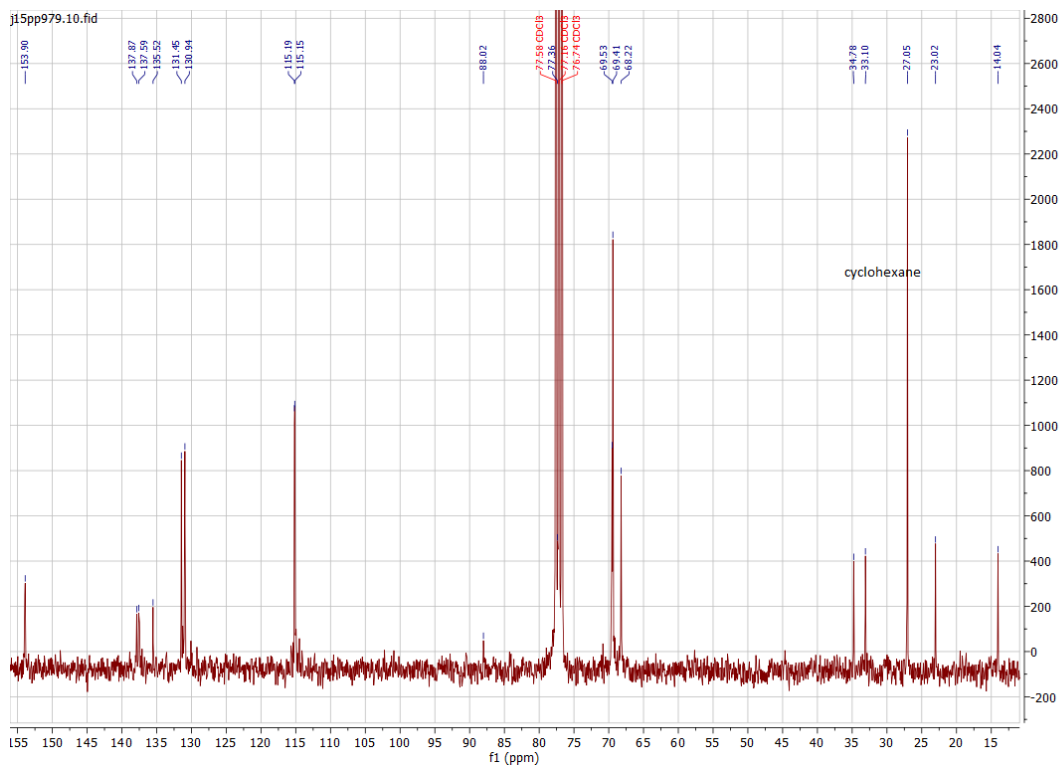
¹H spectrum of 9.



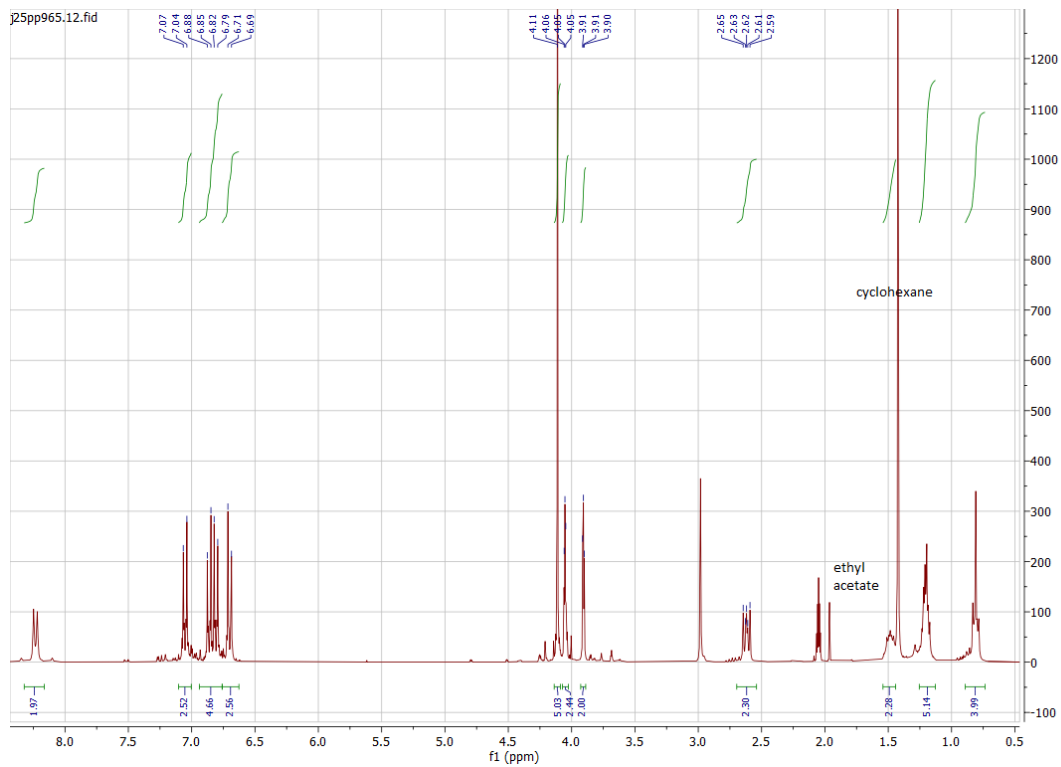
¹³C spectrum of 9.



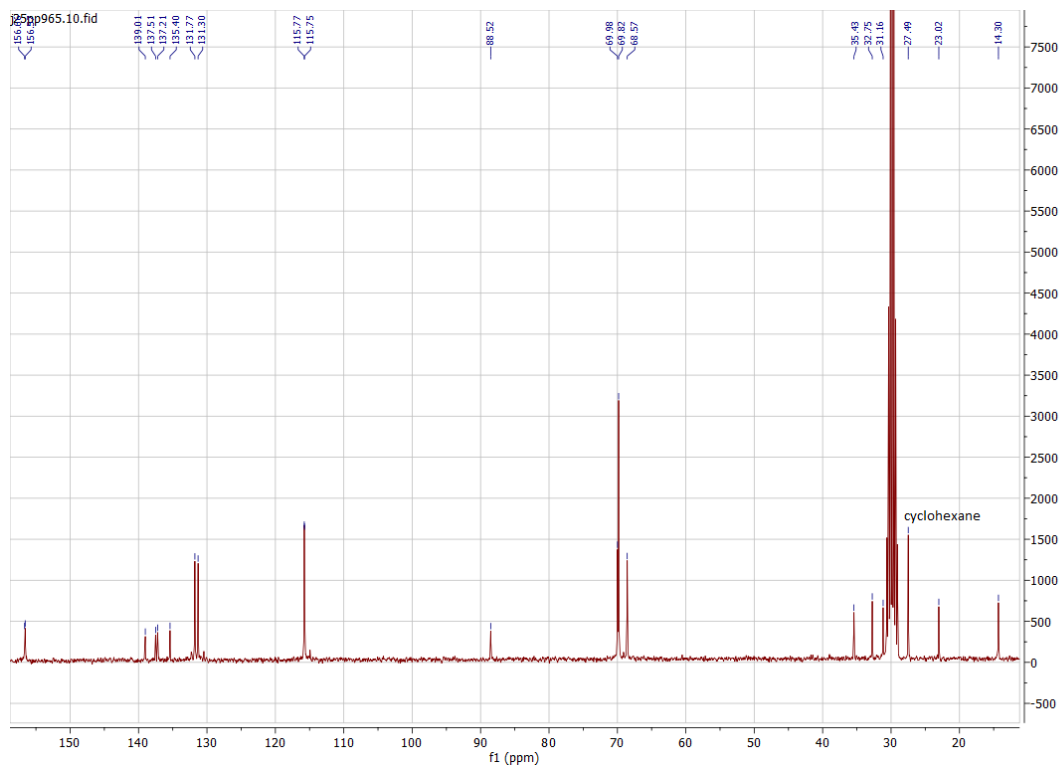
¹H spectrum of 11.



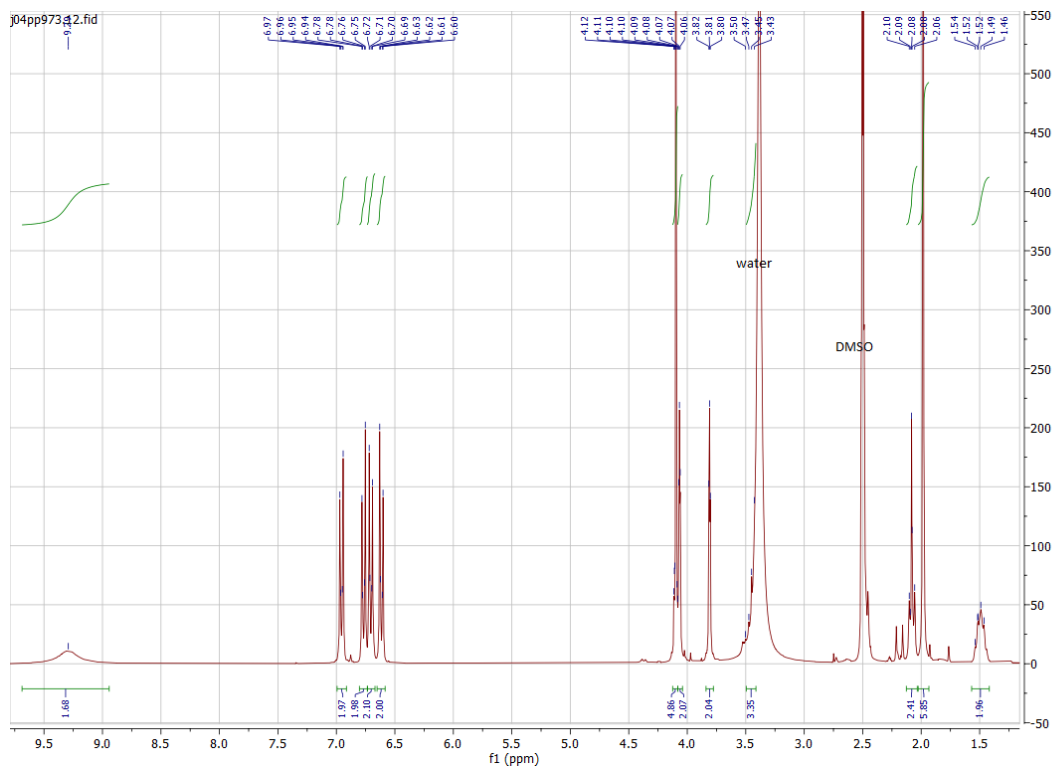
¹³C spectrum of 11.



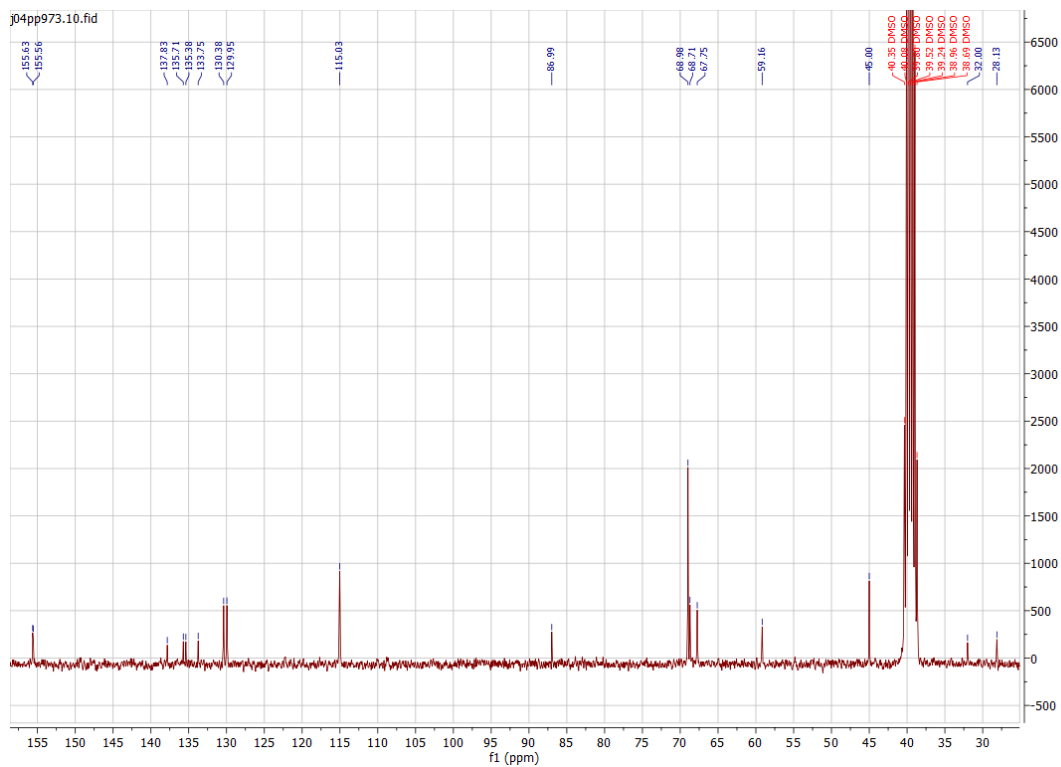
^1H spectrum of **12**.



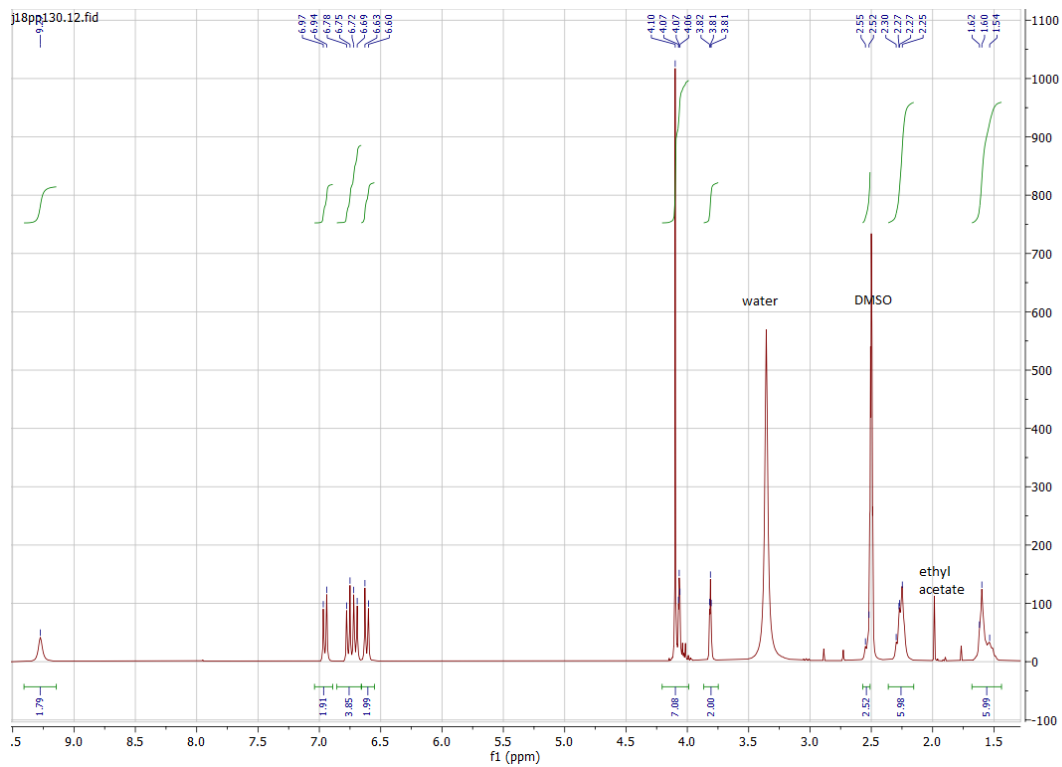
^{13}C spectrum of **12**.



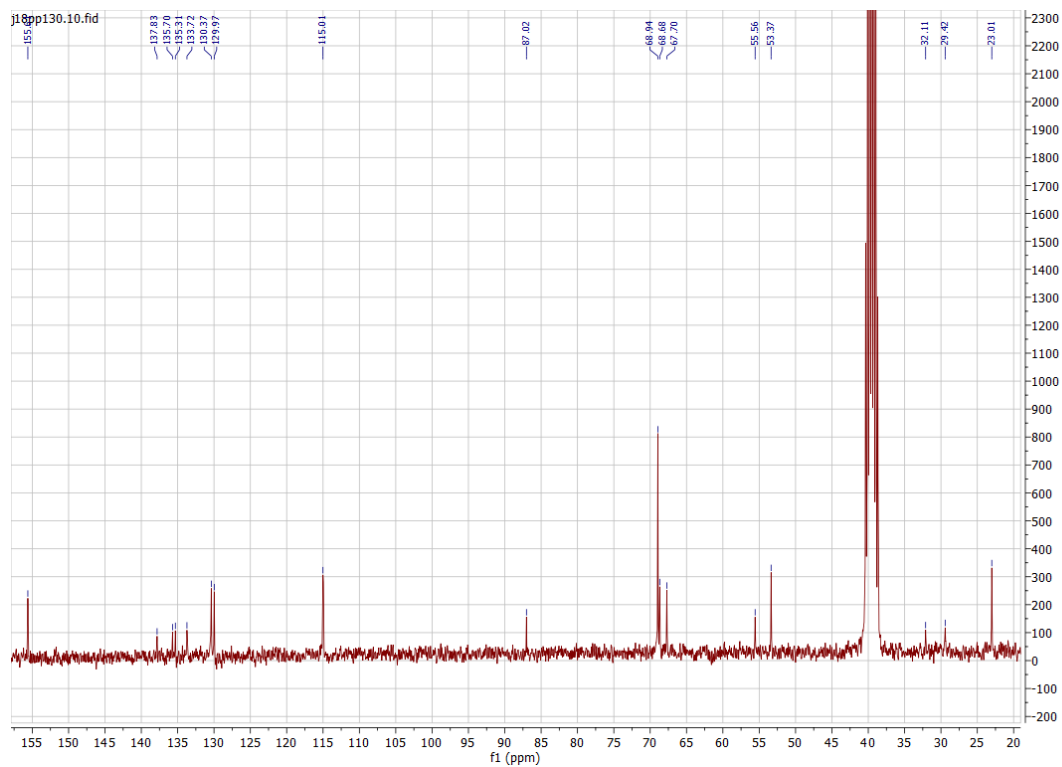
^1H spectrum of **13**.



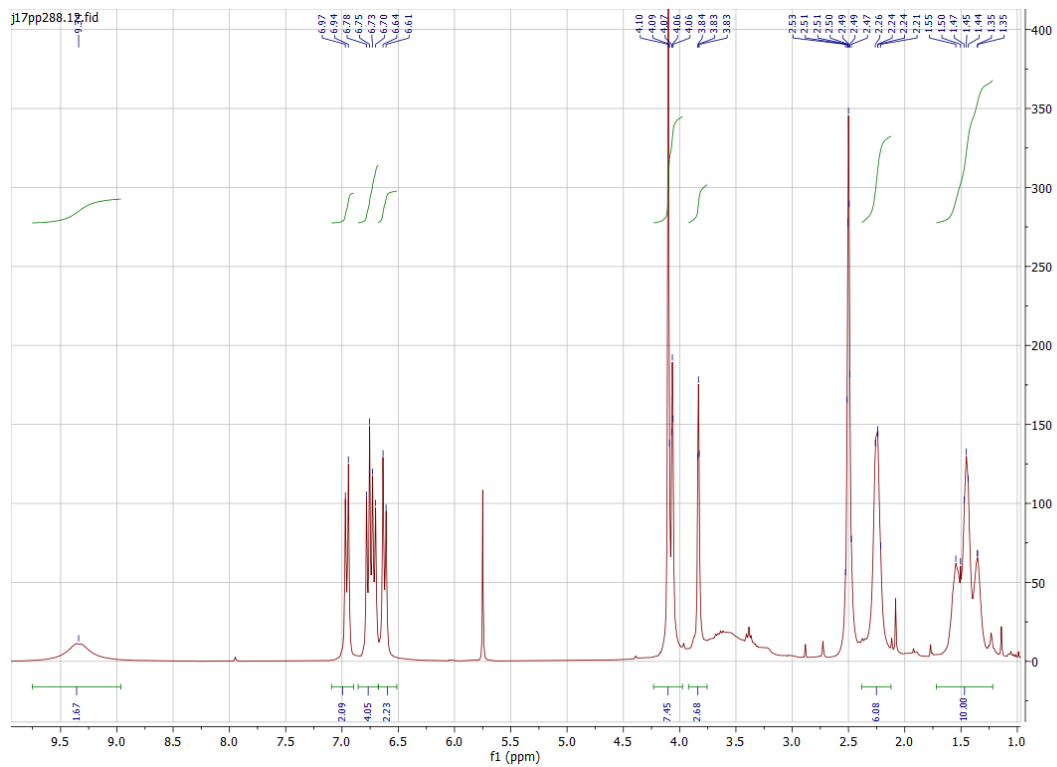
^{13}C spectrum of **13**.



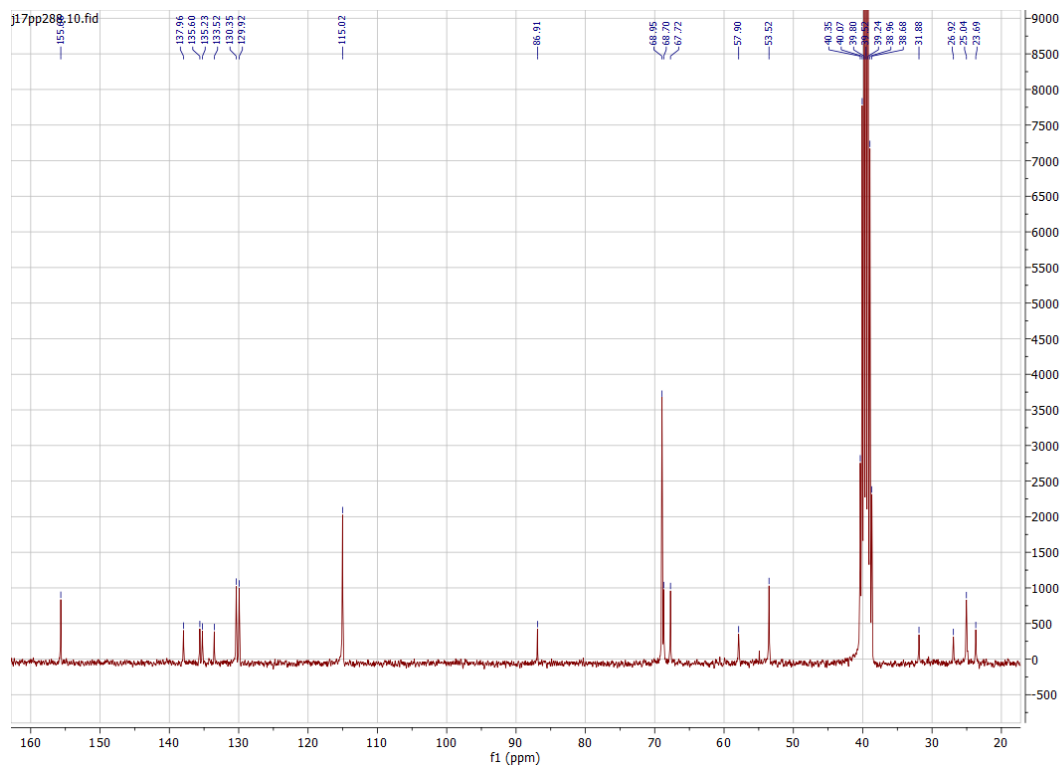
¹H spectrum of 14.



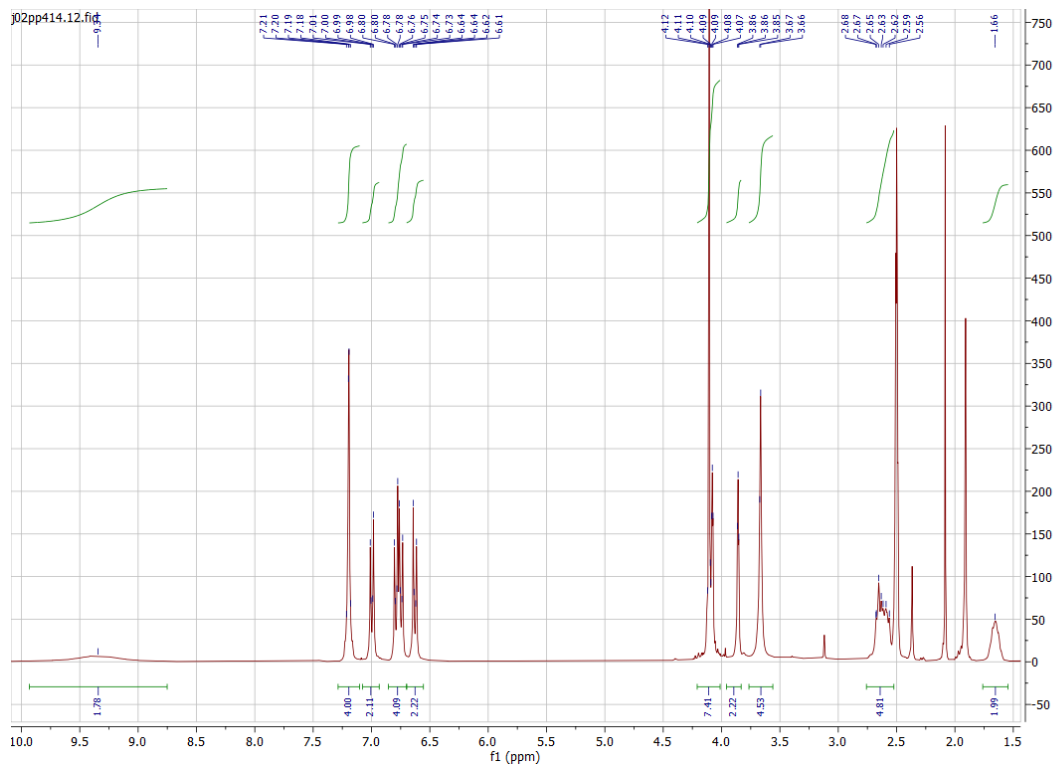
¹³C spectrum of 14.



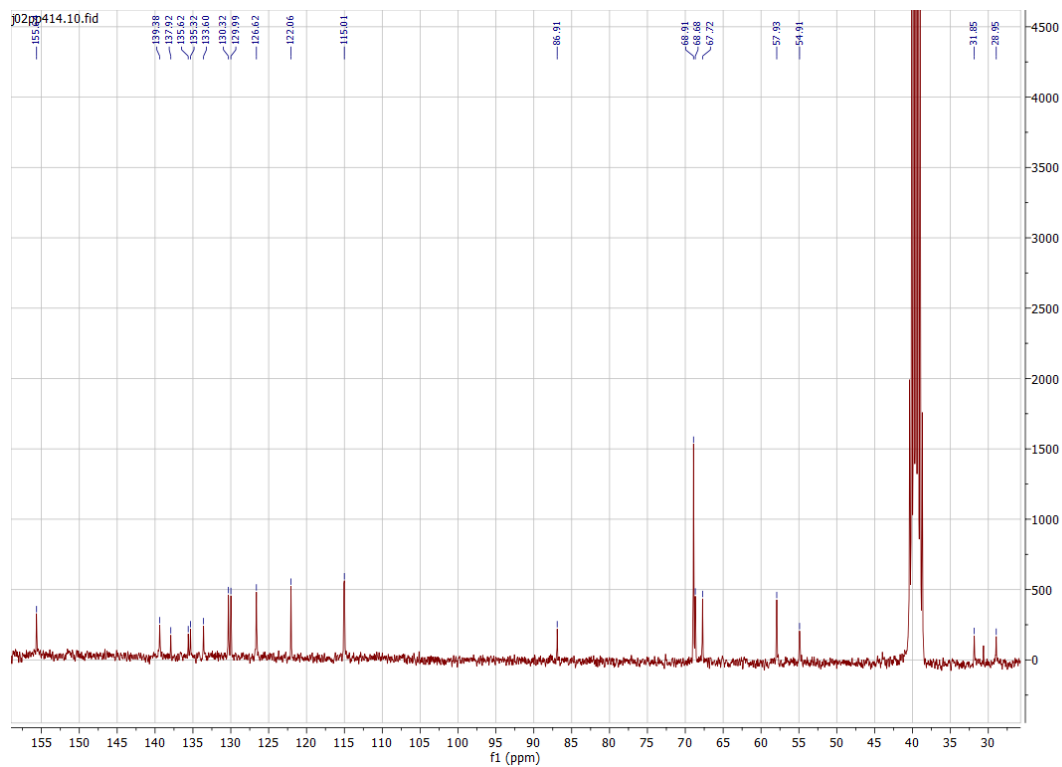
¹H spectrum of 15.



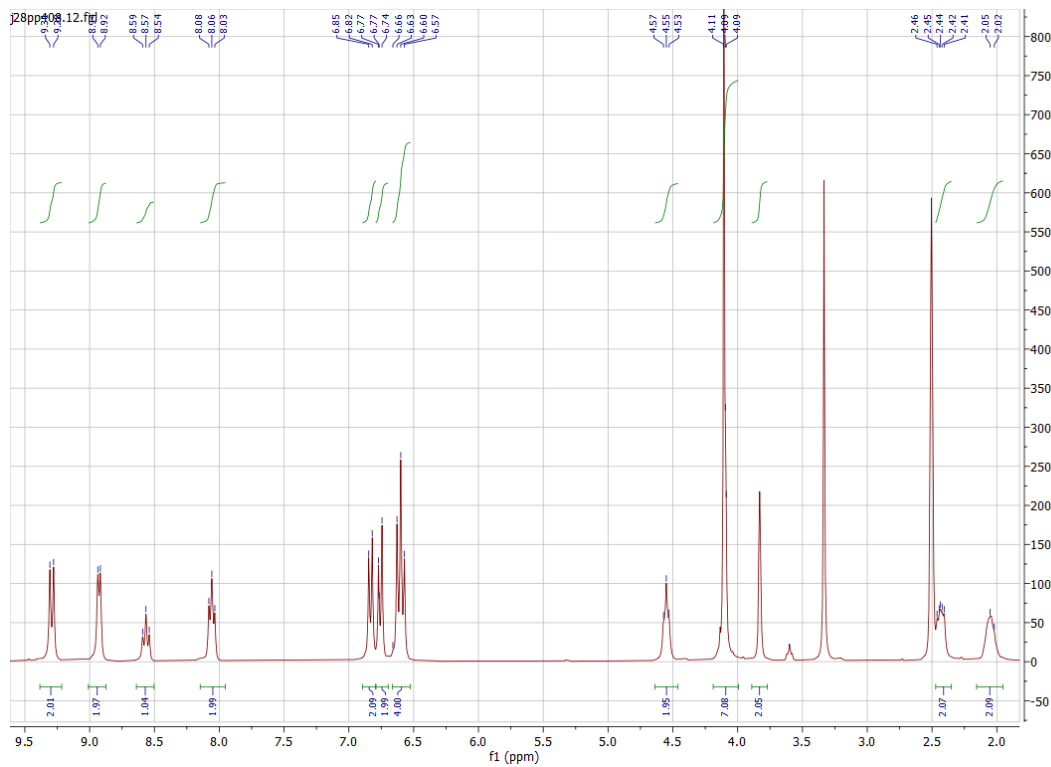
¹³C spectrum of 15.



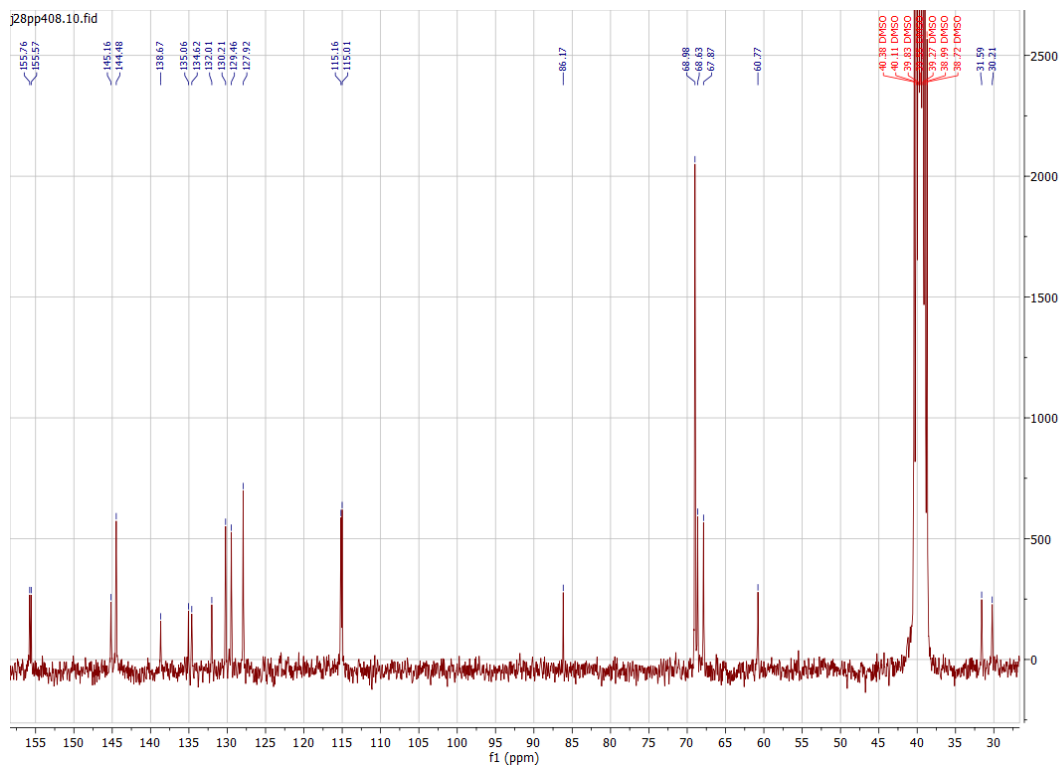
¹H spectrum of 16.



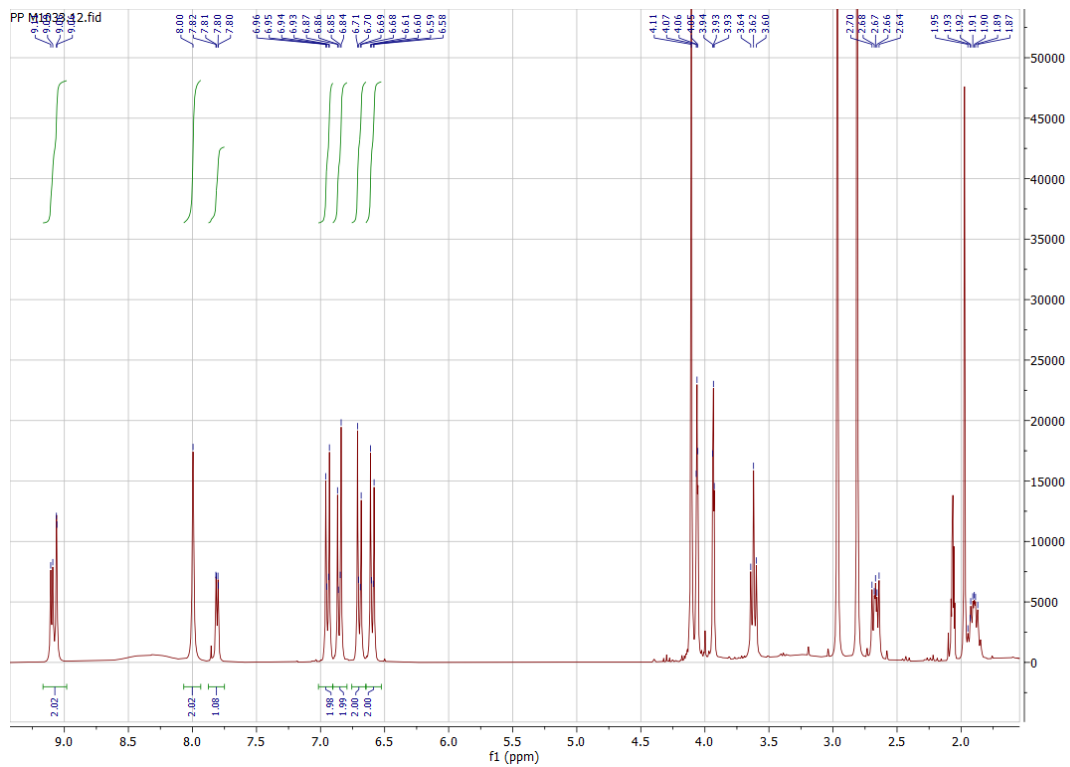
¹³C spectrum of 16.



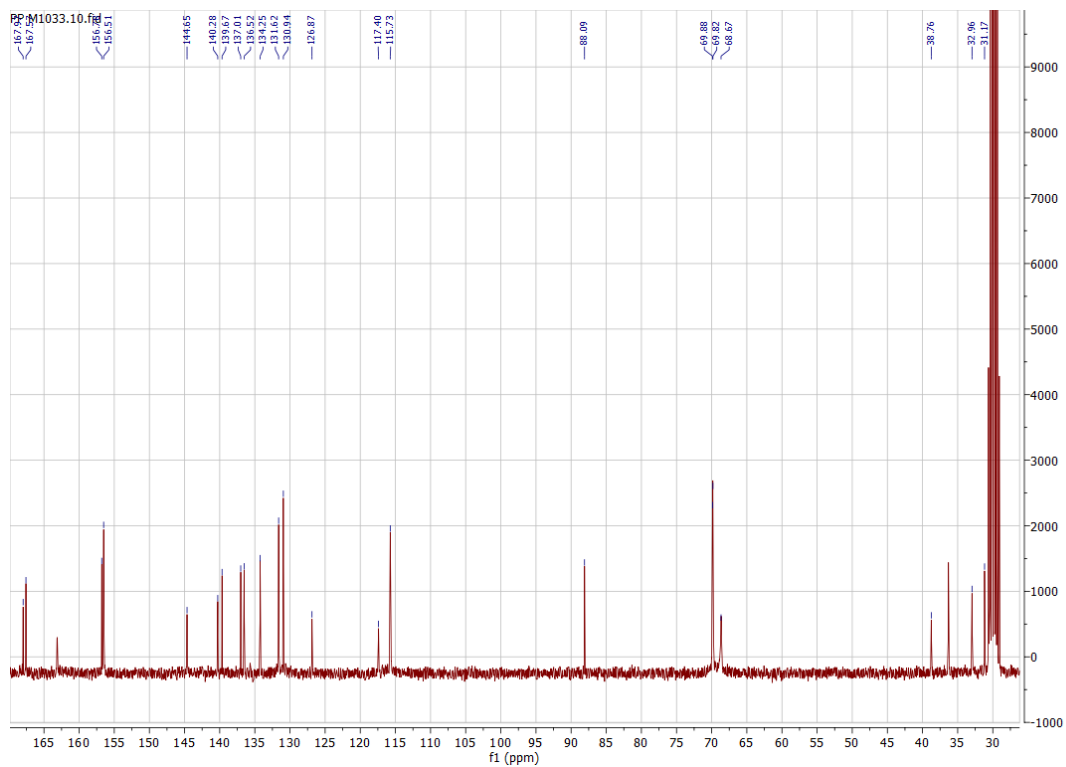
¹H spectrum of 17.



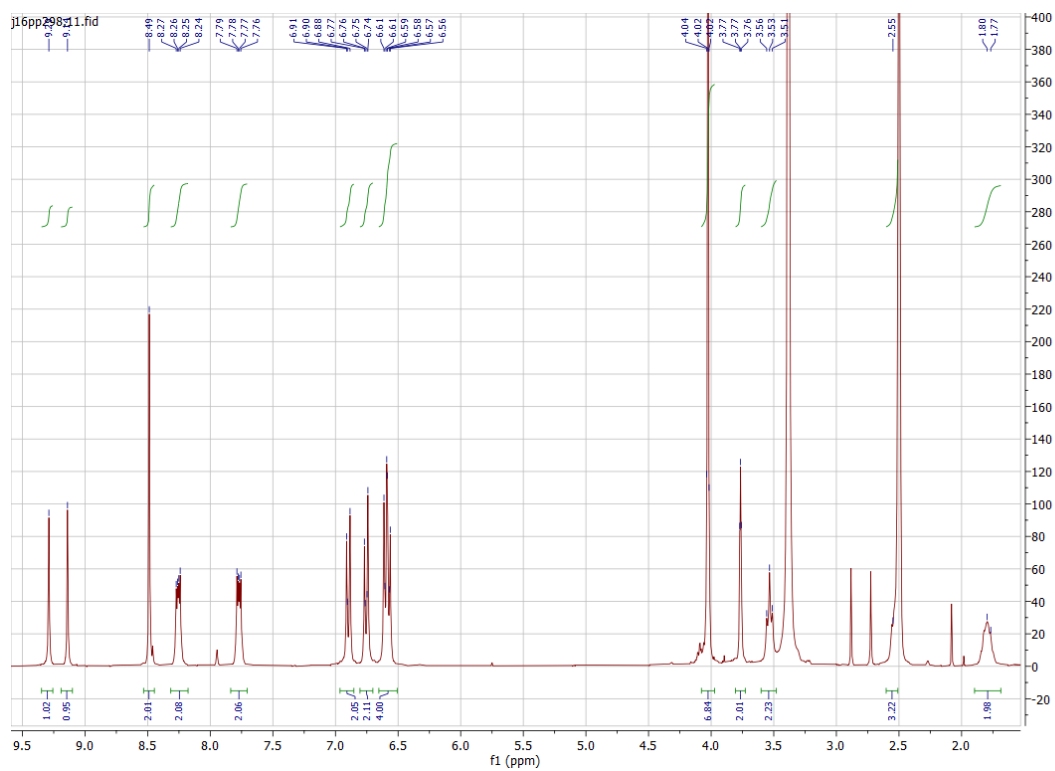
¹³C spectrum of 17.



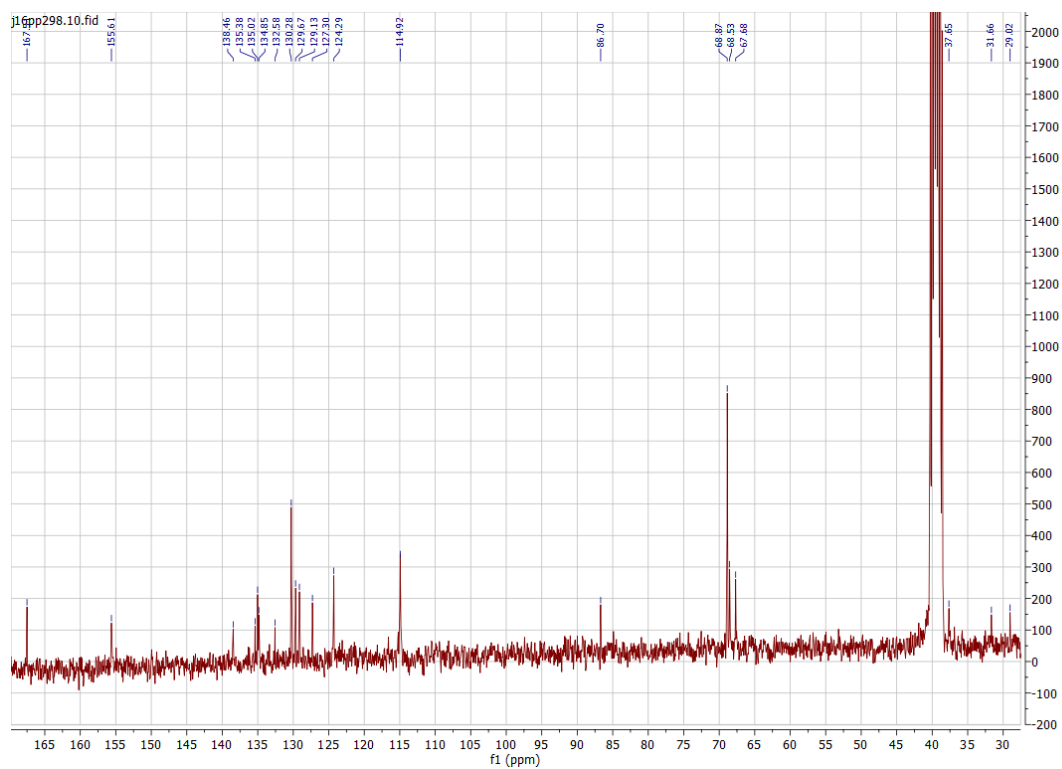
¹H spectrum of 20.



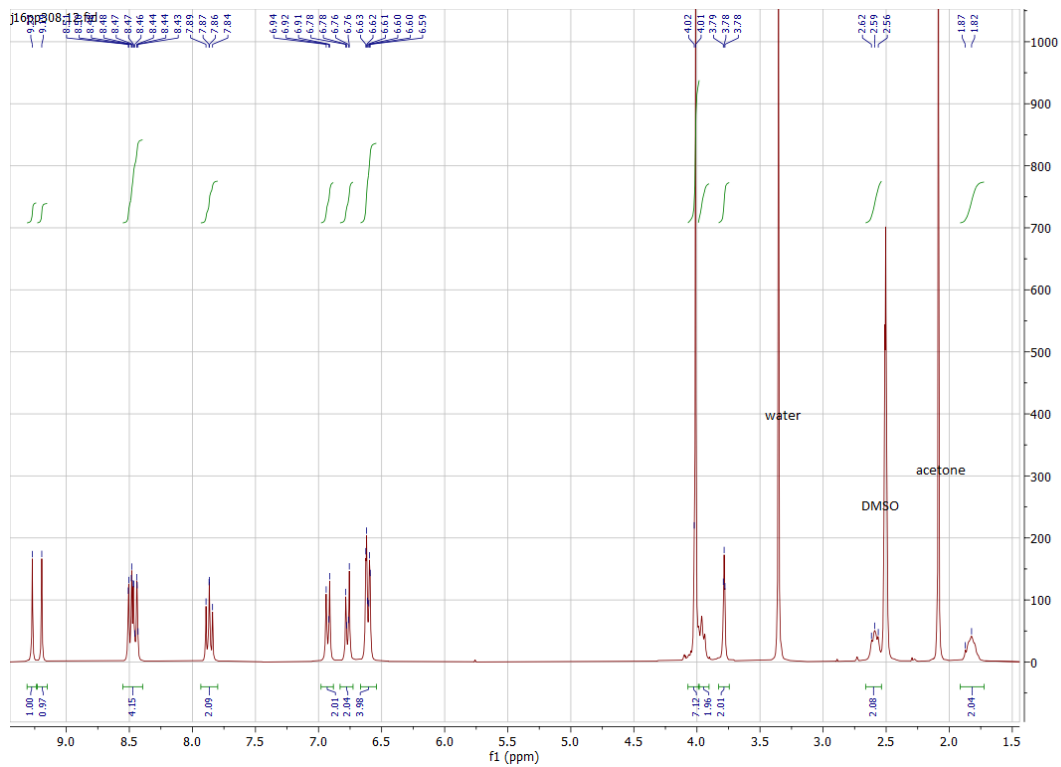
¹³C spectrum of 20.



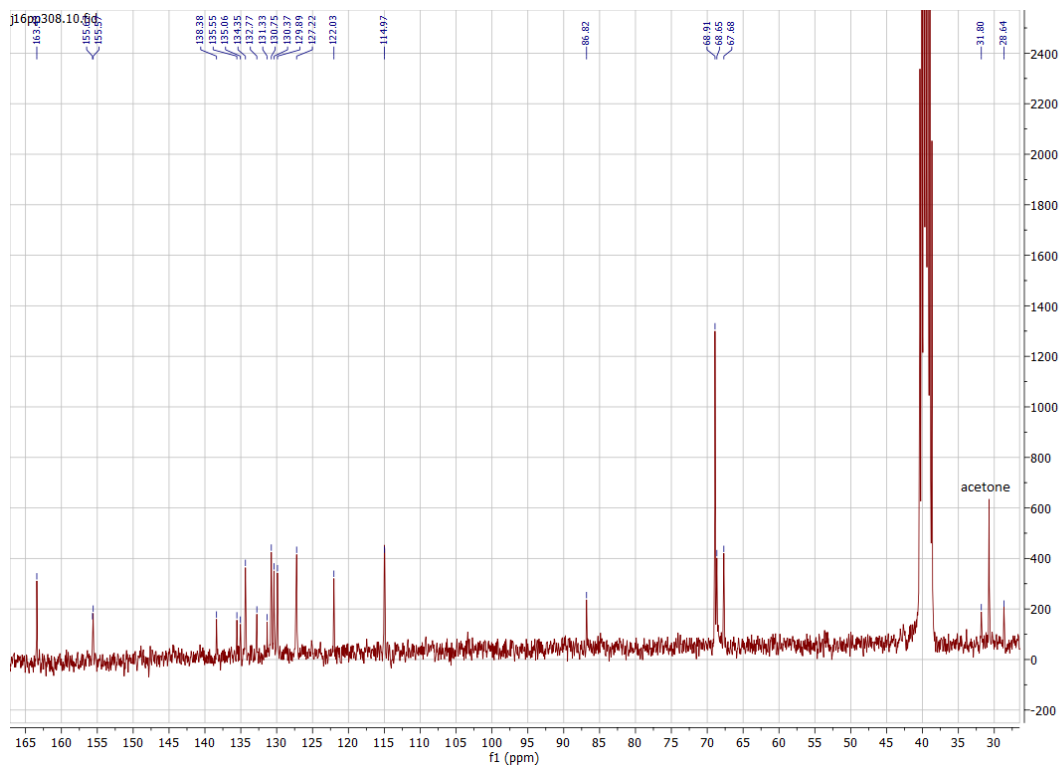
¹H spectrum of 21.



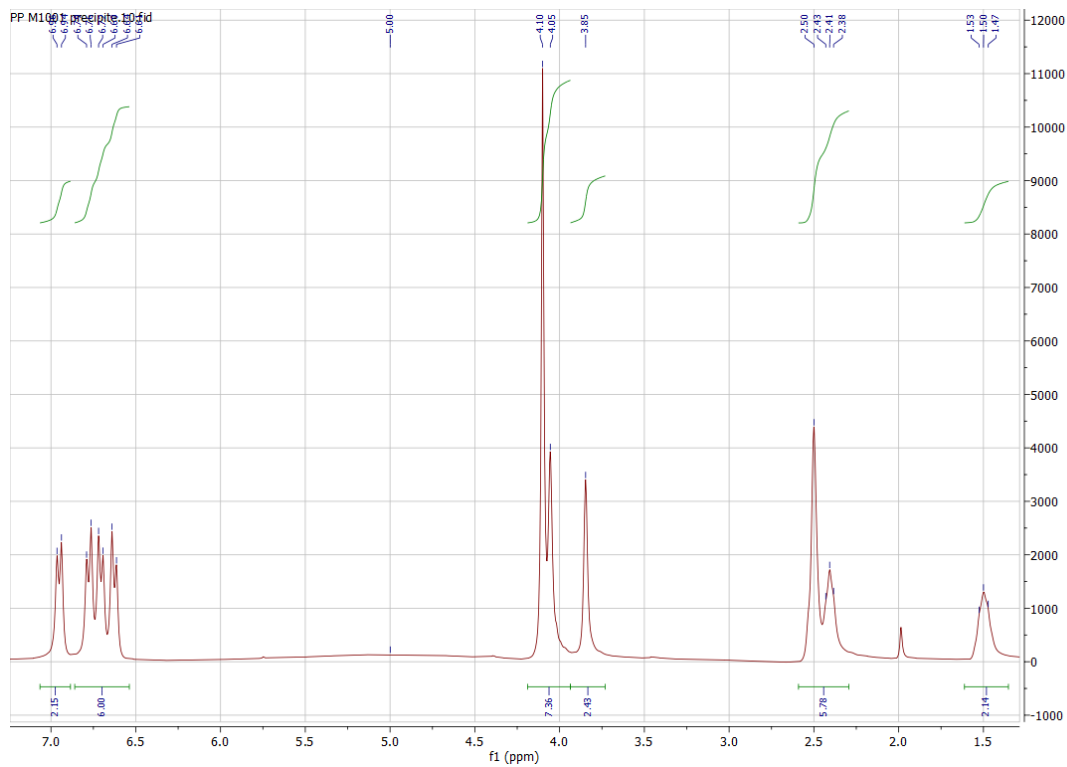
¹³C spectrum of 21.



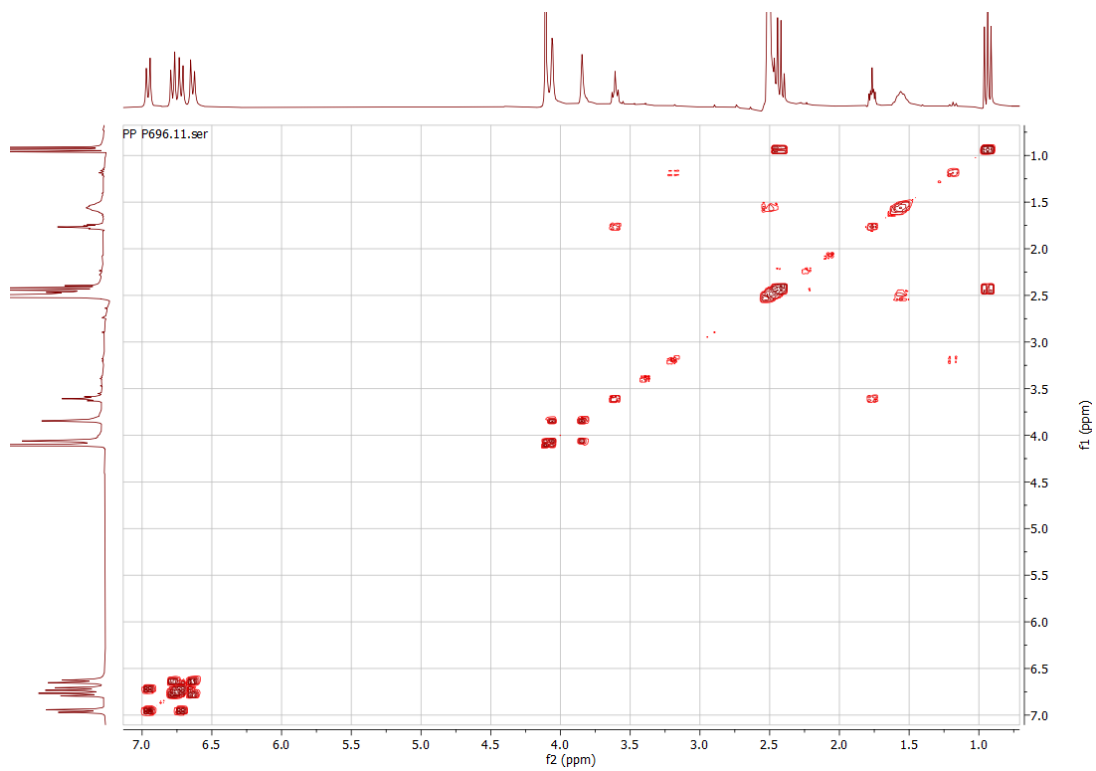
¹H spectrum of 22.



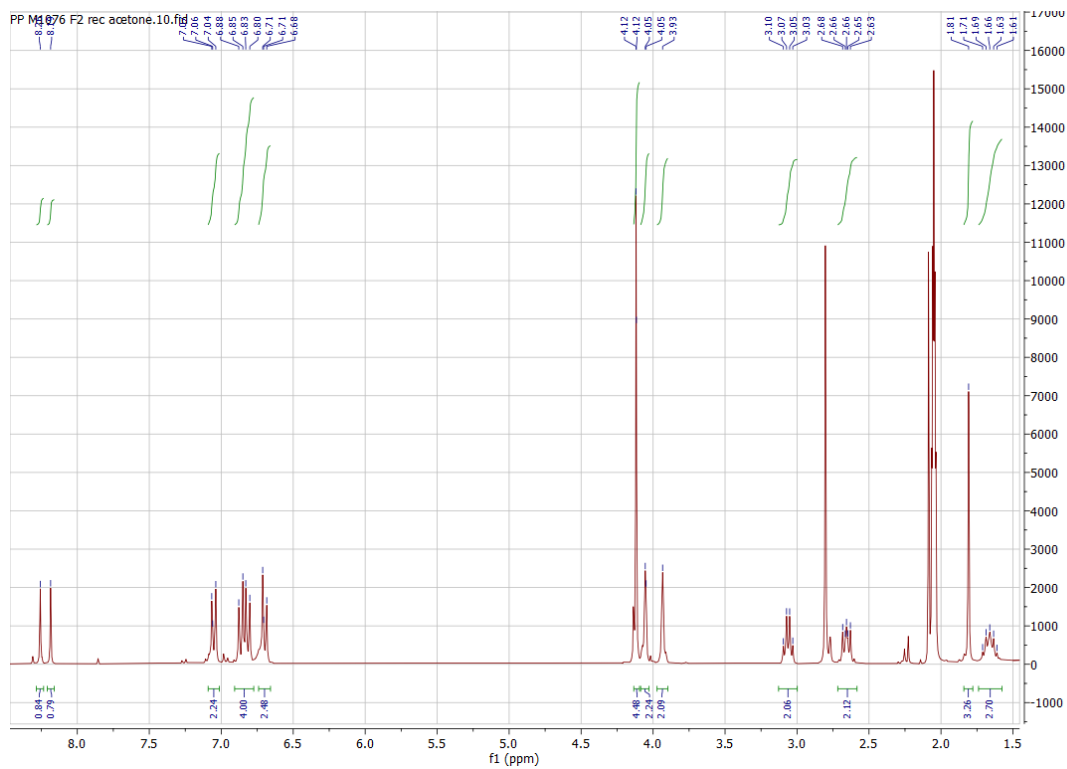
¹³C spectrum of 22.



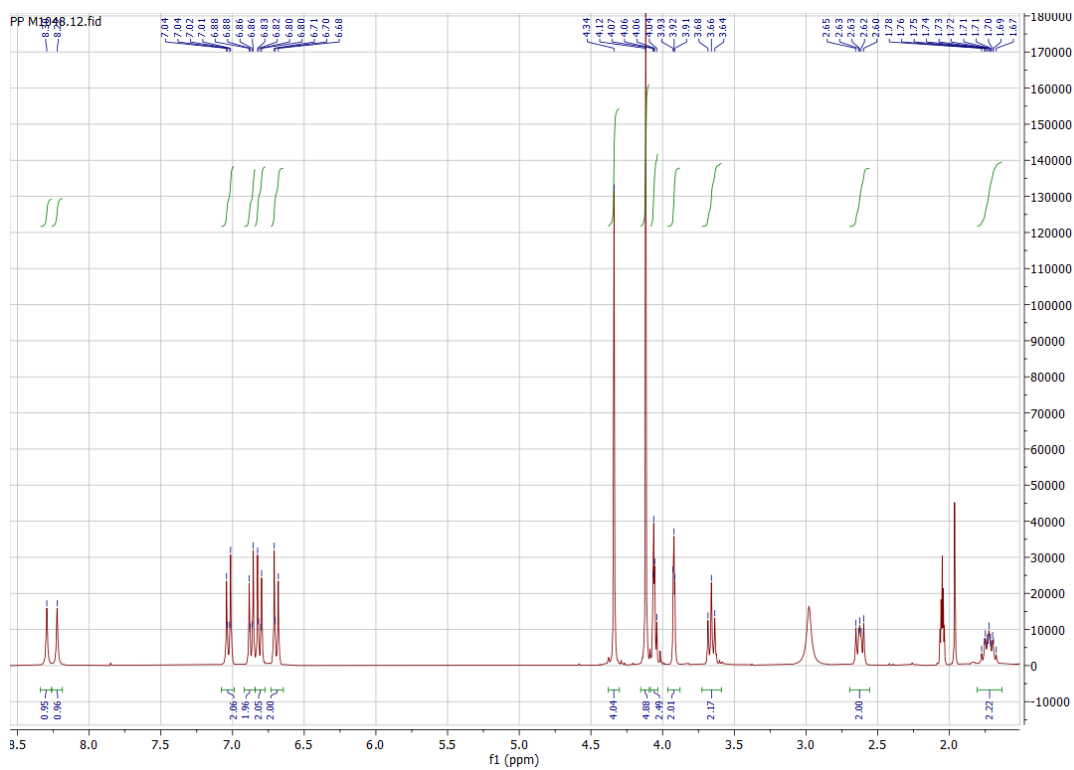
^1H spectrum of **23**.



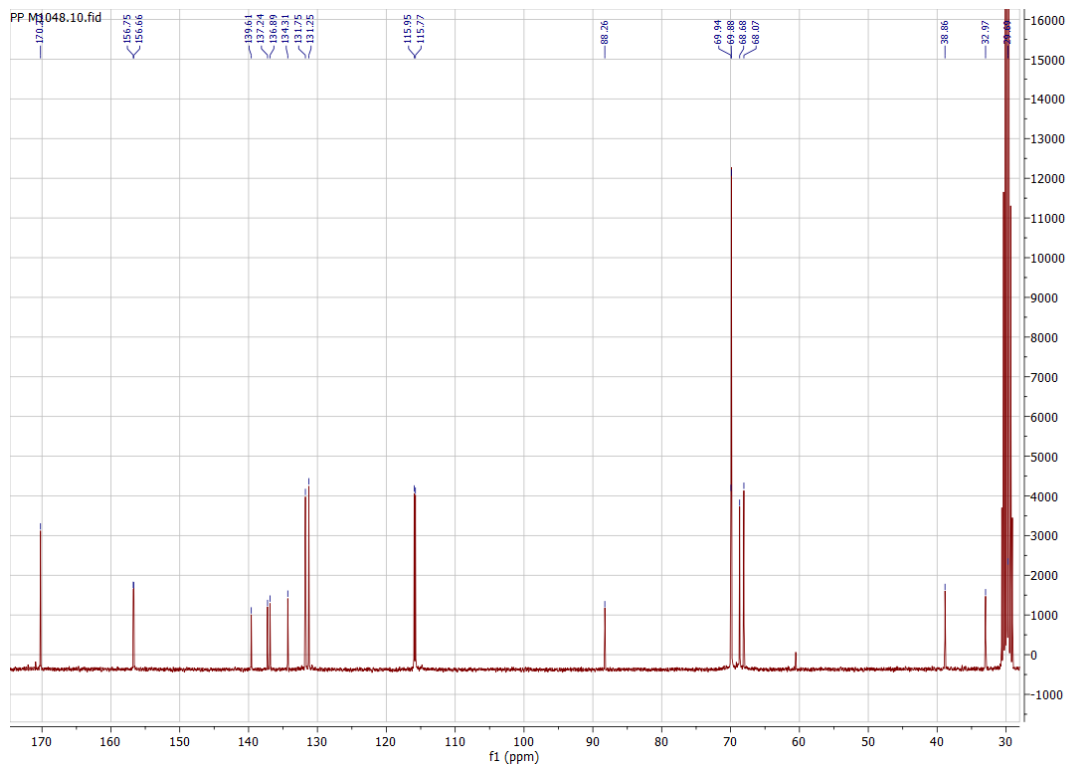
COSY spectrum of **23**.



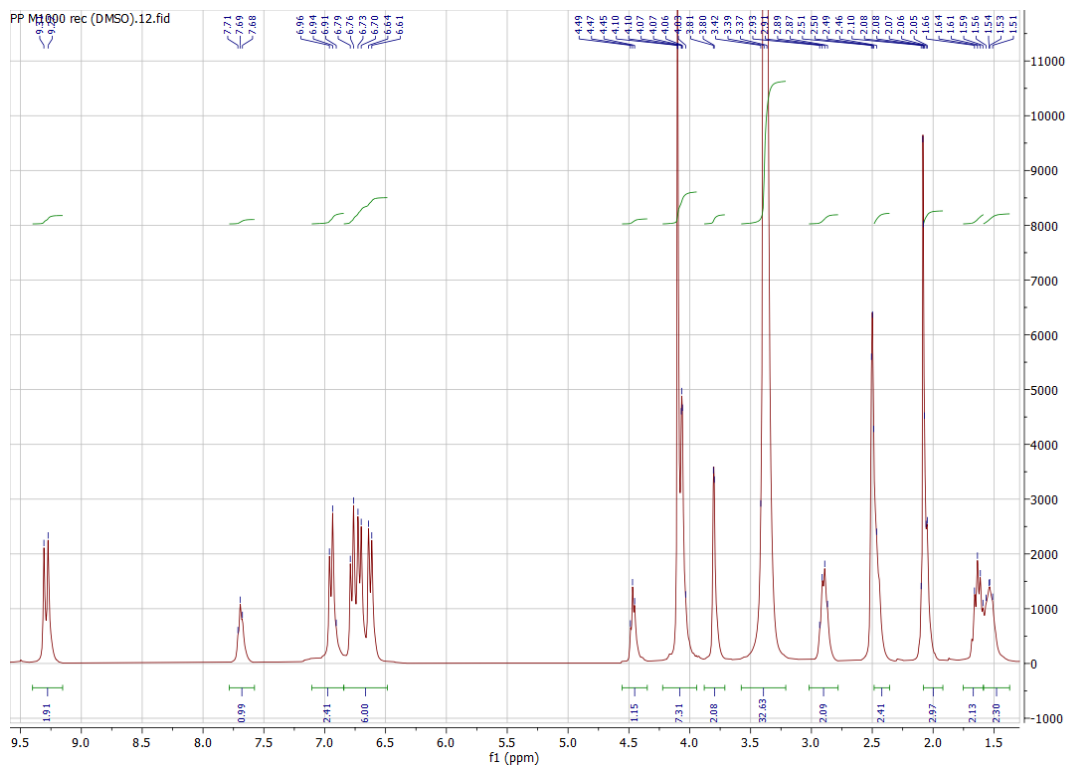
¹H spectrum of 25.



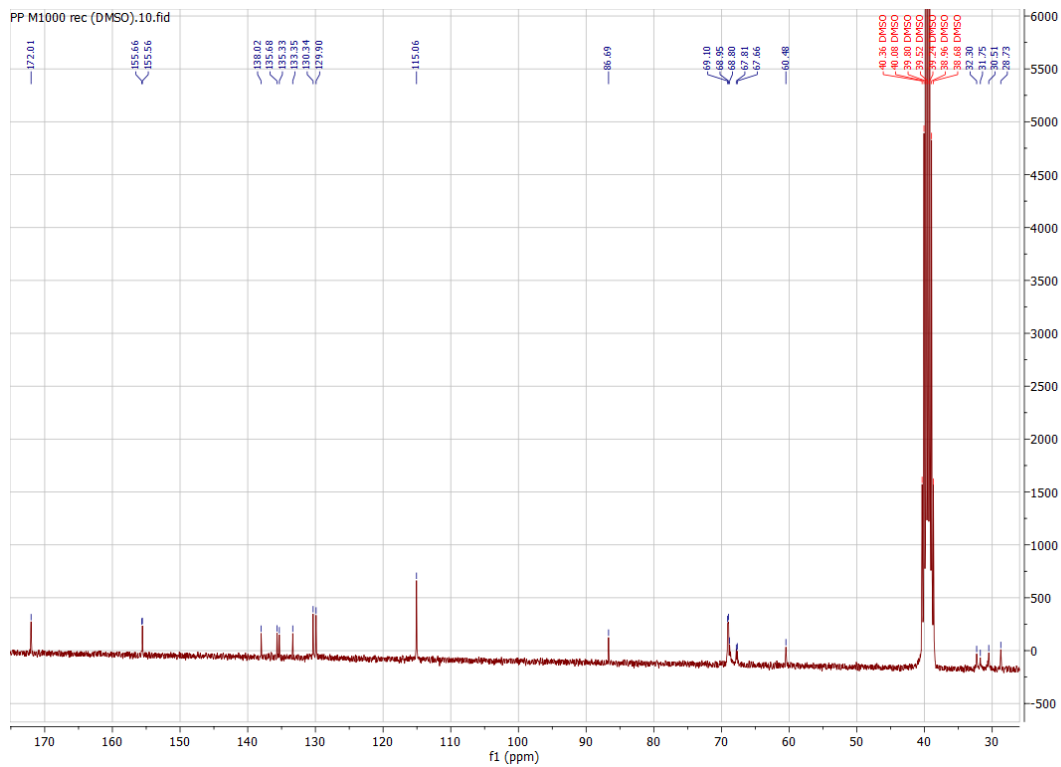
¹H spectrum of 26.



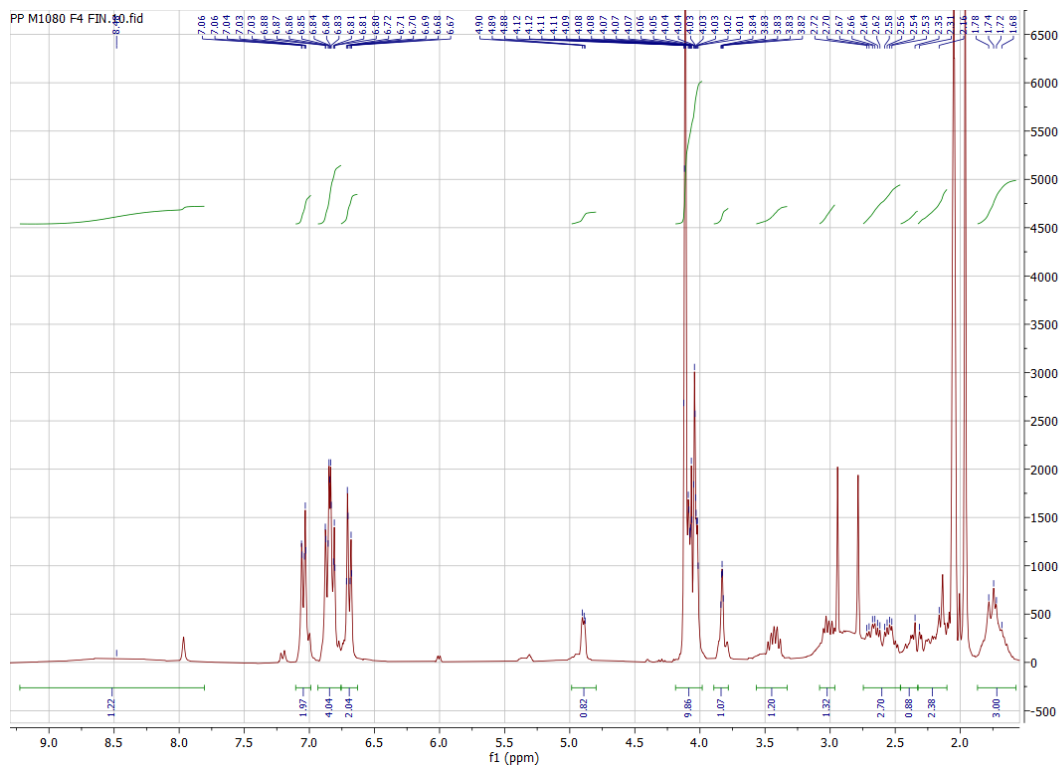
^{13}C spectrum of **26**.



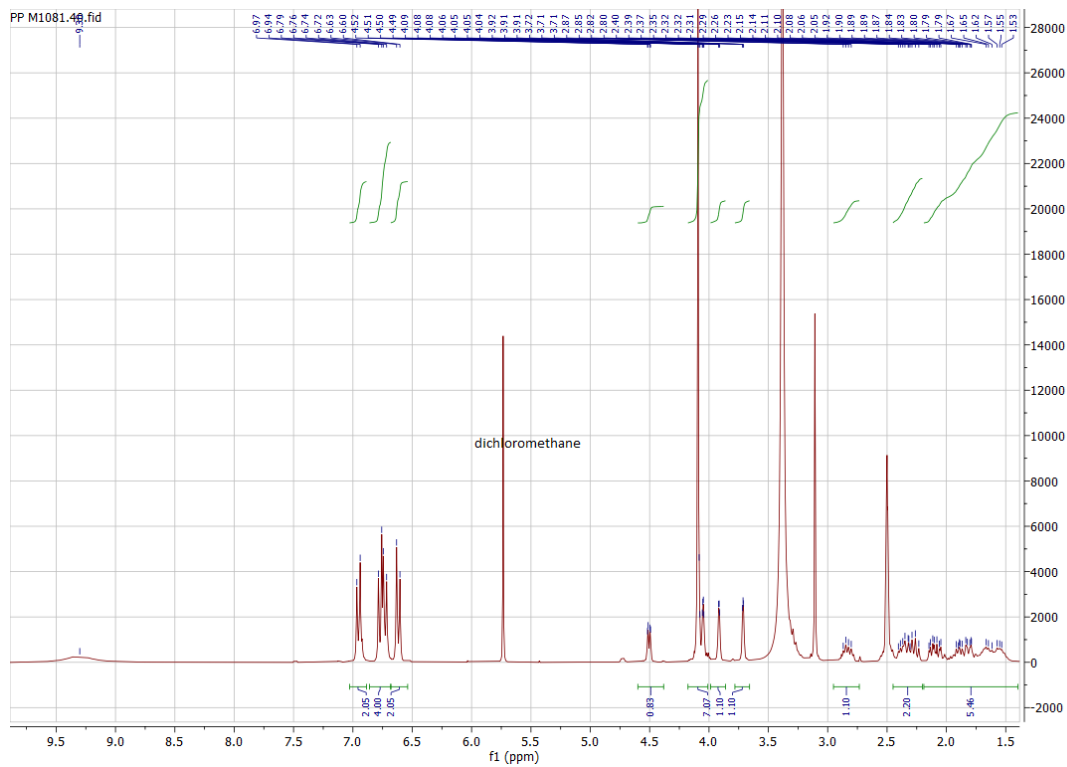
^1H spectrum of **27**.



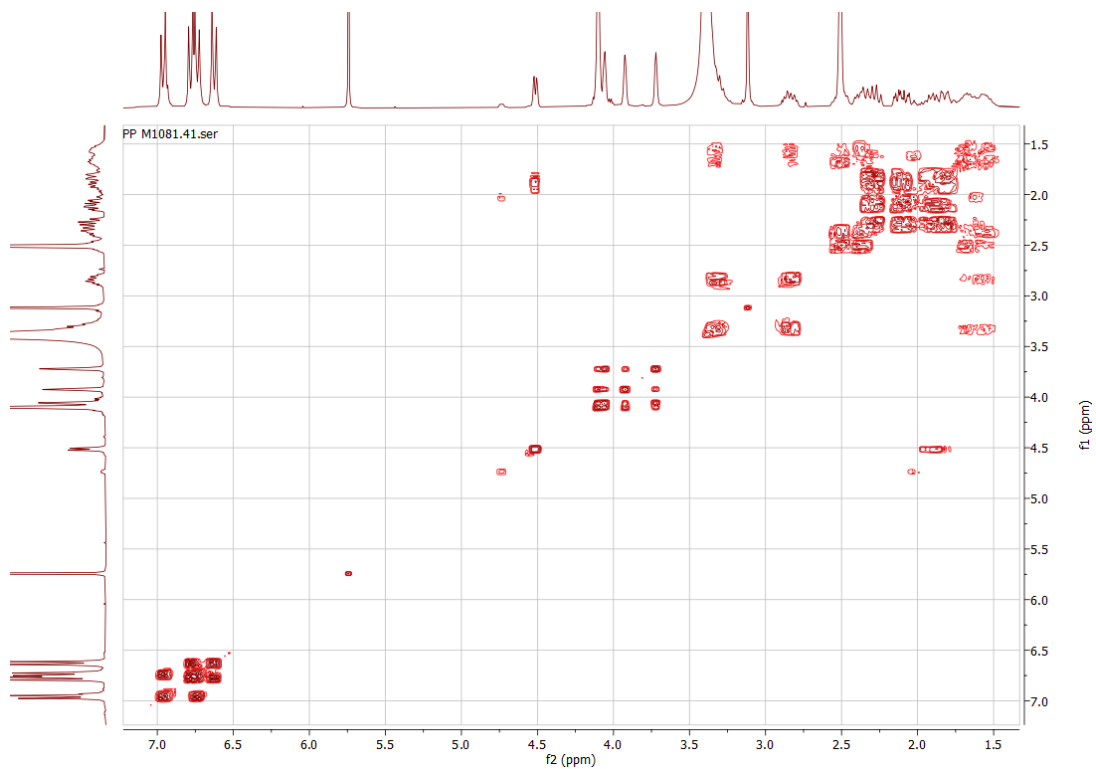
^{13}C spectrum of **27**.



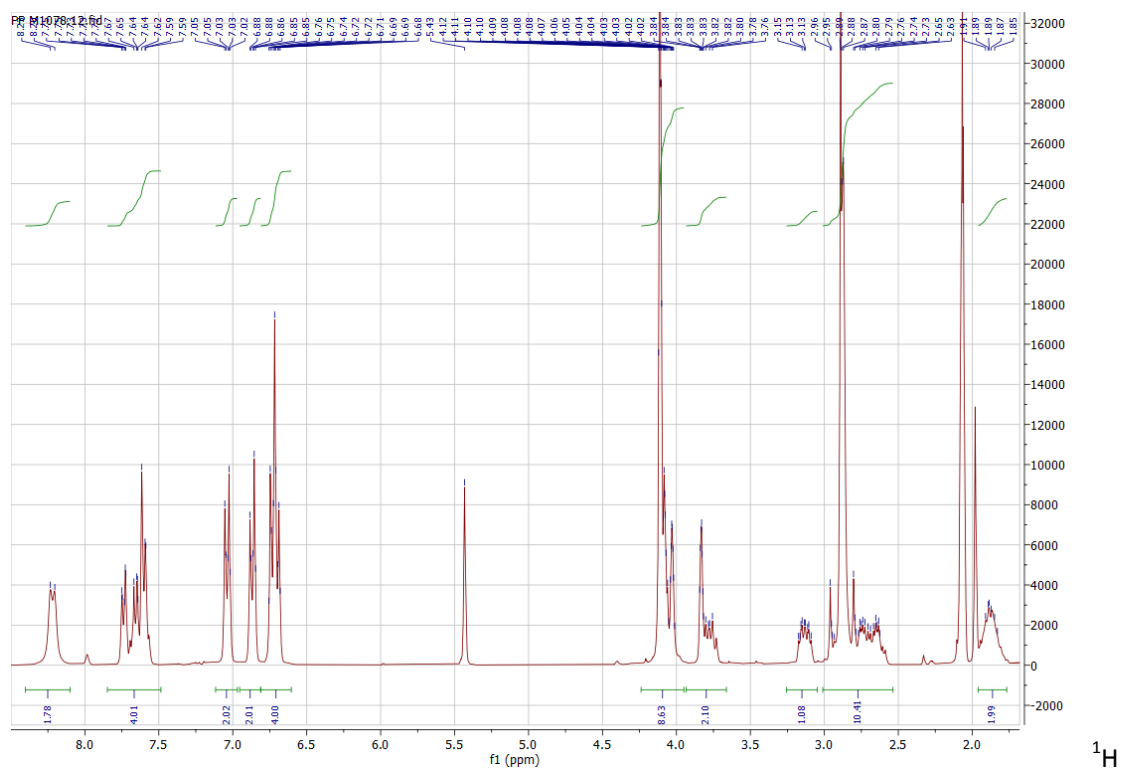
^1H spectrum of **28**.



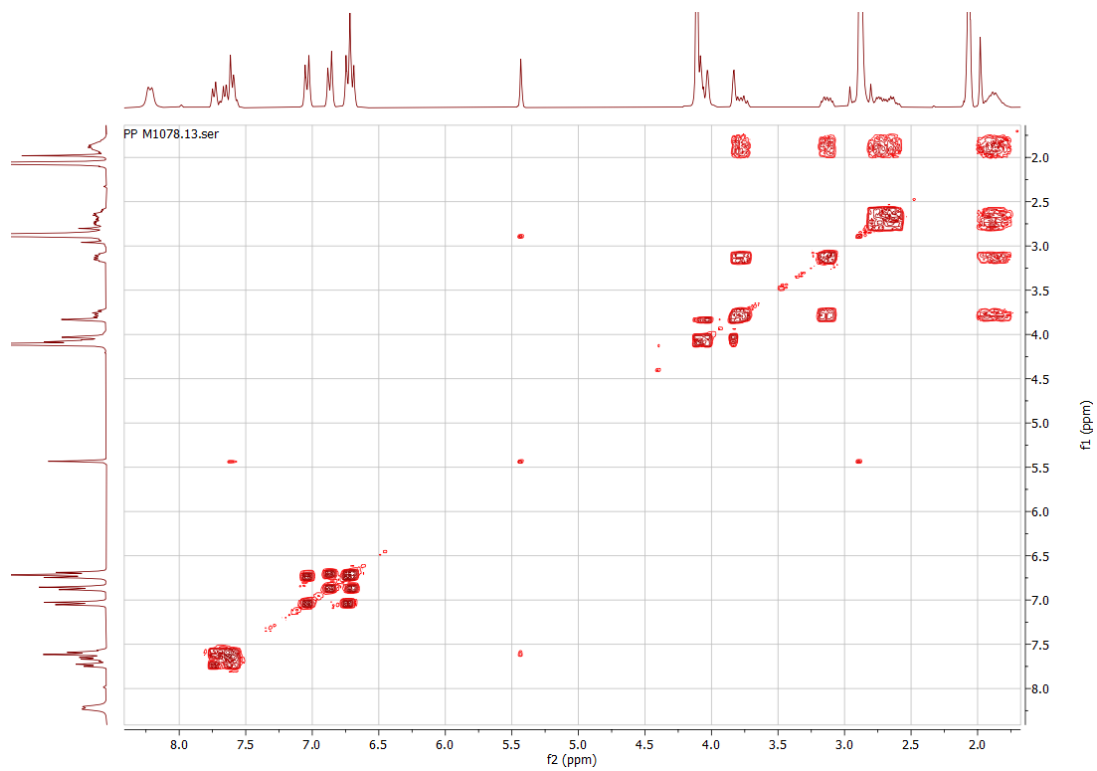
^1H spectrum of **30**.



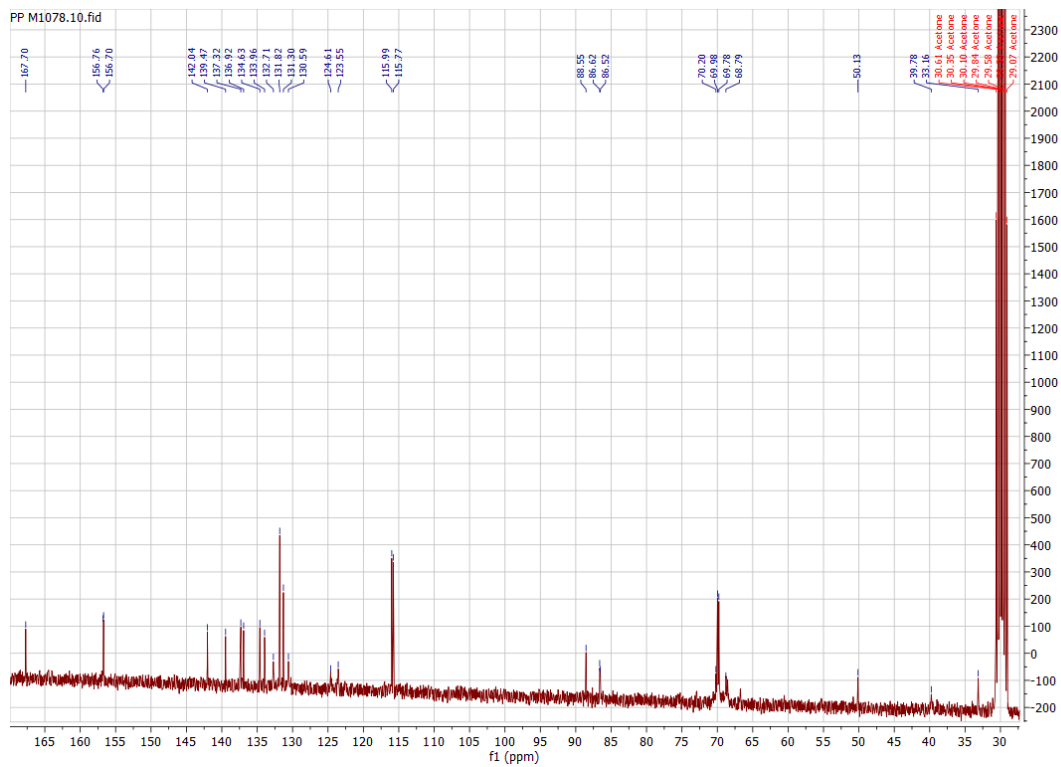
COSY spectrum of **30**.



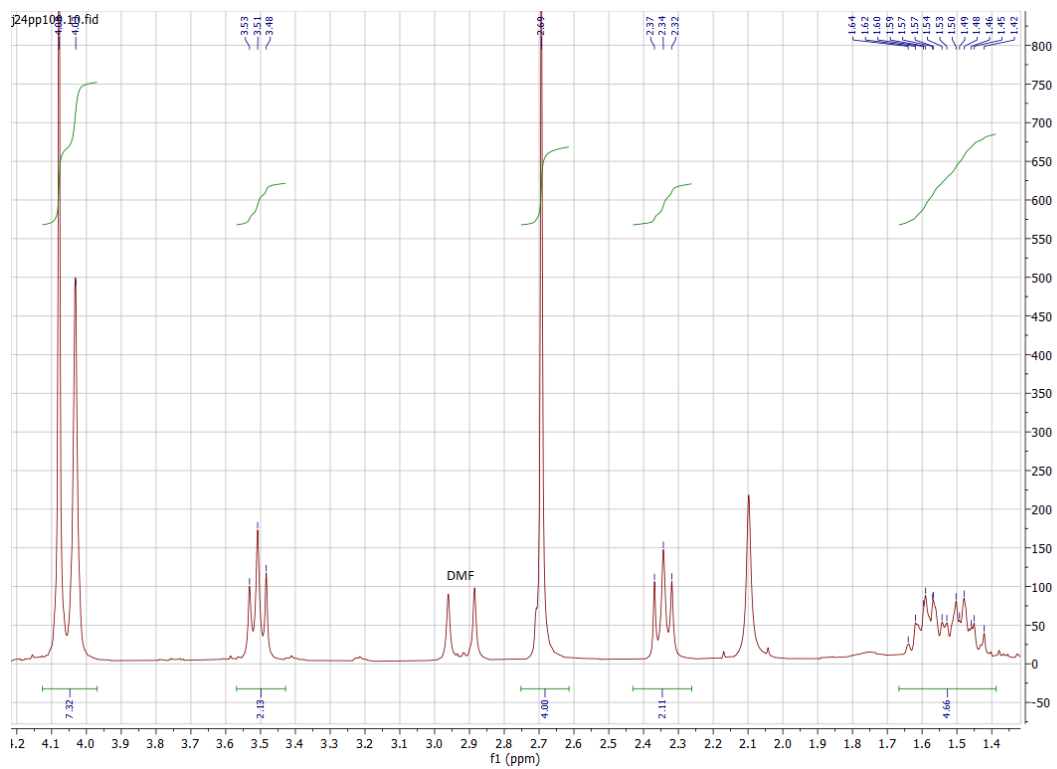
spectrum of **31**.



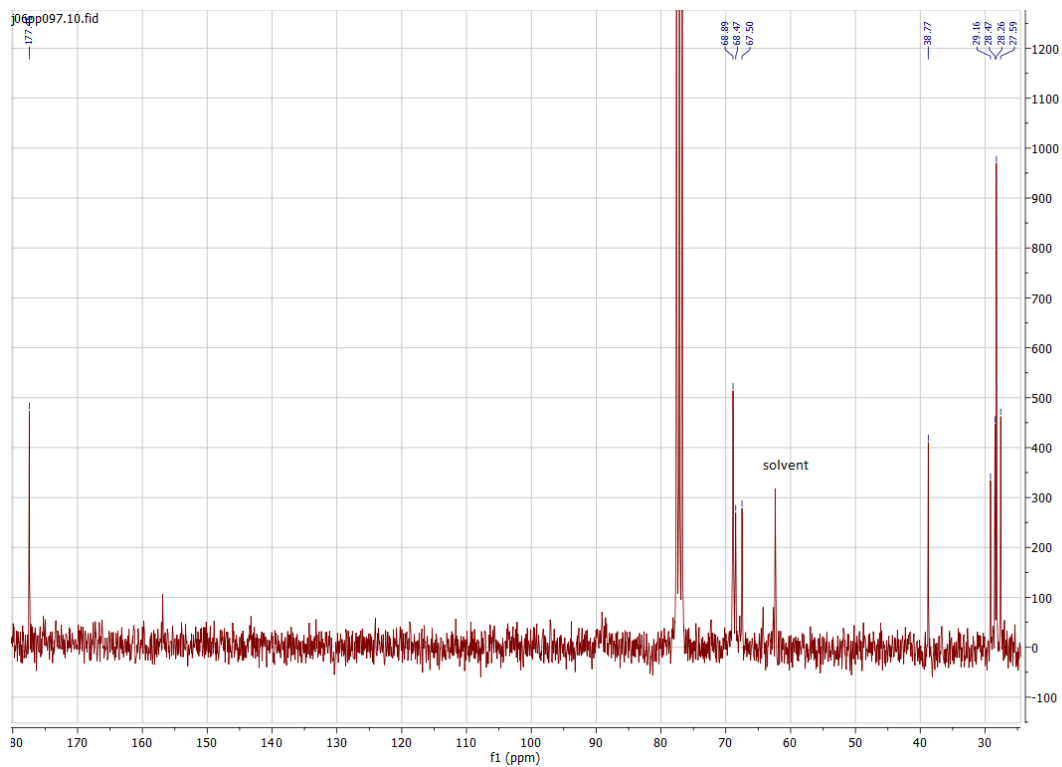
COSY spectrum of **31**.



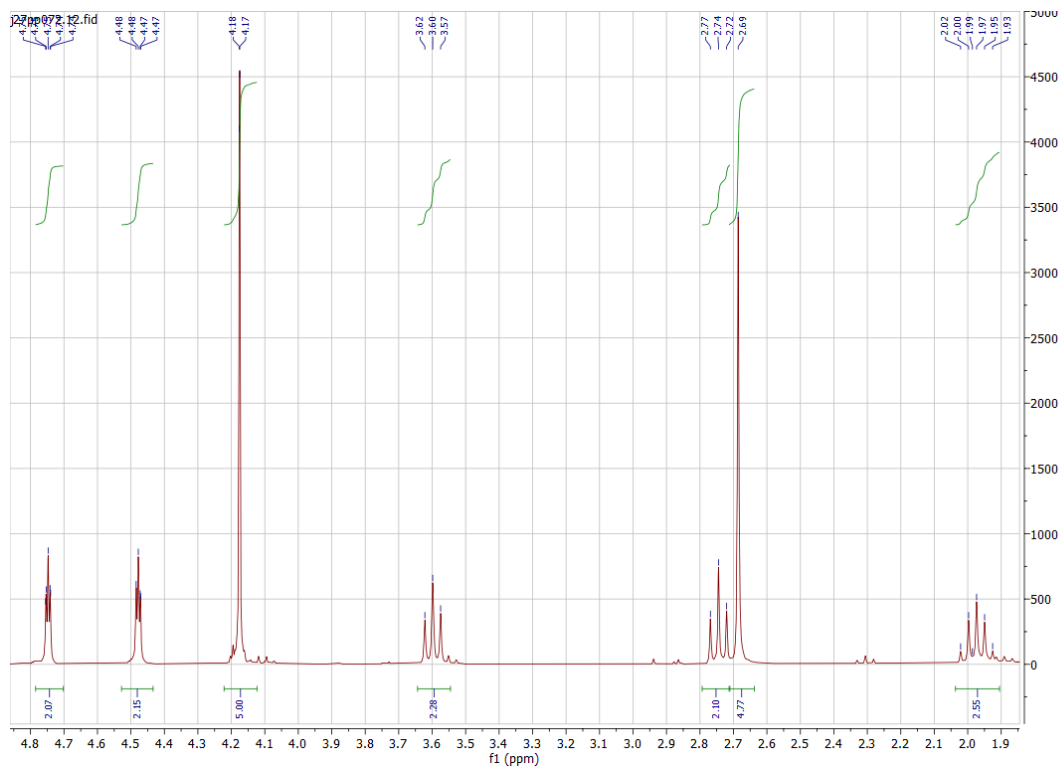
^{13}C spectrum of **31**.



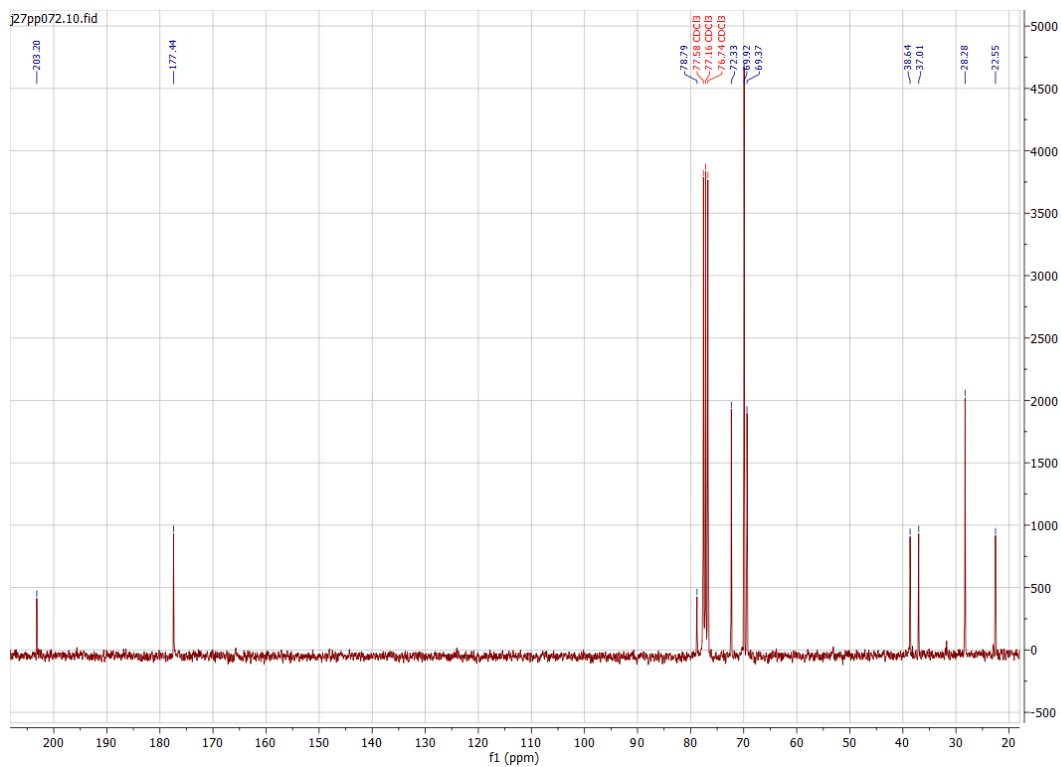
^1H spectrum of **38**.



^{13}C spectrum of **38**.



¹H spectrum of 39.



¹³C spectrum of 39.